JOURNAL OF PETROLOGY | VOLUME 45 | NUMBER 4 | PAGES 793–834 | 2004 | DOI: 10.1093/petrology/egg112

Flood and Shield Basalts from Ethiopia: Magmas from the African Superswell

BRUNO KIEFFER[1,4], NICHOLAS ARNDT[1]*, HENRIETTE LAPIERRE[1], FLORENCE BASTIEN[1], DELPHINE BOSCH[2], ARNAUD PECHER[1], GEZAHEGN YIRGU[3], DEREJE AYALEW[3], DOMINIQUE WEIS[4], DOUGAL A. JERRAM[5], FRANCINE KELLER[1] AND CLAUDINE MEUGNIOT[1]

[1]LABORATOIRE DE GÉODYNAMIQUE DES CHAÎNES ALPINES, UMR 5025 CNRS, BP 53, 38041 GRENOBLE CEDEX, FRANCE

[2]ISTEM, CC 066, UNIVERSITÉ MONTPELLIER II, PLACE E. BATAILLON, 34095 MONTPELLIER CEDEX 05, FRANCE

[3]DEPARTMENT OF GEOLOGY AND GEOPHYSICS, SCIENCE FACULTY, ADDIS ABABA UNIVERSITY, P.O. BOX 1176, ETHIOPIA

[4]DÉPARTEMENT DES SCIENCES DE LA TERRE ET DE L'ENVIRONNEMENT, UNIVERSITÉ LIBRE DE BRUXELLES 50, AV. F. D. ROOSEVELT, B-1050, BRUSSELS, BELGIUM

[5]DEPARTMENT OF GEOLOGICAL SCIENCES, UNIVERSITY OF DURHAM, SOUTH ROAD, DURHAM DH1 3LE, UK

RECEIVED JULY 31, 2002; ACCEPTED SEPTEMBER 22, 2003

The Ethiopian plateau is made up of several distinct volcanic centres of different ages and magmatic affinities. In the NE, a thick sequence of 30 Ma flood basalts is overlain by the 30 Ma Simien shield volcano. The flood basalts and most of this shield volcano, except for a thin veneer of alkali basalt, are tholeiitic. In the centre of the province, a far thinner sequence of flood basalt is overlain by the 22 Ma Choke and Guguftu shield volcanoes. Like the underlying flood basalts, these shields are composed of alkaline lavas. A third type of magma, which also erupted at 30 Ma, is more magnesian, alkaline and strongly enriched in incompatible trace elements. Eruption of this magma was confined to the NE of the province, a region where the lava flows are steeply tilted as a result of deformation contemporaneous with their emplacement. Younger shields (e.g. Mt Guna, 10·7 Ma) are composed of Si-undersaturated lavas. The three main types of magma have very different major and trace element characteristics ranging from compositions low in incompatible elements in the tholeiites [e.g. 10 ppm La at 7 wt % MgO (=La_7), La/Yb = 4·2], moderate in the alkali basalts (La_7 = 24, La/Yb = 9·2), and very high in the magnesian alkaline magmas (La_7 = 43, La/Yb = 17). Although their Nd and Sr isotope compositions are similar, Pb isotopic compositions vary considerably; $^{206}Pb/^{204}Pb$ varies in the range of ~17·9–18·6 in the tholeiites and ~19·0–19·6 in the 22 Ma shields. A conventional model of melting in a mantle plume, or series of plumes, cannot explain the synchronous eruption of incompatible-element-poor tholeiites and incompatible-element-rich alkali lavas, the large range of Pb isotope compositions and the broad transition from tholeiitic to alkali magmatism during a period of continental rifting. The lithospheric mantle played only a passive role in the volcanism and does not represent a major source of magma. The mantle source of the Ethiopian volcanism can be compared with the broad region of mantle upwelling in the South Pacific that gave rise to the volcanic islands of French Polynesia. Melting in large hotter-than-average parts of the Ethiopian superswell produced the flood basalts; melting in small compositionally distinct regions produced the magmas that fed the shield volcanoes.

KEY WORDS: *Ethiopia; flood basalts; shield volcanism; superswell*

INTRODUCTION

According to Hofmann *et al.* (1997), most of the Ethiopian flood basalts erupted 30 Myr ago, during

*Corresponding author. E-mail: arndt@ujf-grenoble.fr

a short 1 Myr period, to form a vast volcanic plateau. Immediately after this peak of activity, a number of large shield volcanoes developed on the surface of the volcanic plateau, after which subsequent volcanism was largely confined to regions of rifting (Mohr, 1983*a*; Mohr & Zanettin, 1988). The rift that opened along the Red Sea and Gulf of Aden separated the Arabian and African continents, and isolated a small portion of the volcanic plateau in Yemen and Saudi Arabia (Chazot & Bertrand, 1993; Baker *et al.*, 1996*a*; Menzies *et al.*, 2001). Volcanic activity continues to the present day along the Ethiopian and Afar rifts.

The Ethiopian flood basalts are the youngest example of a major continental volcanic plateau. Because of their relatively young age and their eruption in a region where plate movements are slow, we find a complete record from the initial, high-flux, flood volcanic phase through to its shutdown and the onset of continental rifting, and finally the initiation of sea-floor spreading. The region represents an ideal situation to study the nature of the mantle source of continental flood volcanism and the manner in which magmas derived from this source interacted with the continental lithosphere, as has been done by researchers such as Mohr & Zanettin (1988), Baker *et al.* (1996*a*), Hofmann *et al.* (1997), Pik *et al.* (1998, 1999) and Baker *et al.* (2000, 2002).

In this study we have focused on the large shield volcanoes and compared their compositions with those of the flood volcanics. We have traced the variations in eruption style and magma flux and studied the petrology, geochemistry and isotopic compositions of lavas with ages ranging from 30 to ~10 Ma, or from the peak of flood volcanism to the onset of major rifting in the northern part of the volcanic plateau. This information has allowed us first to evaluate the roles of crustal contamination and lithosphere melting during the evolution of the province, and then to test conventional models in which flood volcanism is attributed to melting in the head of a large mantle plume.

GEOLOGICAL BACKGROUND

The Ethiopian flood basalts (or traps) cover an area of about 600 000 km^2 with a layer of basaltic and felsic volcanic rocks (Fig. 1). The thickness of this layer is highly variable but reaches 2 km in some regions. The total volume of volcanic and shallow intrusive rocks has been estimated by Mohr (1983*b*) and Mohr & Zanettin (1988) at about 350 000 km^3.

The mineralogical and chemical composition of the flood basalts is relatively uniform. Most are aphyric to sparsely phyric, and contain phenocrysts of plagioclase and clinopyroxene with or without olivine. Most have tholeiitic to transitional compositions (Mohr, 1983*a*; Mohr & Zanettin, 1988; Pik *et al.*, 1998). Interlayered with the flood basalts, particularly at upper stratigraphic levels, are felsic lavas and pyroclastic rocks of rhyolitic, or less commonly, trachytic compositions (Ayalew *et al.*, 1999).

Pik *et al.* (1998, 1999) divided the basaltic rocks into several types on the basis of trace element and Ti concentrations. They recognized a suite of 'low-Ti' basalts (LT) characterized by relatively flat rare earth element (REE) patterns and low levels of Ti and incompatible trace elements. According to Pik *et al.* (1998), these rocks are restricted to the northwestern part of the province, as shown in Fig. 1. Alkali basalts with higher concentrations of incompatible elements and more fractionated REE patterns—the so-called 'high-Ti' basalts (HT1 and HT2)—are found to the south and east. The HT2 basalts are slightly more magnesian than the HT1 basalts and commonly are rich in olivine ± clinopyroxene phenocrysts. They have higher concentrations of incompatible elements and show extreme fractionation of the REE.

Although the post-trap volcanism in the regions of active rifting around Addis Ababa and Djibouti has been the subject of numerous publications (e.g. Justin Visentin *et al.*, 1974; Zanettin *et al.*, 1978; Barrat *et al.*, 1990; Deniel *et al.*, 1994), little attention has been paid to the shield volcanoes. These volcanoes are a conspicuous feature of the Ethiopian plateau and distinguish it from other well-known, but less well-preserved, flood basalt provinces such as the Deccan and Karoo. The shield volcanoes have been described only in overview papers by Mohr (1983*b*) and Mohr & Zanettin (1988) and in a few short specialized papers (Mohr, 1967; Zanettin & Justin Visentin, 1974, 1975; Piccirillo *et al.*, 1979; Zanettin, 1993; Wolde & Widenfalk, 1994; Barberio *et al.*, 1999). The shields are described as being made up predominantly of volcanic rocks with alkaline compositions. The basal diameters of the shields range from 50 to 100 km and the highest point in Ethiopia, the 4533 m high peak of Ras Dashan, is the present summit of the eroded Simien shield. This peak soars almost 2000 m above the top of the flood basalts, which lies at about 2700 m in the northern part of the plateau. If an additional 500 m of eroded material is taken into account (Mohr, 1967), a total original height of about 3 km is estimated for this volcano. Although smaller in diameter, the summits of many of the other shield volcanoes also exceed 4000 m. Mt Choke, the second shield we studied, has a basal diameter of over 100 km and rises to 4052 m, some 1200 m above the surrounding flood volcanics. Guguftu, the third shield, is more highly eroded and its original form is difficult to discern. The 3859 m peak of Mt Uorra is the summit of the present volcano.

A trachytic unit on the flank of the Simien shield has been dated by Rochette *et al.* (1998) at 29·7 ± 0·05 Ma by $^{40}Ar/^{39}Ar$ and by Coulié *et al.* (2003) by K–Ar at

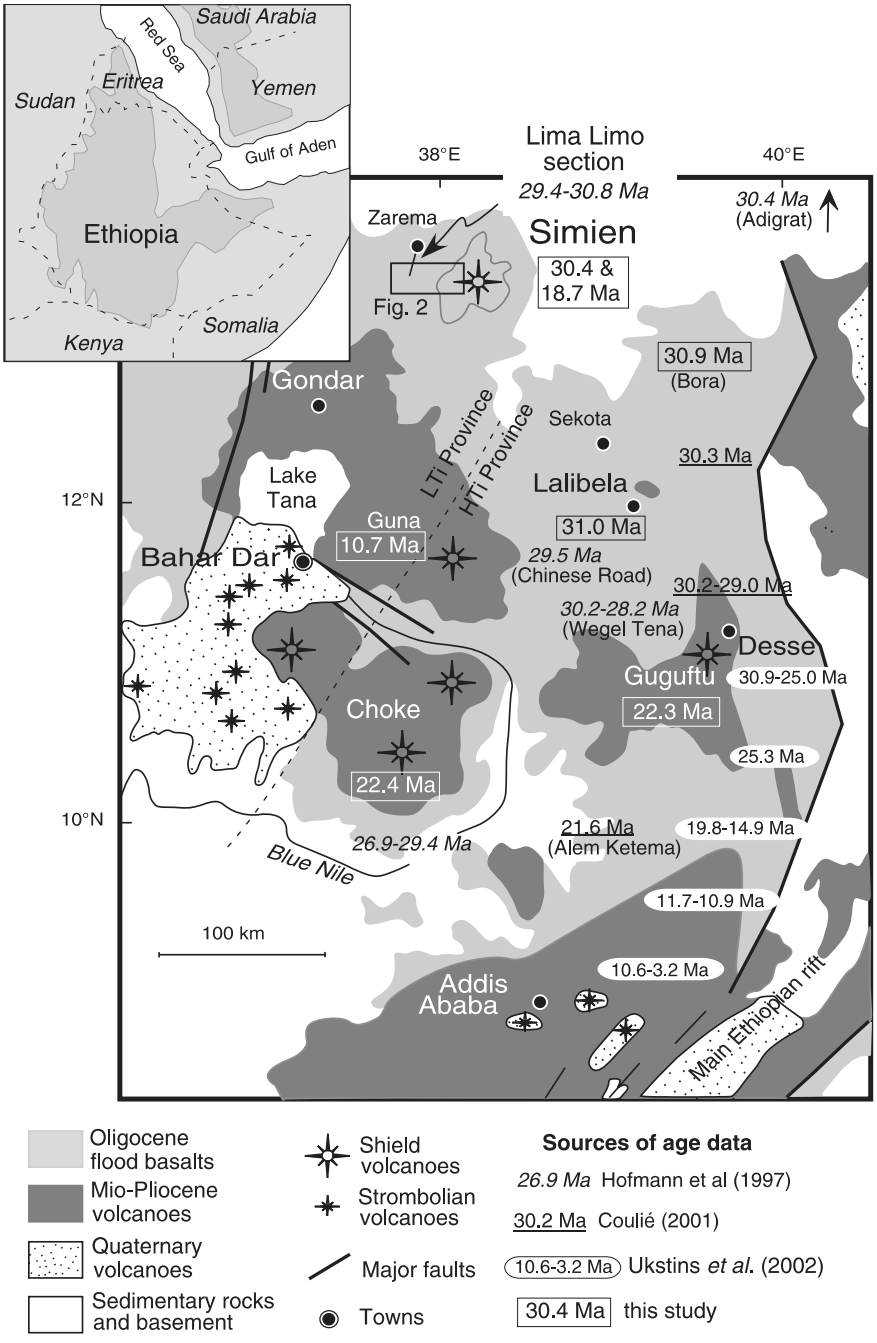

Fig. 1. Map of the northern part of the Ethiopian plateau showing the extent of the flood volcanism and the location and ages of the major shield volcanoes (modified from Zanettin, 1992; Pik *et al.*, 1999), with additional age data from this study and Hofmann *et al.* (1997), Coulié (2001) and Coulié *et al.* (2003), and Ukstins *et al.* (2002). The dashed line shows the boundary between the LT and HT provinces of Pik *et al.* (1999). The inset shows the location of the Ethiopian volcanic plateau (in grey) in the Horn of Africa.

29·1 ± 0·4 Ma. Coulié *et al.* also dated the basalt ETH 199 (labelled EH99 in their paper) from near the present summit by K–Ar at 29·9 ± 0·4 Ma. All these ages are within error of Hofmann *et al.*'s (1997) age of the underlying flood basalts. Most other shields are significantly younger. New $^{40}Ar/^{39}Ar$ ages for the Choke and Guguftu volcanoes (Fig. 1, discussed below) indicate that both erupted around 22 Myr ago (Table 1); another new result for Mt Guna, which is located between Simien and Choke, provides an age of 10·7 Ma. Zanettin (1992) and Ukstins *et al.* (2002) reported that shield volcanoes farther to the south have ages between 20 and 3 Ma.

Table 1: Summary of Ar–Ar ages from the northern part of the Ethiopian plateau

Location	Co-ordinates	Sample	Rock type	Age (Ma)
Simien shield volcano	13°11′16″N, 37°58′19″E	FB16	Alkali basalt	18·65 ± 0·19
Choke shield volcano	10°42′27″N, 37°50′47″E	ETH238	Plag-phyric basalt, trachyte	22·4 ± 0·3
Guguftu shield volcano	10°55′11″N, 39°30′27″E	ETH265	Plag-phyric basalt, trachyte	23·3 ± 0·3
South of Lalibela	11°48′50″N, 38°54′45″E	ETH633	Hyaloclastite, alkaline picrite	30·99 ± 0·13
Bora	12°55′25″N, 39°26′13″E	ETH679	Plag from alkaline picrite	30·86 ± 0·12
Guna shield volcano	11°47′19″N, 38°16′13″E	ETH627	Alkali basalt	10·76 ± 0·05

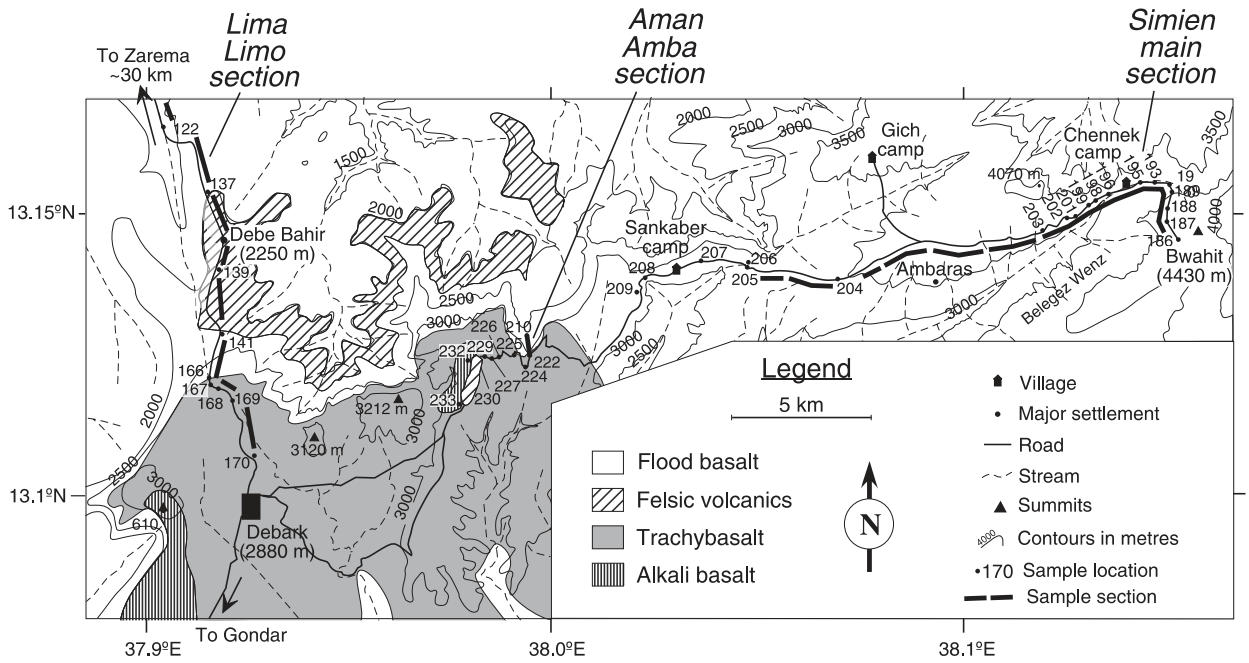

Fig. 2. Map of the Simien shield volcano and underlying flood basalts indicating the distribution of rock types and the locations of the sampled sections.

The lava flows of the shield volcanoes are thinner and less continuous than the underlying flood basalts. They also are more porphyritic, containing abundant and often large phenocrysts of plagioclase and olivine. Like the flood volcanics, the shield volcanoes are bimodal and contain sequences of alternating basalts, rhyolitic and trachytic lava flows, tuffs and ignimbrites, particularly near their summits. The compositions of the lavas in some of the younger volcanoes (e.g. Mt Guna, Fig. 1) are more variable and include nephelinites and phonolites (Zanettin, 1993) in addition to alkali basalts.

SAMPLING STRATEGY AND ANALYTICAL METHODS

The samples analysed in this study come from three regions. Most of our attention was focused on the Simien shield in the northern part of the plateau and its underlying flood basalts (Fig. 1). Other samples were collected from the Choke and Guguftu shields, a little farther to the south. To provide information about the geographical distribution of different magma types, supplementary samples were collected in the Alem Ketema region, just north of Addis Ababa and the Sekota region in the NE (Fig. 1). Reference is also made to the analytical data of Zanettin *et al.* (1976), Zanettin (1992, 1993), Pik *et al.* (1998, 1999) and Rochette *et al.* (1998).

Figure 2 is a map of the Simien volcano. Figures 3 and 4 show the geological relations, the stratigraphy and the rock types collected along three sampled sections within the flood basalts and overlying shield. About 70 lava samples were collected from the principal Lima Limo section, which extends from Zarema, to the north of the area shown in Fig. 2, along the Lima Limo road,

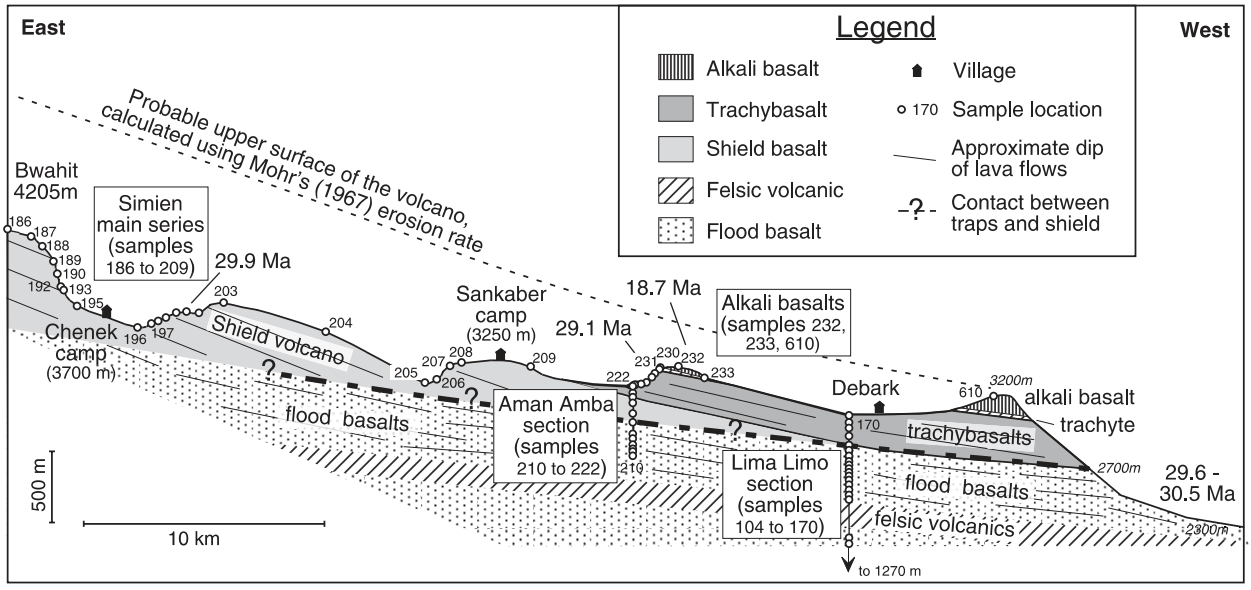

Fig. 3. Diagrammatic section through the Simien shield volcano and underlying flood basalts.

from near the base of the flood basalts to the upper flank of the shield. One other section (Aman Amba) is centred on the transition from plateau to shield volcanism; the third (Simien Main Series) extends out from near the present summit of the shield volcano towards its lower flank (Figs 2 and 3). Samples of peridotite xenoliths and clinopyroxene megacrysts from an alkali basalt flow on the flank of the volcano were also collected and analysed for major and trace elements and Nd isotopes.

A total of 17 samples were collected along the road from the base to the summit of Choke volcano, and 16 samples were taken from the road that bisects Guguftu volcano. The location of these samples is shown in Fig. 5. Petrographic descriptions and locations of all samples collected in this study are given in the Electronic Appendix, which can be downloaded from the *Journal of Petrology* website at http://www.petrology.oupjournals.org.

Samples were ground in an agate mortar. Major elements were analysed by inductively coupled plasma atomic emission spectrometry (ICP-AES) and Ni, Cr and V by inductively coupled plasma mass spectrometry (ICP-MS) at the Centre de Recherche Pétrographique et Géologique in Nancy. The error on these data is less than 5% relative. Other trace elements were analysed by ICP-MS at the University of Grenoble following the procedure of Barrat *et al.* (1996, 2000). For the trace elements Rb, Sr, Ba, Hf, Zr, Ta, Nb, U, Th, Pb, Y and REE, the accuracy is better than 5%; for Cs it is ~10%. Table 2 contains the major and trace element data, along with measurement of standards BIR-1, BHVO-1 and RGM-1. Additional analyses are listed in the Electronic Appendix. The data are plotted in the figures on a volatile-free basis.

Nd, Sr and Pb isotopic analyses (Tables 3 and 4) were carried out at the Université Libre de Bruxelles on a VG 54 mass spectrometer using the procedure described by Weis *et al.* (1987). All samples were leached for 10 min in 2N HCl in an ultrasonic bath, then a second time in dilute HF to remove secondary minerals. To evaluate the effects of leaching, two duplicate analyses were run on unleached samples. Sr isotopic ratios were normalized to $^{86}Sr/^{88}Sr = 0{\cdot}1194$ and Nd isotopic data were normalized using $^{146}Nd/^{144}Nd = 0{\cdot}7219$. The average $^{87}Sr/^{86}Sr$ value for NBS 987 Sr standard was $0{\cdot}710278 \pm 12$ ($2\sigma_m$ on the basis of 12 samples). Analyses of the Rennes Nd standard yielded $^{143}Nd/^{144}Nd = 0{\cdot}511970 \pm 7$ ($2\sigma_m$ on the basis of 12 samples), which is within error of the recommended value of 0·511961 (Chauvel & Blichert-Toft, 2001). The recommended value corresponds to a value of 0·511856 for the La Jolla Nd standard. Chemical preparation for Pb isotopic analyses was carried out at the University of Montpellier. Powdered samples were weighed to obtain ~100–200 ng of lead, and the samples were then leached with 6N HCl for 30 min at 65°C. Samples were dissolved for 36–48 h on a hot plate with a mixture of concentrated distilled HF and HNO_3. Lead was separated using a procedure modified from Manhès *et al.* (1978). Blanks were less than 40 pg and are considered negligible for the present analyses. Lead isotopic compositions were analysed by multicollector ICP-MS using a VG model Plasma 54 magnetic sector system at the École Normale Supérieure de Lyon and the Tl normalization method described by White *et al.* (2000). This technique gives highly accurate and reproducible analyses, with an internal precision better than 50 ppm (2σ) and an external precision of ~100–150 ppm (2σ).

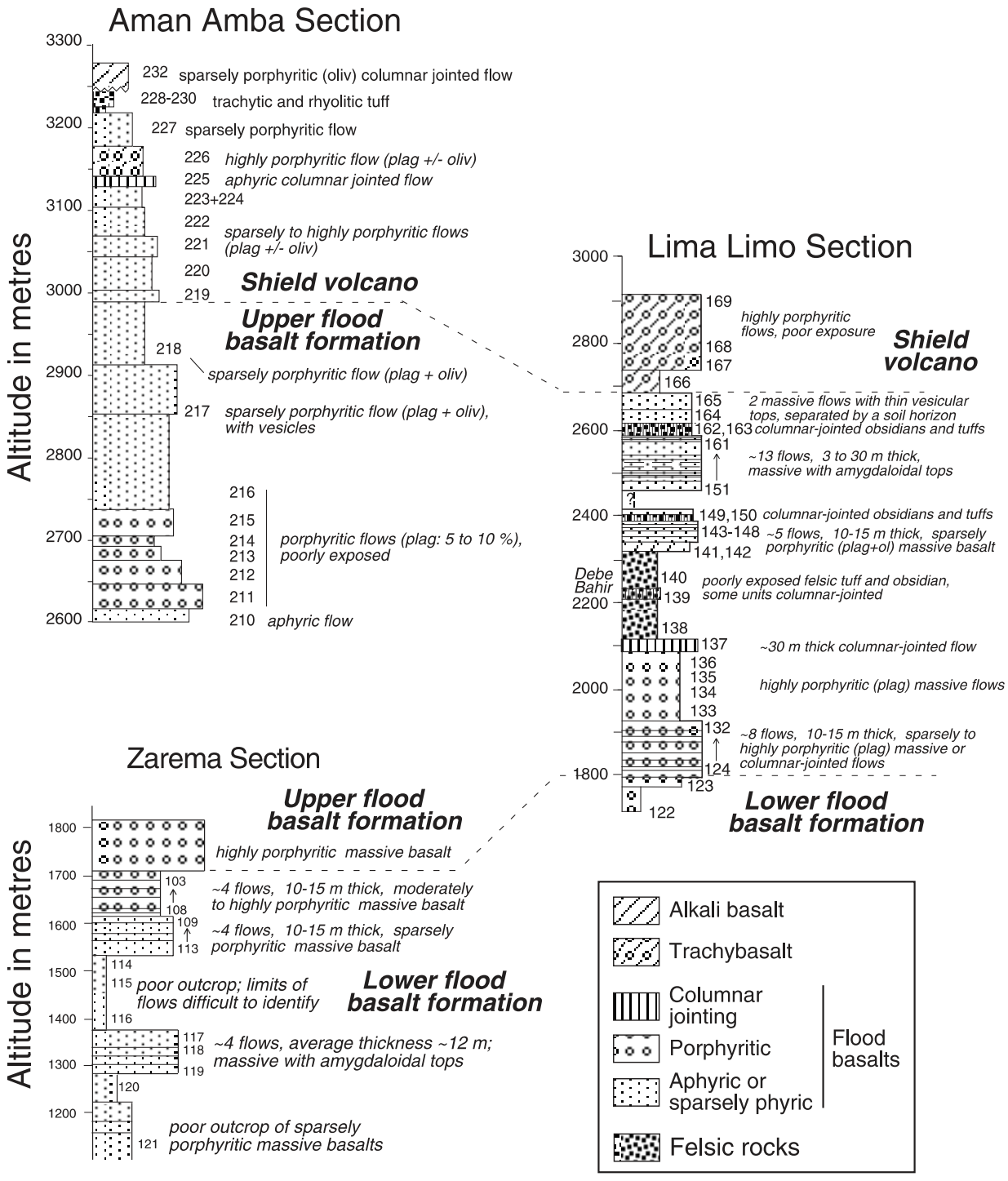

Fig. 4. Stratigraphic logs through the Simien volcano and underlying flood basalts showing rock types and sample locations.

Ar–Ar ages were obtained at the University of Oregon (four samples, analyst R. A. Duncan) and at the Université Blaise Pascal in Clermont Ferrand (four samples, analyst N. Arnaud). At Oregon State University, splits of separated plagioclase or glass, or whole-rock samples were loaded in evacuated quartz vials and irradiated for 6 h at 1 MW power at the Oregon State University TRIGA reactor. The biotite

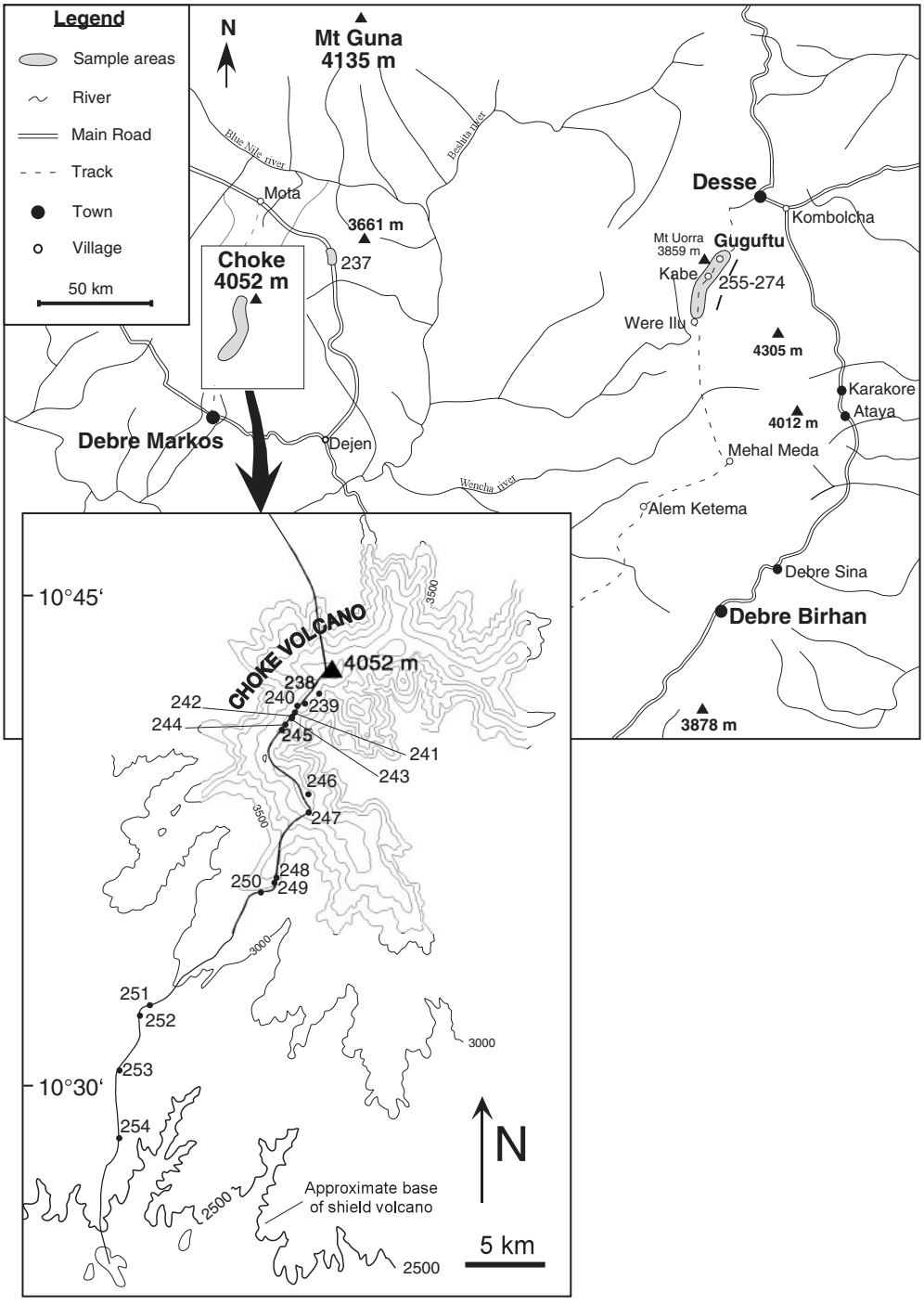

Fig. 5. Maps showing the locations and sample sites on Choke and Guguftu volcanoes.

standard FCT-3 (27·55 ± 0·12 Ma, equivalent to 513·9 Ma for hornblende Mmhb-1; Lanphere *et al.*, 1990) was used to monitor the neutron fluence. The isotopic composition of Ar was determined for each of nine temperature steps using an AEI MS-10S mass spectrometer [see Duncan *et al.* (1997) for experimental details]. Samples run at Clermont Ferrand were irradiated in the Mélusine reactor in Grenoble. Fish Canyon sanidine was used as a standard (27·55 ± 0·08 Ma). Figure 6 shows the age spectra and isochrons; complete analytical data can be found in Table E2 of the Electronic Appendix.

Table 2a: Major and trace element data

	Zarema section																	
Sample no.:	104	105	106	107	108	109	110	111	112	113	114	115	116	117	118	119	120	121
Rock type:	Basalt	Basalt	Basalt	Basalt	Basalt	Basalt	Basalt	Basalt	Basalt	Basalt	Basalt	Basalt	Basalt	Basalt	Basalt	Basalt	Basalt	Basalt
Altitude (m):	1690	1673	1650	1630	1630	1610	1590	1590	1560	1560	1520	1480	1400	1370	1350	1330	1300	1200
wt %																		
SiO_2	48·8	47·9	48·4	49·0	50·3	47·7	49·7	48·6	47·7	49·4	47·9	48·0	48·3	49·6	48·6	48·7	46·2	48·4
TiO_2	1·96	1·73	1·45	1·27	1·45	1·48	1·44	1·35	1·55	1·98	1·79	1·53	1·49	1·51	1·52	1·51	1·32	1·52
Al_2O_3	15·7	15·4	15·2	15·2	15·9	15·9	15·6	15·2	16·6	15·1	15·5	16·3	16·5	15·2	16·0	16·0	13·7	15·3
Fe_2O_3	12·8	11·3	12·2	11·8	12·2	12·2	12·2	11·8	13·1	13·7	12·9	12·9	12·8	11·9	11·9	11·8	11·4	12·1
MnO	0·17	0·16	0·19	0·17	0·17	0·31	0·15	0·16	0·17	0·2	0·17	0·18	0·18	0·16	0·17	0·16	0·16	0·2
MgO	5·67	5·75	6·99	7·68	6·65	6·57	6·64	7·78	6·82	5·65	6·65	6·7	6·54	6·50	6·70	6·78	10·2	7·94
CaO	9·98	10·33	10·25	9·93	9·88	9·96	9·83	9·97	9·21	9·15	9·19	9·21	9·46	9·25	9·72	9·80	10·4	10·2
Na_2O	2·67	2·67	2·23	2·08	2·6	2·61	2·56	2·31	2·73	3·12	2·68	2·73	2·71	3·11	2·68	2·69	1·56	2·62
K_2O	0·56	0·49	0·14	0·69	0·39	0·41	0·28	0·28	0·63	0·69	0·6	0·39	0·31	0·63	0·66	0·64	0·51	0·41
P_2O_5	0·25	0·23	0·14	0·12	0·14	0·14	0·12	0·12	0·18	0·29	0·22	0·22	0·22	0·16	0·21	0·22	0·15	0·18
Total	99·6	100	98·9	99·5	99·9	99·4	99·6	99·1	99·9	100	99·2	99·3	99·5	99·5	99·7	100	100	100
LOI	1·11	3·96	1·67	1·56	0·34	2·14	1·19	1·59	1·2	0·65	1·48	1·16	0·93	1·61	1·61	2·06	4·45	1·26
ppm																		
Cs	0·03	0·07	0·01	0·05	0·05	0·03	0·02	0·03	0·02	0·11	0·03	0·01	0·01	0·01	0·02	0·04	0·03	0·01
Rb	3·87	5·74	0·68	8·35	5·46	5·40	3·10	2·73	6·60	7·51	6·54	1·68	1·11	5·89	7·23	6·78	9·59	3·60
Ba	265	226	77·8	285	138	136	110	107	192	308	257	212	200	229	238	230	133	181
Sr	418	464	280	330	333	307	307	318	440	432	395	406	398	337	384	383	321	349
Th	0·66	0·45	0·50	0·41	0·74	0·74	0·71	0·54	0·39	0·85	0·63	0·32	0·32	0·56	0·57	0·58	0·59	0·49
U	0·22	0·15	0·18	0·14	0·22	0·22	0·20	0·14	0·13	0·30	0·19	0·11	0·12	0·16	0·17	0·19	0·18	0·15
Pb	2·28	2·00	1·22	0·97	1·65	1·57	1·49	1·12	1·18	2·57	2·05	1·36	1·43	1·68	1·87	1·90	0·92	1·47
Nb	8·23	6·81	5·06	4·14	5·64	5·24	5·33	5·64	5·51	8·65	7·34	5·11	4·72	6·25	6·84	6·92	5·96	5·90
Ta	0·51	0·40	0·32	0·25	0·32	0·30	0·33	0·36	0·32	0·53	0·49	0·30	0·29	0·38	0·39	0·40	0·36	0·35
Zr	153	136	94·4	87·6	109	106	103	92·9	111	155	135	109	98·7	112	120	122	89	107
Hf	3·90	3·28	2·43	2·21	2·66	2·63	2·63	2·33	2·77	3·82	3·33	2·72	2·50	2·83	2·96	2·96	2·27	2·70
Y	29·1	26·4	20·1	19·2	22·7	22·6	21·8	20·6	27·3	30·6	28·3	26·6	26·1	24·7	24·8	25·1	22·8	25·9
Cr														65·0	71·0	673		
Ni														112	113	198		
V														262	252	243		
La	12·1	10·5	5·83	4·97	7·82	7·95	7·40	6·75	7·82	12·5	10·1	8·28	7·70	8·55	9·55	9·71	6·64	7·66
Ce	30·0	26·0	15·1	13·0	19·3	19·2	17·7	15·9	19·2	29·6	24·1	20·4	19·1	20·0	22·2	22·5	16·2	18·9

Zarema section

Sample no.:	104	105	106	107	108	109	110	111	112	113	114	115	116	117	118	119	120	121
Rock type:	Basalt	Basalt	Basalt	Basalt	Basalt	Basalt	Basalt	Basalt	Basalt	Basalt	Basalt	Basalt	Basalt	Basalt	Basalt	Basalt	Basalt	Basalt
Altitude (m):	1690	1673	1650	1630	1630	1610	1590	1590	1560	1560	1520	1480	1400	1370	1350	1330	1300	1200
Pr	4·35	3·80	2·30	1·99	2·81	2·80	2·59	2·33	2·89	4·27	3·55	3·09	2·89	2·91	3·17	3·23	2·34	2·93
Nd	20·3	18·1	11·3	9·86	13·2	13·2	12·4	11·1	14·1	19·9	16·7	14·9	14·1	13·7	14·9	15·0	11·3	13·6
Sm	5·32	4·69	3·26	2·94	3·70	3·70	3·48	3·17	4·08	5·26	4·56	4·07	3·91	3·81	3·99	4·04	3·33	4·00
Eu	1·74	1·56	1·17	1·06	1·32	1·30	1·22	1·14	1·43	1·75	1·53	1·41	1·35	1·32	1·37	1·37	1·21	1·41
Gd	5·82	5·12	3·69	3·57	4·09	4·08	3·96	3·67	4·66	5·81	5·20	4·67	4·57	4·50	4·56	4·64	3·90	4·57
Tb	0·92	0·81	0·62	0·57	0·68	0·68	0·66	0·62	0·78	0·93	0·84	0·77	0·76	0·73	0·73	0·74	0·64	0·72
Dy	5·53	4·80	3·77	3·47	4·08	4·11	3·95	3·71	4·75	5·57	5·08	4·73	4·64	4·47	4·43	4·50	3·90	4·38
Ho	1·11	0·96	0·76	0·71	0·82	0·82	0·80	0·75	0·97	1·13	1·04	0·97	0·96	0·90	0·90	0·91	0·79	0·90
Er	2·77	2·33	1·90	1·75	2·04	2·06	2·02	1·86	2·52	2·77	2·55	2·43	2·43	2·27	2·25	2·25	2·17	2·47
Yb	2·55	2·17	1·75	1·60	1·92	1·88	1·85	1·69	2·37	2·66	2·44	2·40	2·41	2·08	2·09	2·13	1·78	2·05
Lu	0·38	0·33	0·26	0·24	0·29	0·29	0·28	0·25	0·36	0·40	0·36	0·36	0·36	0·31	0·32	0·32	0·26	0·31

Lima Limo section

Sample no.:	123	125	126	127	128	129	130	131	132	134	136	137	138	180	139	LL2	234	141	141a	141b	142	143	182
Rock type:	Basalt	Basalt	Basalt	Basalt	Basalt	Basalt	Basalt	Basalt	Basalt	Basalt	Basalt	Basalt	Basalt	Rhyolite	Trachy-andesite	Trachy-andesite	Trachy-andesite	Trachy-basalt	Trachy-basalt	Trachy-basalt	Trachy-basalt	Trachy-basalt	Trachyte
Altitude (m):	1730	1730	1800	1810	1830	1830	1840	1870	1880	1960	2010	2090	2090	2175	2200	2205	2245	2310	2310	2310	2310	2330	2335
wt %																							
SiO_2	49·1	49·8	49·7	50·1	49·8	50·6	50·9	50·2	51·0	47·0	48·4	51·2	46·4	75·4	61·1	57·7	63·8	49·2	50·4	50·0	50·3	49·5	67·2
TiO_2	1·82	1·87	1·90	1·88	1·93	2·03	2·35	2·13	2·18	2·24	1·45	2·36	1·89	0·27	1·33	1·33	1·21	2·63	2·84	2·66	1·91	1·74	0·73
Al_2O_3	15·4	15·1	15·3	15·9	15·9	14·6	13·6	14·0	13·9	17·1	20·1	13·6	15·5	11·4	15·6	14·8	14·5	14·2	15·0	14·3	18·5	15·9	13·5
Fe_2O_3	12·0	12·3	12·4	12·2	11·5	12·7	14·2	13·5	13·7	12·9	9·7	14·7	13·1	2·68	7·80	7·81	7·01	13·2	12·3	13·3	10·2	11·7	5·28
MnO	0·17	0·17	0·17	0·17	0·06	0·19	0·21	0·2	0·2	0·16	0·1	0·22	0·18		0·17	0·16	0·06	0·17	0·17	0·14	0·12	0·16	0·24
MgO	6·10	6·16	5·47	5·14	4·45	5·73	4·7	5·01	5·04	3·5	3·44	5·07	6		1·74	1·91	0·38	2·75	2·14	2·50	2·52	5·14	0·39
CaO	10·9	10·7	10·1	9·84	7·02	10·4	8·82	9·47	9·39	9·65	10·85	8·87	10·43	0·61	4·31	4·72	2·14	7·04	6·80	6·96	7·79	10·16	0·88
Na_2O	2·63	2·63	2·60	2·99	2·66	2·84	3·24	2·96	2·98	3·1	2·94	2·91	2·4	3·34	3·44	3·13	3·31	3·21	2·95	3·15	3·86	2·87	3·20
K_2O	0·28	0·33	0·53	0·52	0·4	0·27	0·52	0·46	0·51	0·57	0·27	0·8	0·18	5·08	4·07	3·36	5·21	2·07	1·74	2·11	1·53	0·44	5·30
P_2O_5	0·24	0·23	0·22	0·22	0·21	0·21	0·3	0·28	0·28	0·28	0·16	0·26	0·21	0·06	0·41	0·45	0·50	0·71	0·81	0·76	0·48	0·21	0·23
Total	99·9	100	100	100·3	98·2	100	99·4	99·9	100	98·3	99·8	99·8	99·9	99·8	100	100	100	100	100	100	100	99·9	100
LOI	1·33	0·84	2·08	1·38	4·46	0·43	0·51	1·57	0·81	1·86	2·42	−0·11	3·56	0·94	3·10	4·63	1·86	4·86	4·97	4·20	2·77	2·08	2·99

Table 2a: continued

	Lima Limo section																						
Sample no.:	123	125	126	127	128	129	130	131	132	134	136	137	138	180	139	LL2	234	141	141a	141b	142	143	182
Rock type:	Basalt	Basalt	Basalt	Basalt	Basalt	Basalt	Basalt	Basalt	Basalt	Basalt	Basalt	Basalt	Basalt	Rhyolite	Trachy-andesite	Trachy-andesite	Trachy-andesite	Trachy-basalt	Trachy-basalt	Trachy-basalt	Trachy-basalt	Trachy-basalt	Trachyte
Altitude (m):	1730	1730	1800	1810	1830	1830	1840	1870	1880	1960	2010	2090	2090	2175	2200	2205	2245	2310	2310	2310	2310	2330	2335
ppm																							
Cs	0·11	0·06	0·08	0·14	0·09	0·36	0·32	0·35	0·48	0·03	0·08	0·35	0·04	0·21	0·64	0·43	0·46	0·62			0·39	0·23	
Rb	2·05	2·18	4·58	5·37	6·70	4·35	12·4	10·4	14·7	7·21	2·99	14·3	1·18	118	68·4	60·3	85·7	39·7			21·3	6·55	
Ba	235	245	277	273	218	145	344	317	295	346	129	298	145	33·3	847	808	1307	1239			769	242	
Sr	420	424	434	374	402	311	382	399	404	471	363	284	325	9·17	510	511	337	759			950	356	
Th	0·80	0·91	1·40	1·82	1·43	0·87	1·57	1·27	1·28	1·35	0·86	2·04	0·58	4·59	1·81	1·93	2·18	1·17			0·83	0·91	
U	0·23	0·24	0·33	0·51	0·48	0·27	0·57	0·45	0·47	0·38	0·30	0·77	0·17	1·15	0·68	0·71	0·67	0·43			0·32	0·24	
Pb	2·81	2·81	3·14	3·94	3·46	1·75	4·49	6·00	3·79	4·00	1·94	4·33	2·38	30·4	16·8	12·7	13·1	9·80			6·58	2·38	
Nb	6·97	7·13	7·34	7·18	7·11	7·76	7·78	9·33	9·84	9·45	4·86	8·42	5·80	37·5	24·6	19·6	22·2	18·7			12·1	6·63	
Ta	0·46	0·45	0·43	0·47	0·46	0·50	0·44	0·55	0·55	0·57	0·28	0·56	0·37	2·81	1·22	1·20	1·42	1·05			0·69	0·40	
Zr	137	143	164	153	165	148	217	198	206	216	109	199	138	933	550	647	672	337			225	135	
Hf	3·68	3·62	3·91	4·03	4·14	3·77	5·09	4·64	4·65	5·32	2·49	5·12	3·64	19·6	11·7	14·0	14·9	7·81			5·31	3·40	
Y	30·0	30·2	34·1	30·9	33·7	35·8	45·7	41·7	42·8	48·3	25·2	46·3	33·2	68·0	49·3	43·2	42·2	50·4			34·1	31·7	
Cr	207						49·0	71·0					97·0	16·6	55·0	10·2	12·3	37·0			24·0	169	
Ni	77·0						34·0	40·0					142	<L.D.	44·0	10·6	<L.D.	24·0			20·0	67·0	
V	318						403	376					325	<L.D.	96·0	98·8	44·0	248			192	303	
La	10·7	10·9	12·0	12·3	12·2	10·0	16·9	14·6	14·6	15·6	6·85	14·0	8·61	99·6	49·7	46·8	46·0	33·1			21·4	10·5	
Ce	27·7	27·2	29·5	30·0	30·0	25·5	41·7	35·6	35·9	38·0	17·2	34·4	22·8	223	114	105	102	79·8			52·1	25·4	
Pr	4·03	4·14	4·32	4·34	4·33	3·90	6·07	5·05	5·21	5·52	2·50	5·00	3·40	27·9	14·7	13·9	14·6	11·1			7·27	3·65	
Nd	18·3	18·9	19·8	20·0	20·0	17·6	28·0	23·8	24·2	25·5	12·0	23·2	16·1	106	58·2	56·8	59·2	47·4			32·0	17·1	
Sm	4·83	5·12	5·31	5·23	5·37	5·02	7·32	6·40	6·41	7·14	3·31	6·54	4·72	19·5	11·6	11·2	12·4	10·7			7·23	4·53	
Eu	1·67	1·71	1·77	1·74	1·83	1·76	2·38	1·93	2·05	2·35	1·32	2·07	1·69	2·64	3·02	2·93	4·26	3·20			2·35	1·53	
Gd	5·36	5·68	6·05	5·73	6·15	6·03	8·03	7·07	7·16	8·18	3·99	7·73	5·50	14·0	10·2	9·58	11·4	10·4			7·07	5·41	
Tb	0·89	0·90	0·99	0·94	1·02	1·07	1·29	1·11	1·16	1·32	0·67	1·30	0·95	2·25	1·49	1·32	1·49	1·51			1·04	0·91	
Dy	5·24	5·30	5·63	5·55	5·85	6·07	7·65	6·88	6·84	7·81	4·06	7·89	5·69	12·9	8·34	8·09	8·24	8·51			5·95	5·57	
Ho	1·05	1·07	1·16	1·14	1·18	1·25	1·55	1·41	1·37	1·62	0·82	1·64	1·16	2·40	1·66	1·50	1·53	1·69			1·16	1·12	
Er	2·80	2·85	3·09	3·11	3·26	3·37	4·27	3·82	3·79	4·45	2·26	4·50	3·11	6·7395	4·59	4·21	4·32	4·55			3·08	2·80	
Yb	2·37	2·46	2·62	2·60	2·70	2·76	3·75	3·27	3·22	3·74	1·87	3·85	2·61	6·60	4·19	4·29	3·79	3·95			2·65	2·63	
Lu	0·35	0·35	0·38	0·39	0·39	0·41	0·55	0·47	0·46	0·56	0·28	0·56	0·38	0·9742	0·66	0·69	0·57	0·60			0·39	0·40	

	Lima Limo section																						
Sample no.:	144	145	146	147	148	235	151	152	153	154	155	156	157	158	159	160	161	164	165	167	168	169	170
Rock type:	Basalt	Basalt	Basalt	Basalt	Basalt	Trachyte	Basalt	Basalt	Basalt	Basalt	Basalt	Basalt	Basalt	Basalt	Basalt	Basalt	Basalt	Basalt	Basalt	Trachy-basalt	Trachy-basalt	Basalt	Basalt
Altitude (m)	2345	2350	2355	2360	2370	2390	2450	2470	2480	2490	2495	2500	2530	2540	2560	2570	2580	2610	2630	2690	2690	2820	2870
wt %																							
SiO_2	50·6	48·0	49·2	49·8	49·9	65·1	45·9	50·9	51·8	48·8	48·9	49·1	48·2	49·1	48·1	46·2	48·5	48·9	48·6	46·0	49·9	48·1	48·4
TiO_2	2·1	1·96	1·86	1·68	1·63	0·42	2·81	1·68	1·69	1·92	1·72	1·88	1·90	1·94	1·63	1·89	1·91	1·43	2·4	2·92	2·40	2·78	2·72
Al_2O_3	15·2	15·0	13·9	16·1	16·5	13·0	16·7	15·5	15·6	15·4	15·6	15·2	14·8	15·7	16·1	15·5	15·8	17·2	14·8	18·6	19·1	19·0	19·4
Fe_2O_3	12·1	12·3	12·6	11·3	11·2	6·40	14·8	10·6	10·5	11·8	11·3	11·1	12·0	12·3	10·6	10·9	10·5	10·0	13·3	12·1	10·0	10·9	11·0
MnO	0·14	0·15	0·14	0·13	0·13	0·19	0·16	0·14	0·17	0·16	0·21	0·17	0·14	0·18	0·12	0·15	0·14	0·13	0·15	0·13	0·13	0·10	0·13
MgO	4·96	4·50	3·38	5·19	5·35	0·16	5·33	5·21	5·42	5·76	6·39	4·92	6·17	5·79	5·57	3·70	4·68	6·14	5·19	2·47	2·53	2·86	2·66
CaO	9·07	9·77	7·08	9·35	9·37	1·76	6·96	9·85	9·52	10·9	11·3	10·6	11·0	10·3	10·8	10·7	10·1	11·0	10·26	7·65	7·83	7·69	7·74
Na_2O	2·95	2·82	2·13	2·99	3·01	3·63	3·44	2·82	2·88	2·62	2·44	2·53	2·40	2·81	2·59	2·69	2·85	2·66	2·94	3·89	4·20	4·00	4·17
K_2O	0·64	0·50	1·93	0·58	0·55	4·94	0·98	0·54	0·64	0·23	0·26	0·40	0·21	0·31	0·24	0·42	0·48	0·21	0·39	1·22	1·32	1·22	1·22
P_2O_5	0·26	0·25	0·23	0·23	0·23	0·09	0·40	0·20	0·19	0·21	0·19	0·20	0·19	0·23	0·19	0·22	0·24	0·19	0·25	0·46	0·58	0·47	0·46
Total	100	99·9	99·9	99·9	99·9	99·9	100	100	99·9	99·9	99·9	103	99·9	99·9	99·9	99·9	99·9	99·9	100	100	100	100	100
LOI	2·18	4·69	7·50	2·62	2·11	4·25	2·59	2·63	1·54	2·18	1·52	6·64	2·78	1·32	3·94	7·43	4·65	2·04	2·05	4·78	2·09	2·94	2·10
ppm																							
Cs	0·24	0·19	0·21	0·23	0·22	1·00	0·27	0·30	0·41	0·16	0·22	0·17	0·17	0·10	0·11	0·22	0·19	0·07	0·18	0·09	0·60	0·36	0·21
Rb	10·1	8·40	41·9	6·76	6·29	122	13·6	13·2	15·2	3·43	5·46	7·11	5·34	3·27	3·74	8·48	8·34	1·59	4·93	13·9	17·9	15·2	15·3
Ba	335	296	272	322	313	56·0	454	214	242	120	97·5	140	91·1	169	151	275	304	131	217	519	593	535	537
Sr	364	382	281	390	394	14·1	659	332	326	323	321	317	304	340	349	483	472	366	410	827	894	873	880
Th	1·32	1·10	1·05	1·17	1·11	4·72	0·80	1·11	1·15	0·74	0·64	0·66	0·69	0·79	0·71	0·90	0·91	0·58	1·08	1·01	1·15	1·03	1·02
U	0·32	0·31	0·16	0·30	0·30	1·75	0·21	0·75	0·73	0·25	0·21	0·25	0·23	0·26	0·29	0·26	0·32	0·20	0·36	0·39	0·23	0·24	0·27
Pb	2·96	2·65	2·22	3·65	3·64	26·0	4·00	4·05	5·45	2·00	1·75	1·51	1·40	2·41	2·41	3·02	2·66	1·89	3·01	3·57	3·96	3·45	3·58
Nb	9·45	8·97	7·67	7·59	7·42	68·0	11·7	7·50	7·24	7·54	6·58	7·36	7·65	8·07	6·99	8·22	8·58	5·54	11·4	17·6	18·6	17·7	17·6
Ta	0·58	0·54	0·50	0·49	0·48	3·89	0·75	0·49	0·51	0·52	0·45	0·47	0·51	0·54	0·46	0·51	0·53	0·37	0·80	1·07	1·09	1·05	1·04
Zr	185	175	162	149	146	1302·8	219	133	132	126	110	122	126	135	119	157	160	107	191	258	283	261	258
Hf	4·50	4·30	4·09	3·97	3·82	25·9	5·49	3·38	3·57	3·46	3·04	3·08	3·21	3·64	3·20	3·77	3·89	2·89	5·29	5·93	6·43	5·95	5·90
Y	39·5	35·6	30·6	32·0	31·4	74·3	37·3	29·6	31·7	31·8	28·8	28·7	30·1	33·6	28·9	31·4	32·6	26·0	45·9	37·1	39·4	37·3	37·2
Cr		279	65·0	89·0	90·0	14·0	40·0	198	191	211	326	319	275	181	236	135	155	347	126	27·0		20·0	24·0
Ni		178	61·0	77·0	77·0	<L.D.	36·0	74·0	75·0	70·0	101	87·0	94·0	62·0	78·0	44·0	56·0	109	36·0	27·0		19·0	19·0
V		302	259	278	266	<L.D.	297	283	289	339	307	326	329	331	277	286	295	252	370	206		174	171
La	13·9	13·1	11·8	11·8	11·4	91·9	16·5	10·2	10·5	8·66	7·59	8·46	8·86	9·90	8·86	12·4	12·8	7·80	13·5	20·5	22·5	20·5	20·5
Ce	33·1	31·3	28·2	29·4	28·3	216	42·9	24·6	26·1	22·8	20·1	20·9	22·2	25·6	22·9	30·8	31·5	20·3	35·7	49·5	53·9	49·5	49·2

Table 2a: continued

	Lima Limo section																						
Sample no.:	144	145	146	147	148	235	151	152	153	154	155	156	157	158	159	160	161	164	165	167	168	169	170
Rock type:	Basalt	Basalt	Basalt	Basalt	Basalt	Trachyte	Basalt	Basalt	Basalt	Basalt	Basalt	Basalt	Basalt	Basalt	Basalt	Basalt	Basalt	Basalt	Basalt	Trachy-basalt	Trachy-basalt	Basalt	Basalt
Altitude (m)	2345	2350	2355	2360	2370	2390	2450	2470	2480	2490	2495	2500	2530	2540	2560	2570	2580	2610	2630	2690	2690	2820	2870
Pr	4·75	4·48	4·07	4·14	3·96	26·8	6·27	3·54	3·69	3·36	2·96	3·12	3·29	3·74	3·31	4·35	4·58	2·93	5·19	7·14	7·74	7·13	7·07
Nd	21·9	20·4	18·7	18·6	17·7	94·1	28·6	16·3	16·5	15·4	13·8	14·9	15·6	17·1	15·2	19·6	20·3	13·5	24·0	32·7	35·5	32·9	32·8
Sm	5·70	5·38	4·81	4·86	4·61	18·6	7·19	4·37	4·42	4·32	3·95	4·12	4·35	4·73	4·16	4·98	5·16	3·68	6·59	7·98	8·66	7·98	7·90
Eu	1·94	1·71	1·54	1·64	1·59	2·41	2·52	1·44	1·49	1·59	1·45	1·45	1·49	1·68	1·49	1·69	1·71	1·36	2·34	2·69	2·87	2·69	2·69
Gd	6·60	6·23	5·62	5·49	5·31	17·5	7·61	5·09	5·23	5·34	4·76	4·99	5·14	5·63	4·84	5·56	5·77	4·44	7·83	8·26	8·86	8·28	8·12
Tb	1·10	1·04	0·92	0·91	0·87	2·15	1·16	0·87	0·87	0·90	0·82	0·84	0·90	0·94	0·82	0·90	0·90	0·74	1·33	1·23	1·32	1·23	1·23
Dy	6·59	6·32	5·39	5·51	5·37	12·0	6·67	5·22	5·37	5·51	4·97	5·13	5·58	5·79	5·01	5·33	5·53	4·53	8·23	7·01	7·59	7·05	6·98
Ho	1·32	1·28	1·09	1·10	1·09	2·70	1·32	1·07	1·09	1·13	1·02	1·02	1·12	1·18	1·01	1·08	1·12	0·91	1·63	1·36	1·45	1·35	1·35
Er	3·70	3·18	2·66	2·96	2·87	8·31	3·46	2·65	2·91	2·96	2·68	2·55	2·74	3·10	2·69	2·96	2·99	2·40	4·28	3·30	3·47	3·26	3·23
Yb	3·13	2·97	2·36	2·53	2·50	7·70	2·85	2·49	2·49	2·47	2·22	2·28	2·48	2·63	2·27	2·38	2·51	2·04	3·73	2·87	3·17	2·93	2·98
Lu	0·45	0·45	0·35	0·37	0·37	1·40	0·43	0·37	0·37	0·37	0·33	0·33	0·37	0·40	0·33	0·35	0·36	0·30	0·54	0·44	0·48	0·44	0·45

	Simien main section					Aman Amba section																
Sample no.:	186	188	196	201	206	210	211	213	214	215	216	217	219	222	222	223	225	226	227	230	232	610
Rock type:	Trachy-basalt	Basalt	Basalt	Basalt	Basalt	Basalt	Basalt	Basalt	Basalt	Basalt	Basalt	Basalt	Basalt	Basalt	Basalt	Basalt	Basalt	Basalt	Basalt	Trachyte	Basalt	Basalt
Altitude (m):	4205	4100	3525	3630	3150	2610	2645	2690	2695	2735	2775	2860	2995	3100		3120	3135	3165	3205	3225	3265	3050
wt %																						
SiO_2	50·2	50·5	52·0	49·5	50·4	49·1	48·6	49·6	50·7	51·3	49·7	50·0	49·4	48·6	48·7	49·0	50·6	49·6	47·5	60·7	44·5	45·0
TiO_2	2·21	1·98	2·16	1·96	1·80	1·82	2·00	1·90	1·83	1·99	1·91	2·06	3·11	1·97	1·99	2·54	2·95	2·47	2·63	0·93	1·79	2·97
Al_2O_3	14·4	14·4	14·0	15·0	15·0	15·1	15·5	16·0	15·3	15·3	15·3	15·1	14·0	17·3	17·4	17·3	14·0	16·0	15·1	20·7	14·8	16·0
Fe_2O_3	13·4	13·2	13·3	13·0	12·0	11·9	12·1	11·4	11·7	11·4	11·5	12·3	13·6	11·3	11·3	11·3	14·1	12·5	14·0	2·48	11·8	13·3
MnO	0·19	0·18	0·18	0·18	0·16	0·16	0·16	0·16	0·18	0·17	0·17	0·19	0·20	0·15	0·16	0·14	0·17	0·17	0·16		0·19	0·18
MgO	5·7	5·79	4·64	5·81	6·06	6·21	5·13	4·96	5·38	5·05	5·44	5·13	4·84	4·84	4·82	3·57	4·40	4·82	5·57		10·9	6·49
CaO	10·2	10·5	8·3	10·7	10·6	11·4	10·5	10·4	10·3	9·93	10·6	9·95	10·1	10·2	10·3	9·32	8·20	9·39	8·90	1·28	10·5	8·6
Na_2O	2·75	2·65	3·13	2·65	2·63	2·53	2·8	2·98	2·76	2·91	2·60	2·94	3·03	3·00	3·01	3·37	3·25	3·15	3·08	5·56	2·44	3·15
K_2O	0·54	0·44	1·20	0·38	0·55	0·26	0·22	0·43	0·53	0·70	0·38	0·47	0·54	0·25	0·28	0·60	1·12	0·83	0·66	5·73	1·23	1·63

	Simien main section					Aman Amba section																
Sample no.:	186	188	196	201	206	210	211	213	214	215	216	217	219	222	222	223	225	226	227	230	232	610
Rock type:	Trachy-basalt	Basalt	Basalt	Basalt	Basalt	Basalt	Basalt	Basalt	Basalt	Basalt	Basalt	Basalt	Basalt	Basalt	Basalt	Basalt	Basalt	Basalt	Basalt	Trachyte	Basalt	Basalt
Altitude (m):	4205	4100	3525	3630	3150	2610	2645	2690	2695	2735	2775	2860	2995	3100		3120	3135	3165	3205	3225	3265	3050
P_2O_5	0·29	0·28	0·30	0·25	0·24	0·23	0·26	0·26	0·22	0·26	0·21	0·31	0·36	0·27	0·22	0·26	0·32	0·30	0·29	0·21	0·39	0·11
Total	100	99·9	99·9	99·9	99·9	99·9	99·9	99·9	99·9	99·9	99·8	100	99·9	99·9	100·2	99·9	99·9	99·9	100·1	100·1	100·5	99·6
LOI	0·44	0·00	0·8	0·5	0·51	1·28	2·58	1·75	1·06	0·9	2·05	1·55	0·73	2·03	2·08	2·46	0·85	0·65	2·27	2·53	1·86	2·04
ppm																						
Cs	0·14	<L.D.	0·14	<L.D.	0·17	0·06	0·03	0·09	0·18	0·31	0·14	0·21	0·14	0·04	0·05	0·14	0·12	0·18	0·17	0·1	0·41	0·54
Rb	8·85	8·48	19·0	6·7	10·8	3·99	1·37	5·82	11·8	15·0	7·41	8·84	10·9	2·77	2·89	8·00	17·41	12·32	9·99	72·7	32·8	28·5
Ba	148	134	516	128	178	122	188	237	213	258	140	288	244	177	185	324	380	307	234	2874	450	509
Sr	306	280	302	291	318	310	373	366	339	325	326	364	369	431	451	447	356	461	391	125	558	1081
Th	0·93	0·90	1·71	0·95	0·87	0·80	1·05	1·05	1·20	1·38	0·93	1·10	1·33	0·94	0·91	1·40	1·78	1·40	0·99	6·2	4·13	4·08
U	0·41	0·32	0·44	0·32	0·28	0·27	0·15	0·30	0·38	0·78	0·27	0·29	0·39	0·24	0·23	0·35	0·48	0·45	0·25	1·9	0·97	1·15
Pb	1·95	1·87	3·95	2·03	1·80	1·72	2·08	2·67	2·98	4·48	1·89	2·63	2·22	1·88	1·95	2·89	4·36	3·66	2·27	22·3	2·58	1·88
Nb	8·68	6·37	10·1	6·48	7·96	7·29	8·07	8·49	7·72	8·38	8·42	10·4	15·0	8·48	7·76	11·8	9·20	12·3	11·0	74·7	55·6	43·5
Ta	0·55	0·54	0·62	0·54	0·49	0·46	0·50	0·51	0·49	0·57	0·53	0·57	0·92	0·56						4·18		
Zr	161	121	198	122	136	123	150	152	137	145	139	196	226	135	132	202	219	203	167	1208	150·4	188
Hf	4·08	3·25	5·05	3·3	3·41	3·15	3·83	3·81	3·48	3·77	3·52	4·30	5·52	3·44						25·9		
Y	38·5	29·4	43·5	29·1	32·4	31·7	42·2	34·4	33·5	33·4	34·0	42·1	50·6	31·3	31·5	47·0	47·3	39·7	39·2	76·4	25·3	26·5
Cr	123	116	32·7	168	218	196				114		123	126	87·8								
Ni	49·9	55·1	32·9	62·7	58·6	67·2				46·8		38·5	39·3	75·5								
V	350	331	324	333	298	310				319		313	409	276								
La	10·7	8·81	15·2	9·31	9·57	8·43	13·9	11·3	10·4	10·8	9·96	13·8	16·0	10·6	10·8	16·6	17·9	16·6	12·5	75·3	29·4	36·3
Ce	27·3	23·0	36·5	25·1	24·3	21·9	28·1	27·8	25·7	26·3	24·6	34·0	40·3	25·5	26·9	38·9	44·3	40·4	30·7	142	56·8	72·5
Pr	4·04	3·37	5·24	3·54	3·56	3·24	4·55	4·04	3·71	3·79	3·64	4·96	5·87	3·75	3·88	5·79	6·48	5·86	4·51	23·3	6·86	8·76
Nd	18·8	15·3	23·7	16·6	16·4	15·2	20·9	18·6	16·9	17·4	16·9	22·5	27·4	17·5	17·6	25·7	29·1	25·9	20·6	92·7	26·9	34·6
Sm	5·22	4·18	6·20	4·53	4·60	4·33	5·66	5·01	4·64	4·75	4·70	5·95	7·51	4·77	4·83	6·87	7·81	6·77	5·79	20·5	5·58	7·12
Eu	1·80	1·70	2·01	1·73	1·64	1·53	1·90	1·74	1·63	1·64	1·66	2·02	2·43	1·69	1·72	2·31	2·50	2·21	1·98	6·5	1·72	2·35
Gd	6·28	5·31	7·23	5·56	5·33	5·14	6·77	5·86	5·53	5·68	5·56	6·88	8·67	5·56	5·61	8·09	8·76	7·60	6·79	18·4	5·39	6·47
Tb	1·08	0·84	1·22	0·90	0·91	0·89	1·13	0·97	0·94	0·94	0·94	1·11	1·44	0·92	0·93	1·32	1·46	1·23	1·14	2·9	0·78	0·93
Dy	6·53	5·49	7·21	5·41	5·42	5·31	6·79	5·84	5·68	5·72	5·65	6·58	8·51	5·43	5·47	7·67	8·44	7·00	6·75	16·4	4·55	5·01
Ho	1·32	1·12	1·48	1·05	1·11	1·07	1·43	1·19	1·16	1·17	1·15	1·33	1·71	1·08	1·10	1·52	1·70	1·40	1·36	3·1	0·90	0·96
Er	3·53	2·86	4·09	2·97	2·98	2·86	3·87	3·23	3·06	3·10	3·15	3·58	4·61	2·95	2·95	4·09	4·53	3·64	3·64	8·4	2·45	2·52
Yb	2·94	2·45	3·48	2·41	2·49	2·36	3·12	2·72	2·58	2·66	2·61	3·07	3·76	2·47	2·44	3·32	3·85	3·02	3·04	7·9	2·12	1·99
Lu	0·42	0·36	0·50	0·37	0·36	0·35	0·45	0·39	0·37	0·38	0·36	0·44	0·55	0·35	0·35	0·48	0·57	0·44	0·44	1·2	0·33	0·30

Table 2a: continued

	Choke shield													Guguftu shield											
Sample no.:	237	238	239	240	242	243	245	246	249	250	251	253	254	255	259	260	262	263	264	265	267	268	272	273	274
Rock type:	Basalt	Rhyolite	Trachyte	Trachy-andesite	Basalt	Trachy-andesite	Trachy-basalt	Basalt	Basalt	Basalt	Basalt	Basalt	Basalt	Basalt	Basalt	Basalt	Basalt	Basalt	Trachyte	Rhyolite	Basalt	Basalt	Basalt	Basalt	Dacite
Altitude (m):	2615	3870	3880	3875	3800	3795	3845	3880	3560	3470	2845	2760	2680	2585	3070	3250	3205	3410	3425	3405	3560	3545	3360	3070	3540
wt %																									
SiO_2	46·0	75·2	62·8	58·2	44·5	54·3	47·6	47·0	46·9	48·0	45·1		45·9	52·4	48·4	50·8	47·1	46·8	67·3	68·8	44·0	44·6	46·5		60·5
TiO_2	2·02	0·21	0·44	1·10	1·61	0·86	2·31	2·29	2·84	2·24	1·45		2·29	2·37	1·56	1·72	1·89	2·32	0·50	0·31	2·74	1·79	1·85		0·09
Al_2O_3	19·3	13·1	14·3	15·4	21·0	13·7	16·5	17·3	14·7	16·1	17·7		15·6	15·2	15·3	17·8	17·4	17·8	18·0	16·3	15·0	12·9	15·9		12·8
Fe_2O_3	12·1	1·89	6·69	9·25	10·4	8·81	13·5	13·8	15·5	14·0	11·4		14·7	11·6	11·3	10·1	11·3	12·4	1·10	2·67	13·4	11·7	12·9		1·05
MnO	0·16	<L.D.	0·21	0·22	0·10	0·21	0·25	0·18	0·24	0·23	0·17		0·23	0·21	0·19	0·24	0·21	0·21	<L.D.	<L.D.	0·20	0·18	0·19		<L.D.
MgO	3·82	<L.D.	0·23	1·09	3·85	1·45	3·47	5·53	4·42	4·04	7·25		5·25	3·98	6·52	3·16	4·79	4·53	<L.D.	<L.D.	7·74	11·2	5·71		1·42
CaO	10·9	<L.D.	1·78	3·33	13·1	4·69	8·07	8·84	9·16	8·78	12·2		10·6	7·96	8·89	7·37	9·64	9·05	0·15	0·13	11·41	13·2	11·1		9·40
Na_2O	2·76	2·17	4·67	5·68	2·22	2·69	4·39	3·44	3·50	3·59	2·02		2·99	3·61	3·52	5·28	4·04	4·42	6·40	5·30	2·27	1·37	2·93		4·17
K_2O	0·81	5·13	4·62	3·09	0·42	3·20	1·28	0·87	1·30	1·34	0·58		1·00	1·31	1·15	2·06	1·47	1·33	5·80	4·84	1·22	0·77	0·84		1·85
P_2O_5	0·30	0·06	0·10	0·33	0·26	0·21	0·57	0·34	0·44	0·42	0·26		0·35	0·38	0·58	0·54	0·61	0·78	0·08	0·05	0·49	0·37	0·34		0·10
Total	99·9	99·8	100·0	100·1	99·9	99·9	99·9	99·9	99·9	99·9	99·9		99·7	99·9	100	100	99·9	100	100	99·8	99·5	100	99·9		99·9
LOI	1·62	2·01	4·12	2·43	2·48	9·75	2·03	0·34	0·91	1·19	1·80		0·79	0·92	3·07	1·46	1·45	0·41	1·11	1·39	1·01	2·37	1·58		8·56
ppm																									
Cs	0·07	3·86	1·24	1·02	0·30	1·06	0·88	<L.D.	0·13	0·25	0·09	0·07	<L.D.	0·57	0·77	1·05	0·57	0·39	0·23	0·70	0·18	0·16	0·42	1·20	0·04
Rb	17·7	186	126	74·2	9·34	97·0	31·1	19·8	26·1	43·4	15·4	11·4	25·1	39·6	18·4	56·9	37·8	36·2	178	177	26·4	25·9	19·6	52·0	22·5
Ba	243	61·8	929	826	175	909	420	293	410	457	182	191	266	366	493	882	577	588	82·0	136	305	211	247	255	1455
Sr	600	5·14	64·3	310	510	213	489	429	367	455	410	370	394	394	582	813	583	997	15·6	5·37	894	864	470	224	298
Th	1·19	17·7	12·0	6·65	1·14	7·87	3·27	1·78	3·05	5·02	1·71	1·64	2·65	4·87	1·81	5·45	3·66	5·34	22·0	22·4	3·07	2·43	2·55	1·75	2·16
U	0·31	2·96	2·65	1·69	0·28	1·91	0·78	0·43	0·34	1·22	0·39	0·38	0·58	1·02	0·36	1·31	0·98	1·16	3·76	1·48	0·72	0·55	0·53	0·28	0·21
Pb	2·13	17·3	12·5	10·6	1·62	11·9	3·92	3·38	3·67	4·41	1·48	1·38	2·38	6·57	4·38	5·09	3·55	2·82	24·0	27·7	2·72	2·24	3·39	3·69	12·8
Nb	15·2	142	119	42·5	16·0	68·2	43·2	18·1	37·0	54·2	20·1	20·4	28·1	30·2	23·6	74·8	43·4	69·0	141	120	40·4	29·9	27·6	24·0	2·14
Ta	0·92	8·26	6·73	3·41	0·96	3·40	2·49	1·45	2·25	3·08	1·21	1·24	2·13	2·33	1·24	4·15	3·07	3·73	8·44	6·93	2·38	1·71	1·55	1·23	0·15

	Choke shield													Guguftu shield											
Sample no.:	237	238	239	240	242	243	245	246	249	250	251	253	254	255	259	260	262	263	264	265	267	268	272	273	274
Rock type:	Basalt	Rhyolite	Trachyte	Trachy-andesite	Basalt	Trachy-andesite	Trachy-basalt	Basalt	Basalt	Basalt	Basalt	Basalt	Basalt	Basalt	Basalt	Basalt	Basalt	Basalt	Trachyte	Rhyolite	Basalt	Basalt	Basalt	Basalt	Dacite
Altitude (m):	2615	3870	3880	3875	3800	3795	3845	3880	3560	3470	2845	2760	2680	2585	3070	3250	3205	3410	3425	3405	3560	3545	3360	3070	3540
Zr	109	934	801	320	109	556	283	167	223	283	117	110	163	261	160	269	171	202	830	615	173	126	137	153	86·1
Hf	2·74	23·3	18·0	8·38	2·61	11·4	6·28	4·06	5·56	6·59	3·03	2·84	4·08	6·82	3·61	5·83	3·81	4·37	19·7	15·1	4·25	3·01	3·34	3·50	2·20
Y	24·5	116	91·4	46·9	22·4	72·1	50·9	29·2	43·9	52·4	23·4	23·8	31·4	37·5	28·2	43·5	29·4	33·4	66·9	50·3	27·9	21·5	25·5	24·5	3·91
Cr	21·2			13·9	25·1	<L.D.		15·5		<L.D.			5·30	13·0		56·2	92·3			<L.D.	147	445	30·5		<L.D.
Ni	8·87			<L.D.	23·5	<L.D.		28·1		6·31			12·3	19·0		19·2	37·4			<L.D.	63·0	180	38·3		16·7
V	324			2·45	302	<L.D.		281		240			342	267		87·2	193			<L.D.	314	305	302		26·6
La	12·4	101	78·7	44·1	10·4	60·5	28·2	16·6	27·6	38·2	14·6	14·3	21·6	30·4	22·0	48·9	33·9	46·5	109	117	29·2	21·1	19·2	21·0	4·06
Ce	26·9	182	155	92·7	22·7	127	61·2	36·9	58·9	81·0	31·5	30·8	45·7	67·5	46·5	102	67·8	92·3	204	211	63·5	43·7	40·2	45·8	5·67
Pr	3·68	21·2	18·4	11·5	3·04	15·6	8·08	4·79	7·62	10·0	4·02	3·94	5·85	8·85	5·99	12·4	8·34	11·1	22·8	24·3	8·18	5·47	5·11	5·86	0·68
Nd	16·3	75·3	69·0	45·8	13·3	60·4	34·7	21·8	32·1	40·9	16·8	16·7	24·7	36·6	24·8	48·5	32·1	43·2	77·7	81·5	33·7	22·0	21·4	24·4	2·63
Sm	3·91	13·9	14·4	10·0	3·39	12·7	8·36	5·16	7·46	9·13	3·95	3·95	5·76	8·16	5·39	9·52	7·12	8·32	13·7	14·2	7·08	4·75	4·90	5·18	0·59
Eu	1·50	0·80	3·20	3·41	1·29	3·82	2·81	1·84	2·48	2·94	1·40	1·38	2·03	2·43	1·81	3·45	2·44	2·78	1·79	1·15	2·20	1·50	1·61	1·78	1·29
Gd	4·50	14·7	14·5	9·59	3·78	12·9	8·89	5·96	8·26	9·63	4·32	4·28	6·11	7·67	5·62	9·59	6·12	8·39	12·5	12·7	6·73	4·64	5·07	5·19	1·57
Tb	0·69	2·72	2·41	1·33	0·62	1·92	1·43	0·85	1·27	1·48	0·67	0·67	0·90	1·17	0·82	1·32	0·89	1·09	1·87	1·85	0·95	0·69	0·78	0·76	0·10
Dy	4·20	17·7	14·6	8·26	3·70	11·2	8·35	5·11	7·58	8·65	4·02	4·04	5·17	6·78	4·67	7·41	5·32	5·85	10·7	9·89	5·12	3·81	4·44	4·21	0·58
Ho	0·85	3·91	3·11	1·71	0·77	2·34	1·70	1·03	1·57	1·79	0·82	0·83	1·04	1·30	0·95	1·50	1·05	1·17	2·17	1·90	0·99	0·75	0·89	0·85	0·13
Er	2·35	11·9	9·27	4·74	2·10	6·68	4·79	2·69	4·37	5·01	2·30	2·31	3·03	3·69	2·63	4·10	2·77	3·16	6·39	5·38	2·61	2·01	2·43	2·35	0·37
Yb	2·09	11·3	9·11	4·71	1·89	6·39	4·18	2·81	3·82	4·42	1·98	1·96	2·96	3·29	2·34	3·68	2·69	2·59	6·32	5·52	2·12	1·68	2·01	2·09	0·39
Lu	0·30	1·61	1·34	0·79	0·28	0·94	0·62	0·44	0·59	0·66	0·30	0·30	0·44	0·55	0·35	0·55	0·39	0·40	0·95	0·86	0·32	0·25	0·31	0·31	0·06

L.D., limit of detection. 141, 141a and 141b are different samples from the same flow. The prefix 'ETH' has been excluded from the sample names.

Table 2b: Trace element data for standards

Sample no.:	BHVO-1 Average of 27 analyses	BHVO-1 Eggins (1997)	BR Average of 8 analyses	BR Eggins (1997)	RGM-1 Average of 8 analyses	RGM-1 Eggins (1997)	BHVO-1 Calibration values
ppm							
Cs	0·10	0·10	0·81	1	9·9	9·60	0·10
Rb	9·13	9·50	51·4	47	145	149	9·20
Ba	132	133	1006	1050	824	807	132·9
Sr	395	390	1294	1320	102	108	399
Th	1·25	1·26	9·95	10·87	14·9	15·1	1·25
U	0·41	0·42	2·23	2·46	5·38	5·80	0·41
Pb	2·06	2·10	4·65	4·77	28·4	24·0	2·06
Nb	19·4	19·5	112	98	9·41	8·90	19·7
Ta	1·20	1·20	5·37	5·79	0·95	0·95	1·21
Zr	182	180	290	250	240	219	184
Hf	4·47	4·30	5·85	5·62	6·11	6·20	4·49
Y	27·8	28·0	31·3	30	24·3	25·0	28·0
La	15·5	15·5	77·3	82	22·8	27·0	15·5
Ce	37·7	38·0	145	151	45·1	47·0	38·0
Pr	5·42	5·45	16·7	17·36	5·27	5·30	5·45
Nd	24·6	24·7	63·6	65	19·0	19·0	24·7
Sm	6·17	6·17	11·8	12	3·96	4·30	6·17
Eu	2·05	2·06	3·5	3·7	0·55	0·66	2·06
Gd	6·17	6·22	10·0	9·5	3·76	3·70	6·22
Tb	0·95	0·95	1·28	1·25	0·60	0·66	0·95
Dy	5·27	5·25	6·22	6·20	3·61	4·08	5·25
Ho	1·00	1·00	1·08	1·087	0·77	0·95	1·00
Er	2·57	2·56	2·60	2·4	2·32	2·60	2·56
Yb	1·99	1·98	1·8	1·9	2·47	2·60	1·98
Lu	0·28	0·28	0·3	0·25	0·38	0·41	0·28

STRATIGRAPHY AND CONSTITUTION OF THE VOLCANIC SEQUENCES

Simien shield volcano and Lima Limo flood basalts

The lowermost sample of flood basalt was collected at an altitude of 1200 m near the town of Zarema, near the base of the sequence (Fig. 1). The upper contact, between flood basalts and the shield volcano, lies at an altitude of 2670 m on the Lima Limo road. This contact was defined by the appearance of highly porphyritic plagioclase-phyric lavas, the presence of a distinctive layer of mafic breccias, and by a change in chemical composition, as discussed below. The breccia layer is easily followed in cliff faces and river valleys along the northern escarpment of the plateau, and, in such exposures, the contact is seen to have a distinct dip, at about 3–4°, radially away from the summit of the Simien volcano (Fig. 3).

Except for the uppermost part of the sequence, where small differences in dip are observed, the flood basalts are flat lying. There is no evidence of deformation of the type that Merla *et al.* (1979) and Berhe *et al.* (1987) used in other parts of the plateau to distinguish between a lower deformed formation (Ashangi) and an upper undeformed formation (Aïba). Although a marked change in geomorphology—from subdued relief to steep cliffs—is observed midway through the sequence, this change does not correspond to any observable petrological or chemical characteristic of the flows (Violle, 1999). For these reasons, like Pik *et al.* (1998), we avoid the formation names Ashangi and Aïba, and will speak only of the upper and lower flood basalt formations (Figs 3 and 4).

We describe the basaltic flow units using the terminology of Jerram (2002). Classic-tabular facies, in which the flow units are about 20 m thick, alternate with

Table 3: Sr and Nd isotopic data

Sample	Rock type	Age (Ma)	$^{143}Nd/^{144}Nd$ measured	$^{143}Nd/^{144}Nd$ initial	$\varepsilon(Nd)_i$	$^{87}Sr/^{86}Sr$ measured	$^{87}Sr/^{86}Sr$ initial
Lima Limo flood basalts							
153	basalt	30	0·512914 ± 06	0·512882	5·5	0·704493 ± 06	0·704436
157	basalt	30	0·512983 ± 05	0·512950	6·8	0·703544 ± 05	0·703522
159	basalt	30	0·512924 ± 05	0·512892	5·7	0·703778 ± 06	0·703765
164	basalt	30	0·512940 ± 05	0·512907	6·0	0·703655 ± 06	0·703649
165	basalt	30	0·512932 ± 05	0·512899	5·9	0·703631 ± 05	0·703616
Simien trachybasalts							
167	trachybasalt	30	0·512925 ± 10	0·512896	5·8	0·703604 ± 06	0·703583
168	trachybasalt	30	0·512875 ± 06	0·512846	4·8	0·703641 ± 06	0·703616
169	trachybasalt	30				0·703599 ± 06	0·703577
Aman Amba section							
216	basalt	30	0·512963 ± 04	0·512930	6·5	0·703784 ± 04	0·703756
222	basalt	30	0·512913 ± 05	0·512880	5·5	0·703653 ± 06	0·703645
225	basalt	30	0·512902 ± 05	0·512870	5·3	0·704031 ± 04	0·703971
227	basalt	30	0·512931 ± 04	0·512898	5·8	0·703618 ± 04	0·703587
230	trachyte	30	0·512823 ± 05	0·512796	3·8	0·704703 ± 06	0·703988
Simien main series							
186*	basalt	30	0·512966 ± 04	0·512933	6·5	0·703675 ± 06	0·703639
186	basalt	30	0·512985 ± 05	0·512952	6·9	0·703574 ± 04	0·703538
196	basalt	30	0·512859 ± 05	0·512828	4·5	0·704200 ± 04	0·704123
206	basalt	30	0·512993 ± 05	0·512960	7·0	0·703793 ± 06	0·703751
Simien alkali basalts							
232	alkali basalt	18·7	0·512886 ± 04	0·512871	5·0		
233	alkali basalt	18·7	0·512912 ± 05	0·512897	5·5	0·70360 ± 04	0·70358
Xenoliths and megacrysts							
	Cpx peridotite	18·7	0·513586 ± 06	0·513555	18·3	0·702108 ± 06	0·70216
	Cpx megacryst	18·7	0·512929 ± 06	0·512914	5·8		
Choke shield							
238	rhyolite	23	0·512792 ± 05	0·512776	3·2	0·736979 ± 07	0·703587
239	trachyte	23	0·512850 ± 04	0·512832	4·3	0·705785 ± 06	0·703980
242	basalt	23	0·512972 ± 08	0·512949	6·6	0·703390 ± 04	0·703373
245	basalt	23	0·512936 ± 07	0·512914	5·9	0·703440 ± 06	0·703382
249	basalt	23	0·512874 ± 05	0·512853	4·8	0·703529 ± 06	0·703463
251	basalt	23	0·512875 ± 05	0·512854	4·8	0·703423 ± 04	0·703389
253	basalt	23	0·512866 ± 04	0·512845	4·6	0·703406 ± 04	0·703377
Guguftu shield							
260	basalt	23	0·512849 ± 04	0·512832	4·3	0·704064 ± 04	0·703999
263	basalt	23	0·512836 ± 05	0·512819	4·1	0·703884 ± 06	0·703851
264	trachyte	23	0·512702 ± 07	0·512687	1·5	0·730139 ± 07	
267	basalt	23	0·512838 ± 05	0·512819	4·1	0·703773 ± 06	0·703746
267*	basalt	23	0·512820 ± 04	0·512801	3·7	0·703832 ± 05	0·703805
272	basalt	23	0·512813 ± 04	0·512792	3·6	0·704431 ± 06	0·704393
270	cpx	23	0·512861 ± 04	0·512836	4·4		

Error on the sixth decimal place. The prefix 'ETH' has been excluded from the sample names.
*Not leached.

Table 4: Pb isotopic data

Sample no.	Rock type	$^{206}Pb/^{204}Pb$ measured	$^{206}Pb/^{204}Pb$ initial	$^{207}Pb/^{204}Pb$ measured	$^{207}Pb/^{204}Pb$ initial	$^{208}Pb/^{204}Pb$ measured	$^{208}Pb/^{204}Pb$ initial
Lima Limo flood basalts							
104	basalt	18·112	18·084	15·506	15·505	37·643	37·615
107	basalt	18·708	18·666	15·557	15·555	38·268	38·227
119	basalt	18·272	18·243	15·530	15·529	38·695	38·665
123	basalt	18·161	18·132	15·513	15·511	37·789	37·751
123	duplicate	18·133	18·104	15·510	15·509	37·792	37·754
146	basalt	18·193	18·172	15·514	15·513	37·895	37·85
153	basalt	18·562	18·523	15·540	15·538	37·614	37·594
159	basalt	18·220	18·185	15·507	15·505	37·775	37·747
164	basalt	18·358	18·327	15·524	15·522	37·844	37·814
165	basalt	18·304	18·269	15·512	15·510	37·915	37·881
Simien trachybasalts							
139	basalt	17·942	17·930	15·512	15·511	37·372	37·361
139b	basalt	17·932	17·920	15·508	15·507	37·365	37·355
141	trachybasalt	17·989	17·976	15·506	15·505	37·410	37·399
142	trachybasalt	17·989	17·975	15·506	15·505	37·431	37·419
142	duplicate	17·991	17·977	15·505	15·504	37·425	37·413
167	trachybasalt	18·024	17·993	15·497	15·496	37·540	37·513
168	trachybasalt	18·012	17·995	15·498	15·497	37·534	37·506
168*	duplicate	18·016	17·999	15·501	15·500	37·542	37·514
170	trachybasalt	18·014	17·992	15·497	15·496	37·540	37·513
Simien alkali basalts							
232	alkali basalt	18·993	18·986	15·584	15·583	38·721	38·716
232	duplicate	18·995	18·987	15·585	15·584	38·720	38·715
Choke shield							
242	basalt	19·593	19·553	15·683	15·681	39·504	39·450
245	trachybasalt	19·556	19·510	15·690	15·688	39·499	39·435
251	basalt	19·251	19·190	15·689	15·687	39·391	39·303
253	basalt	19·284	19·221	15·695	15·692	39·434	39·343
Guguftu shield							
263	trachybasalt	19·378	19·283	15·643	15·639	39·348	39·203
263	duplicate	19·380	19·284	15·644	15·641	39·352	39·213
272	basalt	19·068	19·032	15·654	15·653	39·330	39·273

The prefix 'ETH' has been excluded from the sample numbers.

compound-braided facies made up of many thin (~1–2 m) pahoehoe lobes in packages up to 30 m thick. Thin scoriaceous zones and lighter-coloured tuff-rich zones are found at the tops of the units, and soils are relatively common. Thicker columnar-jointed units, which may represent ponded flows, are present, although rare, in most regions. Sequences of thicker, cliff-forming flows can be traced for several kilometres along strike in parts of the escarpment to the north of Debark (Fig. 2).

A conspicuous ~100 m thick layer of felsic volcanic rocks, mainly rhyolitic tuffs and ignimbrites at an elevation of 2200 m (Figs 3 and 4), and two thinner felsic units higher in the sequence, have been described by Ayalew *et al.* (1999).

Flows within the Simien shield dip at 4–6° radially away from the summit. Except for a thin felsic unit on the western flank of the volcano, all rocks of the shield in the regions we studied have basaltic compositions. The lava flows are thinner and less continuous along strike than the flood basalts. Some are massive throughout, but most contain 1–3 m thick massive lobes distributed within thicker sequences of scoriaceous breccia.

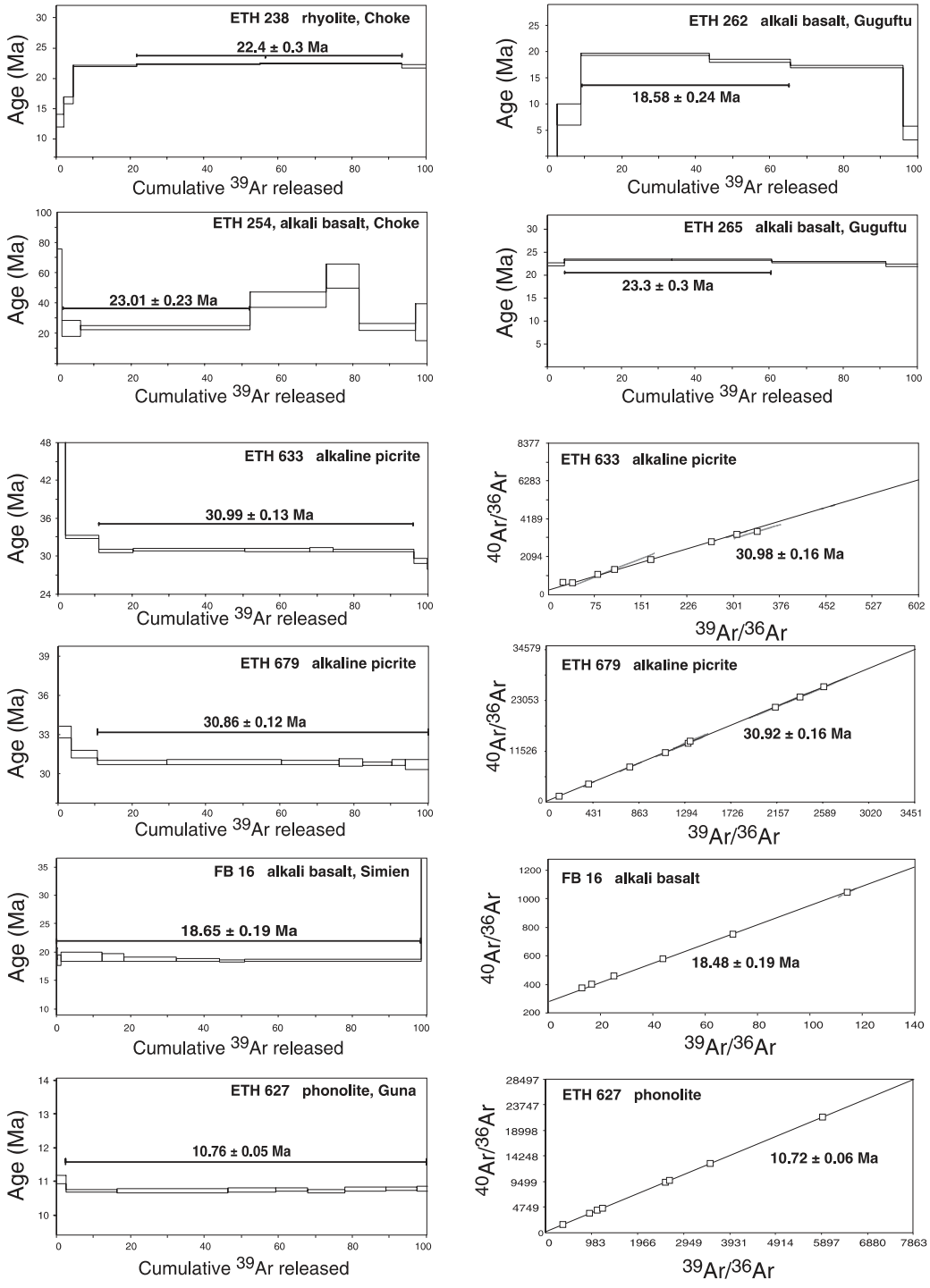

Fig. 6. Ar–Ar spectra and isochrons illustrating the ages of samples dated in this study.

The petrology of the flood basalts has been well described by Pik *et al.* (1998, 1999) and will not be repeated here. Within the shield, four petrological groups are distinguished using a combination of geographical location, petrology and geochemistry (Fig. 4).

Basalts of the Main Series of the Simien shield

The term 'Main Series' describes the rocks that constitute the bulk of the Simien volcano. They extend from the basal contact to the present summit and were sampled in sections east of Sankaber camp (Figs 2 and 3). They

consist of aphyric to sparsely plag ± cpx-phyric basalts (with rare highly phyric units) whose petrology and geochemistry differ little from those of the underlying flood basalts.

Highly porphyritic trachybasalts

These rocks are restricted to a small region on the western flank of the volcano above the Lima Limo section and around the town of Debark (Figs 3 and 4). They contain abundant, very large phenocrysts of plagioclase, less abundant and smaller phenocrysts of clinopyroxene, and little to no olivine. Two trachybasaltic units (samples 141–142) occur in the flood basalt sequence at an altitude of 2450 m, some 300 m below the basal contact of the shield volcano (Fig. 4). These units have distinctive volcanic structures (one is a highly vesicular volcanic breccia) that show that they are not younger sills intruding the flood basalts. Their presence within the flood basalt sequence indicates that trachybasaltic volcanism of the type that formed the western flank of the shield volcano started before the flood volcanism had ceased.

Felsic volcanic rocks

A thin (10 m) unit of felsic volcanic rocks (samples 228–230) is present on the western flank. Although this unit lies at an altitude of only 3250 m, about 1200 m below the eroded summit of the volcano, when the dips of the volcanic strata are taken into account, the felsic sequence is seen to be near the top of the stratigraphic sequence, as shown in Fig. 3. Two rock types are present: (1) friable, poorly exposed quartz-phyric rhyolitic crystal tuff; (2) massive irregular lobes of feldspar-phyric or aphyric trachyte that in places intrude the rhyolitic tuff.

Alkali basalt

Several flows of alkali basalt (samples 232 and 610) directly overlie the felsic volcanic rocks. The lowest flow is massive, in places columnar-jointed; the second is petrologically similar and distinguished, locally, by the presence of small lherzolite xenoliths and megacrysts of clinopyroxene and spinel. $^{39}Ar/^{40}Ar$ dating of an alkali basalt (FB16) gave an age of 18·65 ± 0·19 Ma (Table 1 and Fig. 6).

Choke and Guguftu shield volcanoes

Choke is one of three major shield volcanoes enclosed within a large meander of the Blue Nile (Figs 1 and 5). It is a broad flat symmetrical shield made up dominantly of lava flows that extend radially out from the central conduit with dips of less than 5°. Most of the volcano consists of massive basaltic flows that are morphologically similar to those of the Simien volcano (Fig. 7). Some are aphyric, others porphyritic with phenocrysts of plagioclase ± clinopyroxene ± olivine. Felsic rocks—trachytic and rhyolitic flows and fragmental units—are limited to the upper 300–400 m of the present volcano.

A rhyolite sample (ETH 238) from an altitude of 3870 m, about 200 m below the present summit, gave a plateau age of 22·4 ± 0·3 Ma and an isochron age of 23·0 ± 0·3 Ma (Table 1 and Fig. 6). A basalt sample (ETH 254) from 2680 m, near the base of the shield, yielded a plateau age of 23·01 ± 0·23 Ma and an isochron age of 19·6 ± 1·53 Ma. The age of the underlying flood volcanics is poorly known, being constrained only by ages of 29·4 ± 0·3 Ma to 26·9 ± 0·7 Ma reported by Hofmann *et al.* (1997) for basalts from the Blue Nile valley at a location about 80 km east of the volcano. If we accept the older age, the Choke volcano erupted some 4 Myr after the underlying flood volcanics.

Guguftu is located about 40 km south of the town of Desse (Fig. 5), close to the western margin of the Ethiopian rift and in a region of considerable deformation and erosion. For this reason the overall form of the volcano is not easily established. Most rocks are highly porphyritic basalts containing phenocrysts of olivine, clinopyroxene and plagioclase (Fig. 7). As in the Choke volcano, trachytic volcanic units form a minor component of the volcanic pile in the upper part of the sampled sequence. A lahar composed of all rock types in the region occurs in the middle of the sequence. A feature that distinguishes Guguftu from the other volcanoes is the presence of numerous mafic and felsic dykes oriented between 000° and 045°.

A feldspar-phyric rhyolite (ETH 265) from an altitude of 3405 m at the top of the shield sequence gave a plateau age of 23·3 ± 0·3 Ma and an isochron age of 23·8 ± 0·3 Ma (Table 1 and Fig. 6). ETH 262, a plag–cpx–ol-phyric basalt from a volcanic plug that intrudes basaltic flows in the lower part of the shield, yielded a 18·58 ± 0·24 Ma plateau age. Another plag–cpx–ol-phyric basalt (ETH 255), from an altitude of 2585 m and presumably in the upper part of the flood volcanic sequence, gave a plateau age of 19·1 ± 1 Ma; the last steps of the spectra, however, gave values between 23 and 30 Ma, because of excess Ar. The isochron age is 23·5 ± 1 Ma. This sample was collected 5 m from a felsic dyke and this intrusion may have perturbed the Ar–Ar system. The nearest previously dated samples in the flood basalts, from the Wegel Tena section about 50 km north from Guguftu, yield ages from 30·2 ± 0·1 Ma to 28·2 ± 0·1 Ma (Hofmann *et al.*, 1997). On the other hand, Ukstins *et al.* (2002) obtained ages around 25 Ma in the upper part of the basaltic sequence near Dessie, which suggests that this part of the volcanic plateau had a protracted volcanic history.

Other regions

The village of Alem Ketema is situated on the left bank of the Blue Nile, about 100 km north of Addis Ababa (Fig. 1).

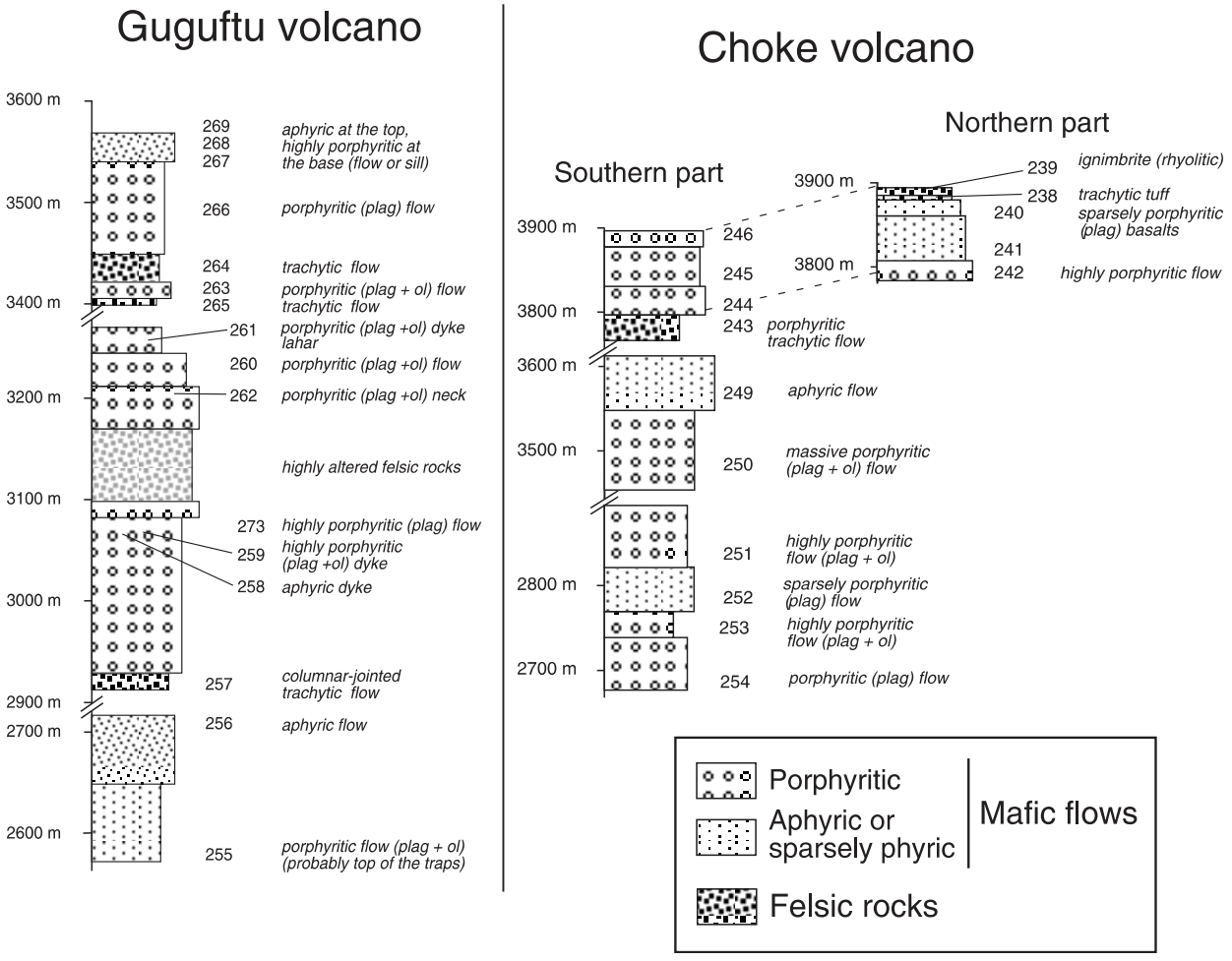

Fig. 7. Stratigraphic logs of sampled sections through Choke and Guguftu volcanoes.

In this region the flood basalts are far thinner than to the north, being limited to several 50–200 m thick sequences of relatively thin flows that alternate with felsic volcanics and clastic sedimentary rocks. The basalts are petrologically similar to flows of the Choke shield. Coulié (2001) and Coulié *et al.* (2003) obtained K–Ar ages between 20·7 and 23·5 Ma for felsic volcanics interlayered with these basalts.

The region between the towns of Sekota, Lalibela and Bora (Fig. 1) contains abundant picrites, ankaramites and alkali basalts with chemical characteristics that correspond to the HT2 magma type of Pik *et al.* (1998, 1999). Unlike the other regions, the rocks from this area are tilted, folded and cut by numerous normal faults; dips up to 40° are common. The thinner flows are massive with scoriaceous tops; thicker units (10–30 m) are internally differentiated with lower parts enriched in phenocrysts of olivine and clinopyroxene. We dated two samples of the HT2 rock type (Table 1 and Fig. 6). Sample ETH 679, from the gabbroic-textured upper part of a differentiated flow, gave a $^{40}Ar/^{39}Ar$ age of 30·86 ± 0·12 Ma. The second, ETH 633, a glassy olivine–clinopyroxene–phyric hyaloclastite that probably formed when a lava flow entered a shallow lake, gave an age of 30·99 ± 0·13 Ma.

PETROGRAPHY OF MAFIC ROCKS OF THE SHIELD VOLCANOES

In this study, emphasis has been placed on the mafic rocks of the shield volcanoes because the flood basalts have been well described in previous studies by Mohr & Zanettin (1988), Zanettin (1993) and Pik *et al.* (1998, 1999).

Simien shield and underlying flood basalts

There is little systematic variation in the characteristics of the dominant basaltic rocks from the base of the flood volcanic sequence to the summit of the shield volcano.

Instead, we see a seemingly random alternation of aphyric, sparsely phyric and highly phyric lavas (Figs 3 and 4). The phenocryst phases are plagioclase and clinopyroxene (ubiquitous) and olivine (present in most samples). Because we sampled the massive flow interiors, most of our samples are sparsely vesicular or non-vesicular.

Plagioclase-phyric basalts (>20% phenocrysts) occur at 1800–1900 m and 2000–2150 m. These rocks are petrologically similar to the porphyritic trachybasalts on the upper western flank of the Simien volcano, but they do not contain the remarkably high abundance of phenocrysts of the latter rocks, nor do they have their distinctive chemical compositions. Olivine-phyric basalts also occur throughout the stratigraphic sequence, particularly at the base and around 2500 m and 2700 m.

The trachybasalts contain abundant (up to 60%), very large (up to 3 cm long) phenocrysts of plagioclase and less abundant smaller phenocrysts of clinopyroxene. Olivine phenocrysts are present in some samples. The matrix consists of plagioclase, clinopyroxene, opaque minerals and olivine.

The alkali basalts of the uppermost series on the upper western flank of Simien are distinguished by the presence, within the volcanic groundmass, of small equant olivine grains. Samples from the second flow in this series, the unit that contains lherzolite xenoliths, are characterized by abundant olivine xenocrysts and megacrysts of clinopyroxene and spinel.

Choke and Guguftu shields

Almost all our samples from the Choke and Guguftu shields are plagioclase-phyric and contain olivine and clinopyroxene phenocrysts. They are distinguished from the basalts of the Simien shield by the presence of small grains of olivine in the matrix, and distinctly pink–brown clinopyroxene grains, features indicating that these basalts belong to the alkaline magma series.

Other regions

The flood basalts from the Alem Ketema region are alkali basalts with characteristics very like the flows of the Choke and Guguftu shields. The HT2 flows from the Sekota–Lalibela–Bora region are sparsely to highly phyric lavas characterized by abundant (up to 50%) rounded to euhedral phenocrysts of olivine and clinopyroxene. The groundmass consists mainly of clinopyroxene, abundant oxides and accessory biotite and apatite; plagioclase is rare or absent. The olivines are rich in forsterite ($Fo_{76–87}$) providing evidence of crystallization from relatively magnesian magmas.

Alteration

Samples from all three shields are variably altered. Olivine, plagioclase and glass in the matrix are partially or, in some samples, completely replaced by secondary minerals; phases such as chlorite, carbonate, zeolites and clay minerals fill vesicles and fractures.

GEOCHEMICAL DATA

Major and trace element compositions of mafic rocks from the Simien shield and underlying flood basaltic sequence

The general characteristics of the basaltic rocks are illustrated in the total alkalis–silica (TAS) diagram (Fig. 8). Flood basalts, and basalts of the Simien Main Series, have compositions that plot, with one or two exceptions, in the subalkaline field or slightly within the alkaline field. To simplify subsequent discussion they will be referred to as tholeiitic basalts. Almost all the other basalts—those from the western flank of the Simien volcano and almost all the rocks from the Choke and Guguftu shields—have lower SiO_2 contents and/or higher $Na_2O + K_2O$ contents and plot in the alkali field. The distinction extends to other incompatible major and trace elements: the trachybasalts and the alkali basalts of Simien volcano, for example, have moderately high TiO_2 and very high Nb, La and Th, compared with the flood basalts and the Simien Main Series (Figs 9 and 10).

In MgO variation diagrams (Fig. 9), the flood basalts and basalts of the Simien Main Series have a relatively restricted range of compositions. Accumulation of plagioclase explains part of the more evolved (low-MgO, high-Al_2O_3) compositions of the trachybasalts. It cannot explain, however, their high contents of TiO_2 and low contents of CaO, elements that are incompatible and compatible, respectively, in plagioclase. Instead, the data show that these rocks formed from relatively evolved, incompatible-element-enriched magmas. The alkali basalts are distinguished from the other lavas by relatively high MgO and low SiO_2 and very high contents of incompatible elements.

Mantle-normalized trace element patterns for the flood basalts and the Simien Main Series are very similar (Fig. 10). They have relatively flat light REE (LREE), moderately sloping heavy REE (HREE), and pronounced negative Th and Ti anomalies (Fig. 10c and d). In these incompatible-element-enriched rocks, Nb/La ratios are distinctly sub-chondritic; were it not for the pronounced Th depletion, the patterns would show large negative Nb anomalies. The trachybasalts from the western flank of the shield have higher contents of the more incompatible elements and steeper patterns (Fig. 10b). Their negative Th, Nb and Ti anomalies are even larger than in the flood basalts. In the alkali basalts (Fig. 10a), the trend to steeper REE patterns persists: concentrations of LREE are higher and concentrations of HREE are lower than in other basalts. Anomalies of Th and Nb are absent, but the negative Ti anomalies remain.

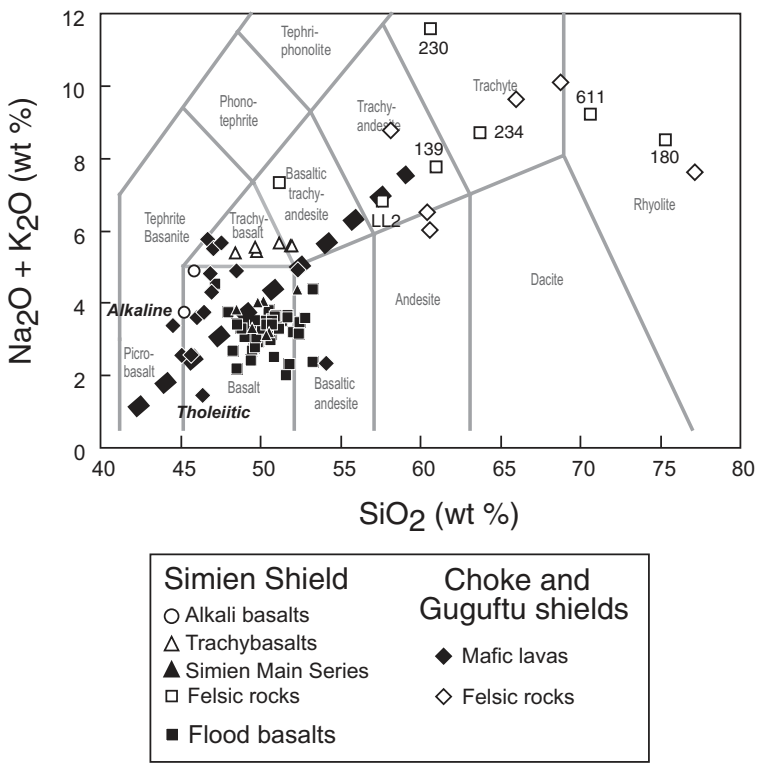

Fig. 8. Total alkalis–silica diagram comparing the geochemical characteristics in the shield volcanoes and the underlying flood basalts. The bold dashed line distinguishes tholeiitic from alkaline basalts (from MacDonald & Katsura, 1964).

Stratigraphic variations of chemical compositions within the flood basalts and Simien shield

The relatively constant composition of flood and shield basalts, from the base of the sequence to the top of the shield, is illustrated in Fig. 11. Silica contents range between 48 and 53% and show no up-sequence trends, apart for a poorly defined increase in the interval 1500–1800 m. A change in composition is more apparent for TiO_2, K_2O and Nd, which increase significantly in this interval, and for MgO, for which the concentration decreases.

The four samples of trachybasalts from the lower portion of the shield volcano in the Lima Limo section (in the interval 2700–3000 m), and also the two lava flows intercalated with the flood basalts (samples 141 and 142, between 2300 and 2400 m), are distinguished from the flood basalts by low MgO, high TiO_2, Al_2O_3, P_2O_5 and K_2O, and high Ba, Sr, Zr, La/Sm and Sm/Yb.

The two samples of alkali basalts are plotted at their current altitude of about 3200 m, well below the summit of the volcano and below the older basalts of the Simien Main Series. They lie in this position because they form part of a later veneer on the flanks of the volcano (Fig. 3). These rocks have moderate to high MgO contents (reflecting their high olivine contents) and low SiO_2 contents; levels of alkalis and incompatible trace elements are comparable with or higher than those of the other basalts.

Choke and Guguftu volcanoes

The petrological and geochemical characteristics of mafic lavas from the two younger shields are identical to those of the alkali basalt on the Simien shield. Samples from Choke volcano are petrologically more evolved and their compositions are influenced by the accumulation of plagioclase phenocrysts, but despite these differences, the geochemical features that characterize the alkali basalts remain. These features include high concentrations of incompatible elements, steeply sloping trace element patterns, and positive Nb anomalies (Figs 12 and 13). Also notable are low contents, relative to elements of similar compatibility, of Th and Ti (Fig. 13). Although our sampling was not sufficiently detailed to investigate stratigraphic variations in the compositions of the volcanoes, the 16–17 samples from each volcano reveal no systematic up-section variations.

Other regions

The flood basalts from Alem Ketema have alkaline compositions and are enriched in incompatible trace

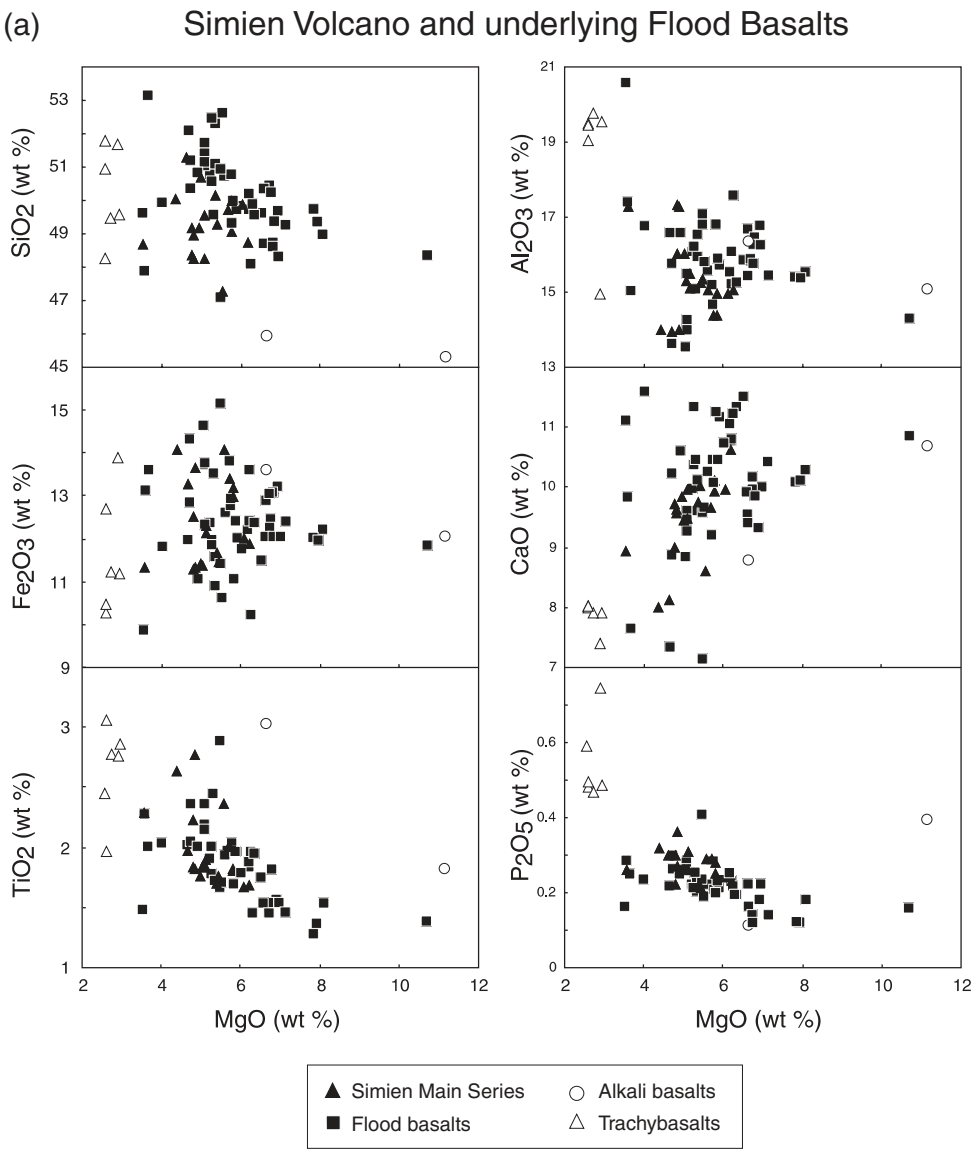

Fig. 9. Variation diagrams of (a) major elements vs MgO (wt %) and (b) trace elements vs Zr and $(La/sm)_N$ in the Simien volcano and underlying flood basalts.

elements, very like the alkali basalts of the Choke and Guguftu shields. The HT2 lavas from the Sekota–Lalibela–Bora region are very different (Figs 12 and 13). They contain moderate to high MgO and low SiO_2, in accord with their abundant olivine and clinopyroxene phenocrysts. Their Al_2O_3 contents are low and their TiO_2, P_2O_5 and incompatible trace element contents are very high. The HREE are strongly fractionated, and Nb anomalies are positive or absent.

ISOTOPIC COMPOSITIONS

Our new Nd and Sr isotopic data are illustrated in Fig. 14. The basaltic samples have a relatively limited range of compositions: $^{143}Nd/^{144}Nd = 0{\cdot}51279–0{\cdot}51296$, $\varepsilon_{Nd(T)} = +3{\cdot}6$ to $+7{\cdot}0$; $^{87}Sr/^{86}Sr = 0{\cdot}70337–0{\cdot}70439$. Flood basalts from the Lima Limo section have compositions similar to the trachybasalts and Main Series tholeiites from the Simien shield. Their $^{87}Sr/^{86}Sr$ ratios are slightly higher than samples from the Choke shield, but when Pik *et al.*'s (1999) data are included, there is almost complete overlap. Samples from the Guguftu shield are displaced to higher $^{87}Sr/^{86}Sr$ and lower $^{143}Nd/^{144}Nd$, and plot largely separately from samples from the Choke shield. However, once again, when the Pik *et al.* (1999) data are included, there is little to discriminate between flood and shield basalts. Most felsic samples have slightly lower $^{143}Nd/^{144}Nd$ than the basalts, but their $^{87}Sr/^{86}Sr$ ratios

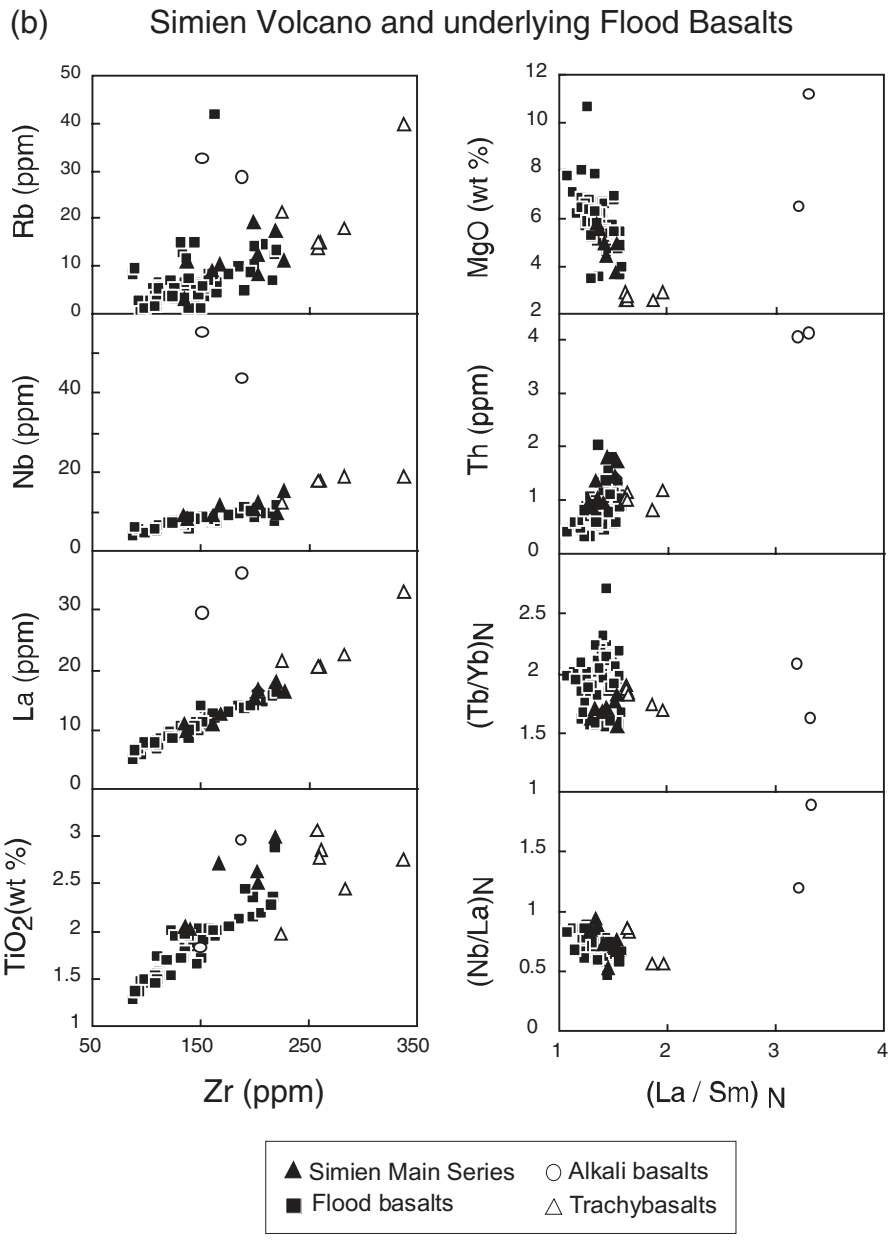

Fig. 9. Continued.

are similar. An exception is a trachyte sample from the Guguftu shield, which has slightly lower $^{143}Nd/^{144}Nd$ and higher $^{87}Sr/^{86}Sr$.

Lead isotopic compositions, in contrast, vary widely (Fig. 15). The Lima Limo flood basalts have relatively low $^{206}Pb/^{204}Pb$ ratios, from 18·1 to 18·7, and, with the exception of one sample, low $^{207}Pb/^{204}Pb$ and $^{208}Pb/^{204}Pb$. Trachybasalts from the Simien shield plot in a single group at still lower $^{206}Pb/^{204}Pb$. The shield basalts have more radiogenic compositions. The thin 18·7 Ma veneer of alkali basalt on the Simien shield has intermediate $^{206}Pb/^{204}Pb$ ratios, and samples from the 23 Ma shields have higher ratios. Choke basalts have a combination of high $^{206}Pb/^{204}Pb$, $^{207}Pb/^{204}Pb$ and $^{208}Pb/^{204}Pb$ and low $^{87}Sr/^{86}Sr$ that distinguishes them from all other samples from the Ethiopian volcanic province. Guguftu basalts have slightly lower Pb isotope ratios but higher $^{87}Sr/^{86}Sr$. Each volcano or volcanic sequence in the region has a distinct Pb–Sr isotopic composition.

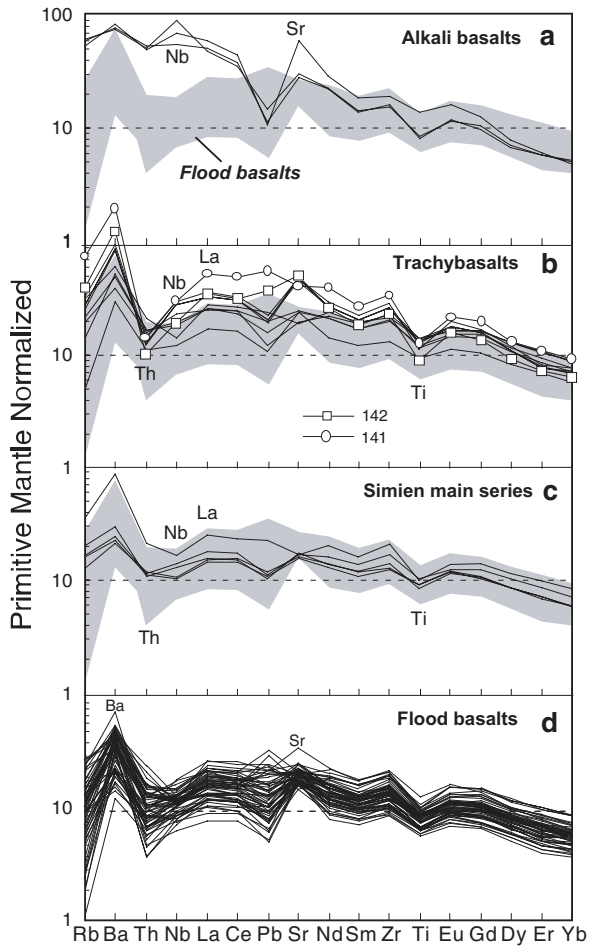

Fig. 10. Trace element concentrations, normalized to primitive mantle of Hofmann (1988), of samples from the Simien volcano and underlying flood basalts.

Lavas from the Ethiopian shield are characterized, therefore, by relatively constant Nd–Sr isotopic compositions but wide ranges in Pb isotope and in trace element concentrations and ratios. In the LT and HT2 lavas, for example, differences of almost an order of magnitude in the concentrations of elements such as Th or La, and major differences in Pb isotope ratios, are present in rocks with almost identical ranges of Nd and Sr isotope compositions.

DISCUSSION

Spatial and temporal distribution of magma types in the northern Ethiopian plateau

The information presented above reveals a complex evolution, in time and space, of volcanism in the northern Ethiopian plateau. The Simien shield appears unique in that it consists predominantly of incompatible-element-poor LT tholeiites, like the flood basalts in this part of the plateau. Although Pik *et al.* (1999) proposed that rocks of the LT series are restricted to the northwestern part of the region, our sampling, and the analyses reported by Zanettin *et al.* (1976), indicates a slightly wider distribution. Thin sequences of LT tholeiites are present to the north of the town of Sekota (Fig. 1), where our unpublished analyses show that the lowest 300 m of the volcanic sequence consists of LT tholeiites, and in the Nile Valley, where Zanettin *et al.* (1976) suggested the presence of LT tholeiites at the base of the sequence, immediately overlying the sedimentary rocks of the basement. Although the LT type of basalt erupted mainly in the northwestern part of the province, it is not entirely restricted to this region. Wherever the LT rocks have been dated, they give ages very close to 30 Ma.

Our analyses of the HT2 flood basalts from the Sekota–Lalibela–Bora region complement the data reported by Pik *et al.* (1998). These rocks, which have elevated concentrations of incompatible trace elements and strongly fractionated trace element patterns, appear to be restricted to a small region in the northeastern part of the plateau bounded approximately by the towns of Sekota, Bora and Desse. They are among the oldest volcanic rocks in the northeastern plateau, having erupted around 31 Ma.

Figures 12 and 13 show that, in terms of their trace element contents, the basalts from the Choke and Guguftu shields, the Alem Ketema flood basalts, and the late veneer of alkali basalt on the Simien shield all resemble Pik *et al.*'s (1998) HT1 type of flood basalt. These rocks share an alkaline magmatic character with relatively high concentrations of incompatible trace elements and moderately fractionated trace element patterns. As in the Simien shield, the magmatic character of the Choke and Guguftu shields matches that of the underlying flood basalts. The ages of HT1 rocks range from about 30 Ma in the north of the province to far younger in the south. The Choke and Guguftu shields and the Alem Ketema flood basalts are about 22 Myr old, and the late veneer of alkali basalt on the Simien shield is 18·7 Myr old.

In the central part of the plateau it is difficult to distinguish between flood and shield basalts: the Alem Ketema basalts, for example, had been mapped as flood basalts (Zanettin *et al.*, 1976), but they are better interpreted as peripheral parts of a 23 Ma shield. The general picture seems to involve protracted but sporadic eruption of alkali basalt, from 30 Ma to <10 Ma, with migration of the centre of eruption from north to south.

The silica-undersaturated rock types (basanites, nephelinites and phonolites) in some of the younger shield volcanoes are still younger (25 to <5 Ma; Zanettin & Justin Visentin, 1974; Zanettin *et al.*, 1976). Mt Guna, which erupted between the Choke and Simien shields, has an Ar–Ar age of 10·7 Ma (Table 1 and Fig. 6).

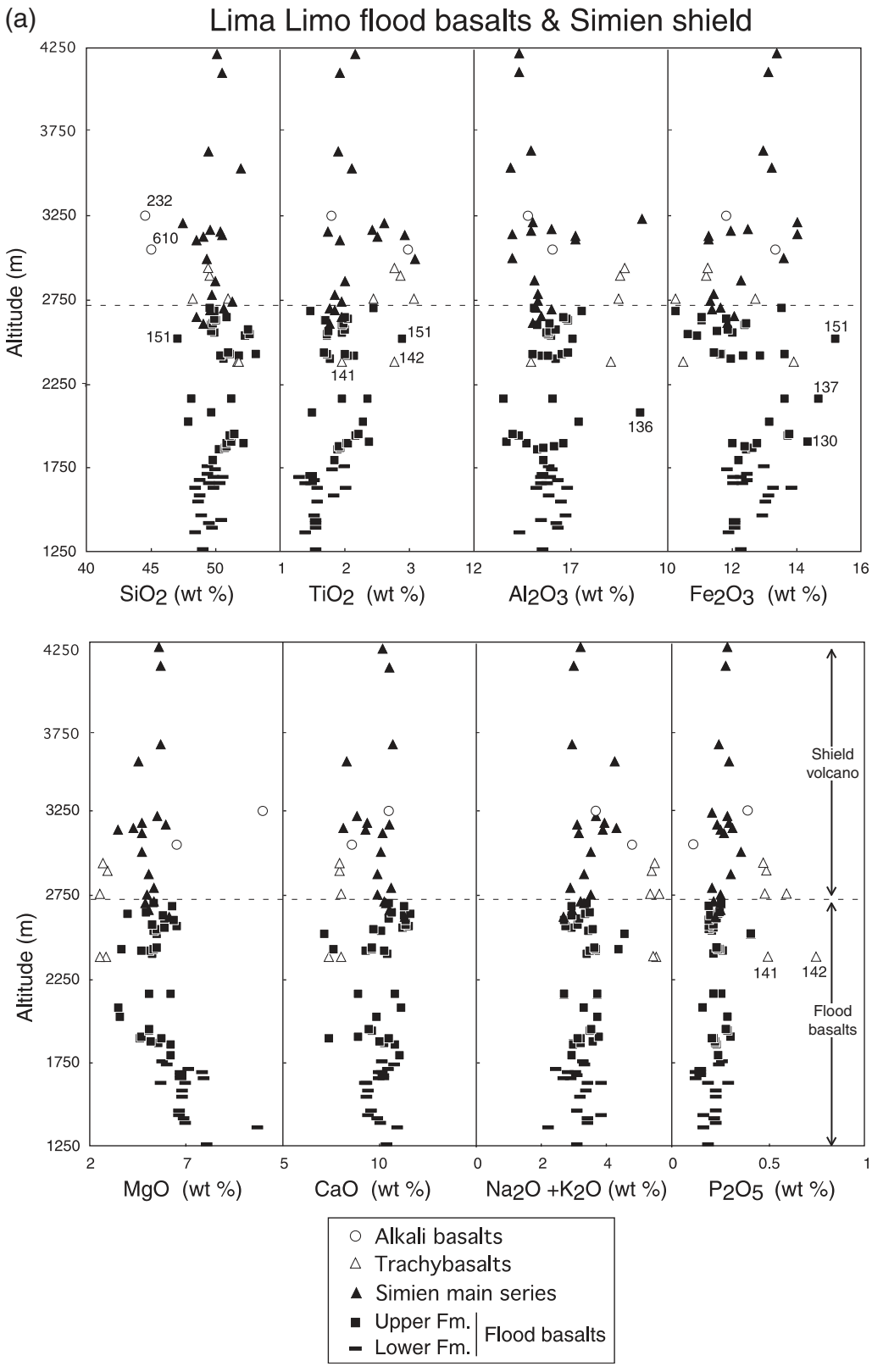

Fig. 11. Diagrams showing variations of (a) major elements and (b) trace elements with stratigraphic height in the Simien shield volcano and underlying flood basalts.

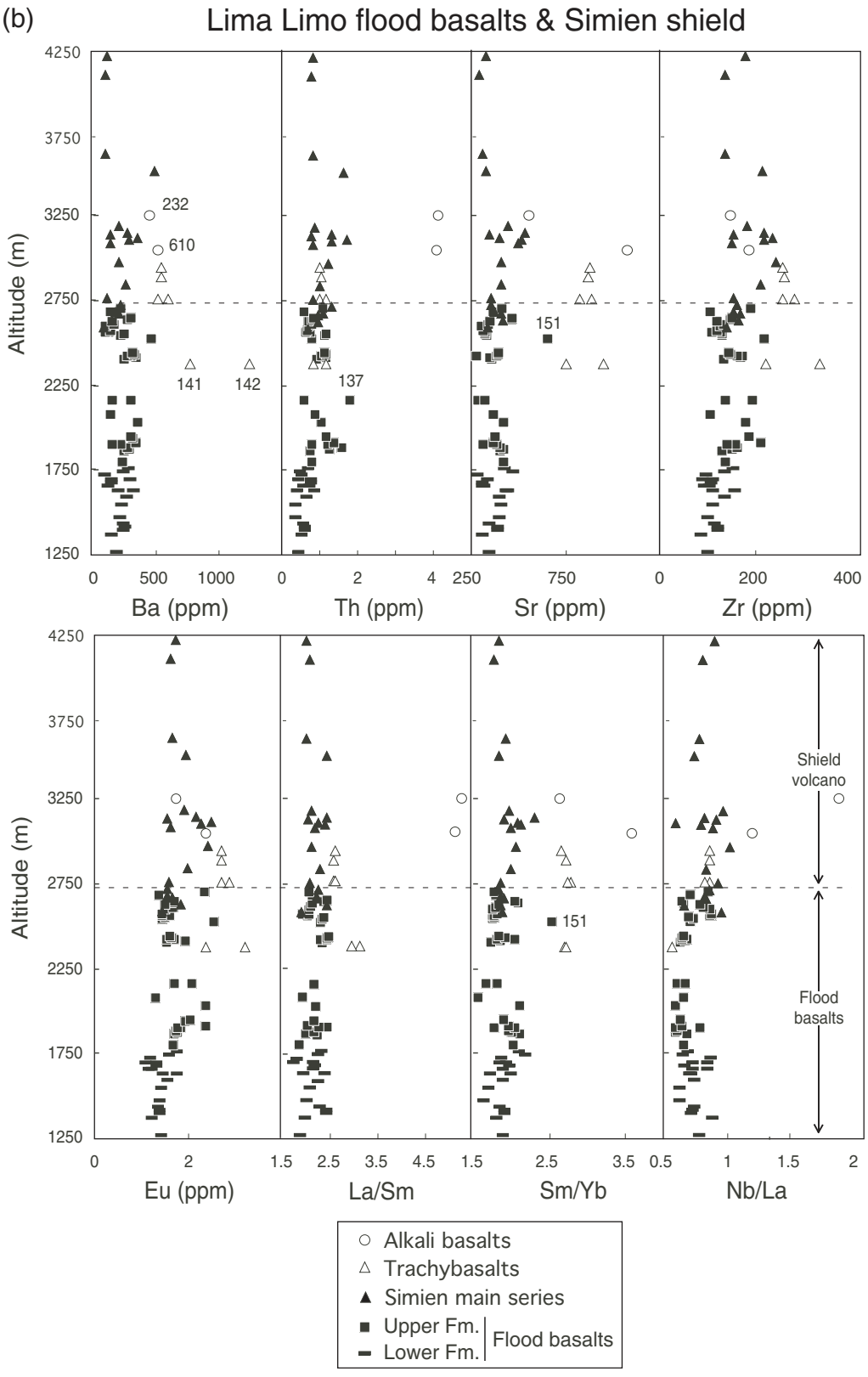

Fig. 11. Continued.

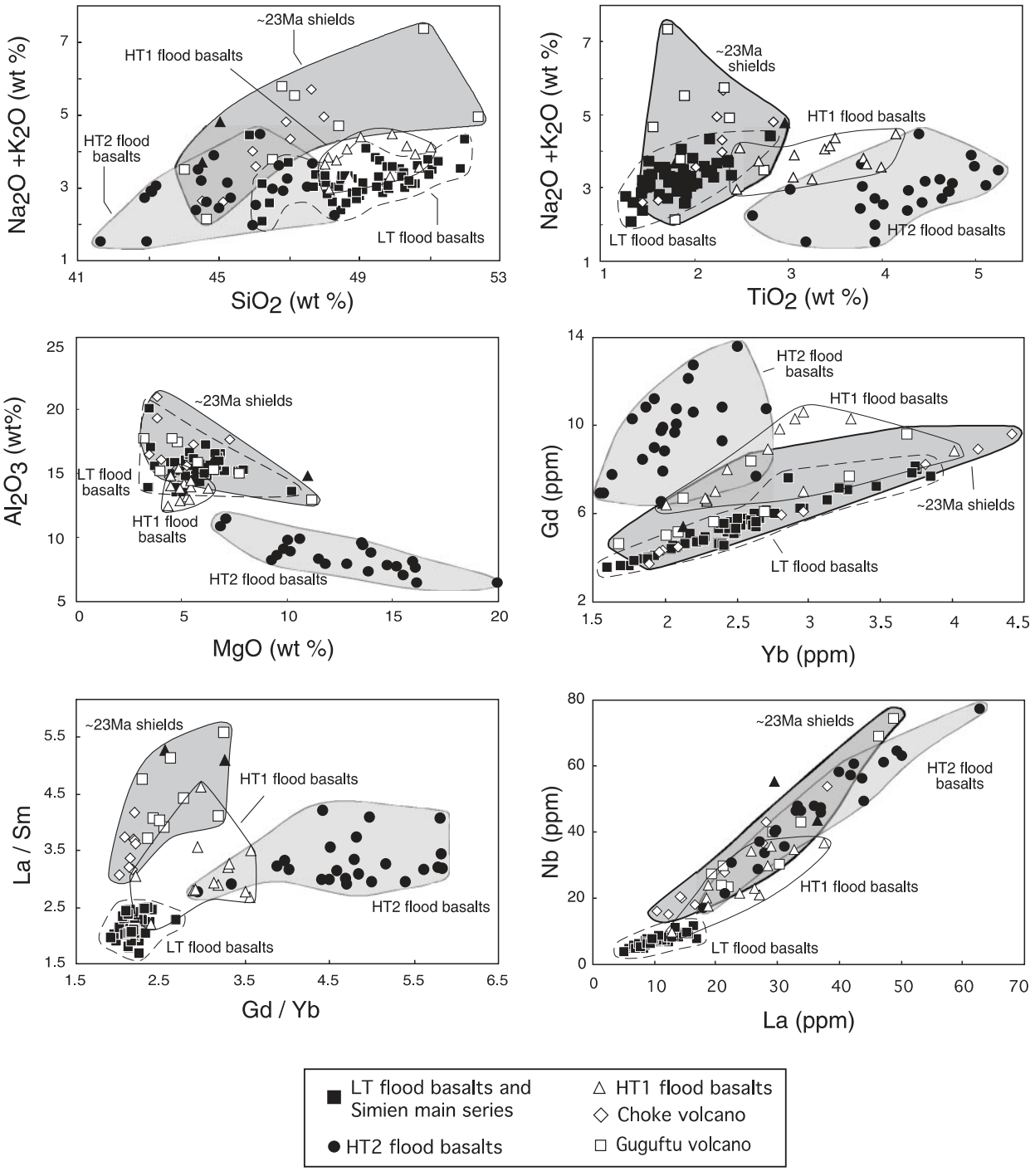

Fig. 12. Major and trace element characteristics of volcanic rocks from Choke and Guguftu volcanoes, compared with those of the underlying HT1 and HT2 flood basalts and with basalts from other parts of the northern plateau. Data from this study, Pik *et al.* (1999) and unpublished analyses.

Is the Ethiopian plateau a typical flood basalt province?

The image of the Ethiopian volcanic province given in the literature, and supported by our study, is very different from that of a 'normal' flood basalt province. Type examples of continental flood basalts, such as those of the Deccan and Karoo provinces, are described as thick, monotonous sequences of thick, continuous, near-horizontal flows of tholeiitic basalt. In contrast, the descriptions of the Ethiopian province by Mohr & Zanettin

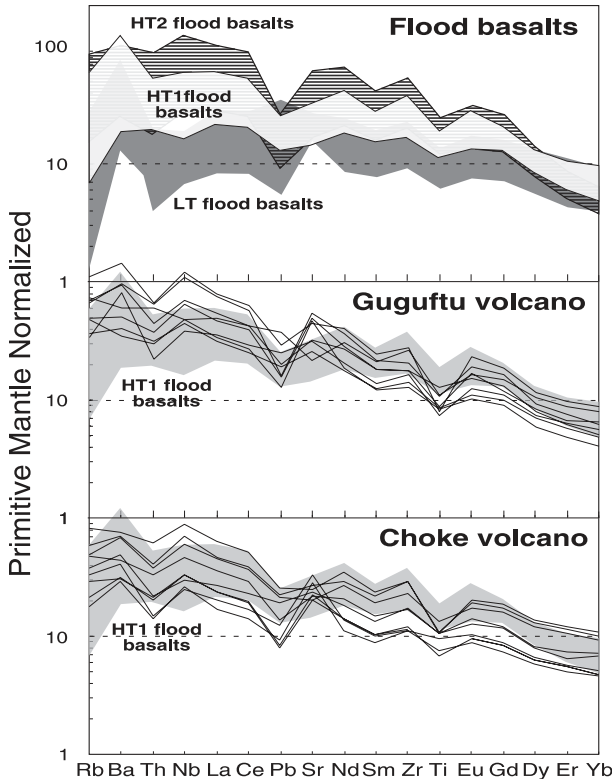

Fig. 13. Trace element concentrations, normalized to primitive mantle, of samples from the Choke and Guguftu volcanoes, compared with those of the underlying HT1 flood basalts. Data from this study and Pik *et al.* (1999).

(1988), and our own field observations and geochemical data, reveal a series of flood basalts overlain by large and conspicuous shield volcanoes. The magmatic character varies from north to south and within each region the character of the shield volcanoes matches that of the underlying flood basalts.

Are the differences between the Ethiopian plateau and the other flood volcanic provinces real, or are they merely apparent, a consequence of differing extents of erosion and degrees of preservation, compounded by incomplete sampling of these vast volcanic structures?

One undeniable difference is the relatively young age of the Ethiopian province. If the small-volume (170 000 km^3, Courtillot & Renne, 2003), and in many ways unusual, Columbia River basalts are excluded, Ethiopia is the youngest major flood basalt province. It is one of the least deformed, and probably the only one in which the uppermost volcanic units are well preserved. Because of the uplift associated with most flood basalt provinces, their upper levels typically are strongly eroded. In the Karoo Province, for example, kimberlite pipes have been eroded to their root zones. However, in both the Deccan and Karoo provinces, there is solid evidence that flat-lying tholeiitic basalt flows erupted from start to finish of the volcanic event, and that shield volcanoes never formed. Cox & Hawkesworth (1985) measured inclinations along a 650-km-long section of the Deccan Traps and concluded that dips were extremely low, between 0·25 and 0·3°. Widdowson (1997) found that a flat-lying laterite at the top of the sequence represents the original, almost horizontal upper surface of the lava pile. Widdowson & Cox (1996) stated that: 'individual flows and formations within the Deccan are known to cover huge areas with only relatively gradual changes of thickness ... After the cessation of the eruptions, the landscape must have been almost devoid of any important topographic features.' Marsh *et al.* (1997), writing of the Karoo province, stated: 'the present structure ... is one of a broad basin with a slight inward dip of the flows', and 'the constancy of thickness ... (of the volcanic formations) ... suggests that the bulk of the lava pile was built on a generally planar surface. There is nothing in the stratigraphy that suggests the presence of geographically focused lava eruption sites ...'

On the other hand, in the Paraná–Etendeka and North Atlantic igneous provinces, shield volcanoes, igneous centres and large volcanic disconformities have been mapped. Jerram & Robbe (2001) described an early shield volcano in the Etendeka province in Namibia. The North Atlantic province contains the well-known intrusive complexes of Skye, Mull and Rum, which probably fed overlying shield volcanoes. Shield volcanoes have also been identified by Planke & Eldholm (1994) in offshore parts of this province, and by Pedersen *et al.* (1996) at the base of the Greenland section.

In each of these examples, the main phase of flood volcanism produced large horizontal flows similar to those of the Deccan. Sequences of flows can be followed for many kilometres, and are difficult to link with any specific volcanic centre. No direct link between flood and shield volcanism can be established. Three key observations suggest that the situation was different in Ethiopia.

(1) The contact between the flood basalts and the lowermost units of the Simien shield dips at a slight (~4°) angle, radially away from the summit of the volcano. Shallow dips (4–7°) in the upper parts of the flood basalt sequence indicate a decrease in magma flux prior to the construction of the Simien shield. These observations, together with the matching compositions of flood and shield basalts, suggest that the two types of eruption were fed by the same conduit system.

(2) The thickness of the flood basalt pile varies from about 1500 m in the thickest sections in the Lima Limo region to less than 200 m to the north of the town of Sekota (Fig. 1) and in the Nile Valley, about 400 km to the south and towards the supposed centre of the province (Fig. 1). Near Alem Ketema, LT tholeiites are absent and the entire volcanic sequence comprises several thin

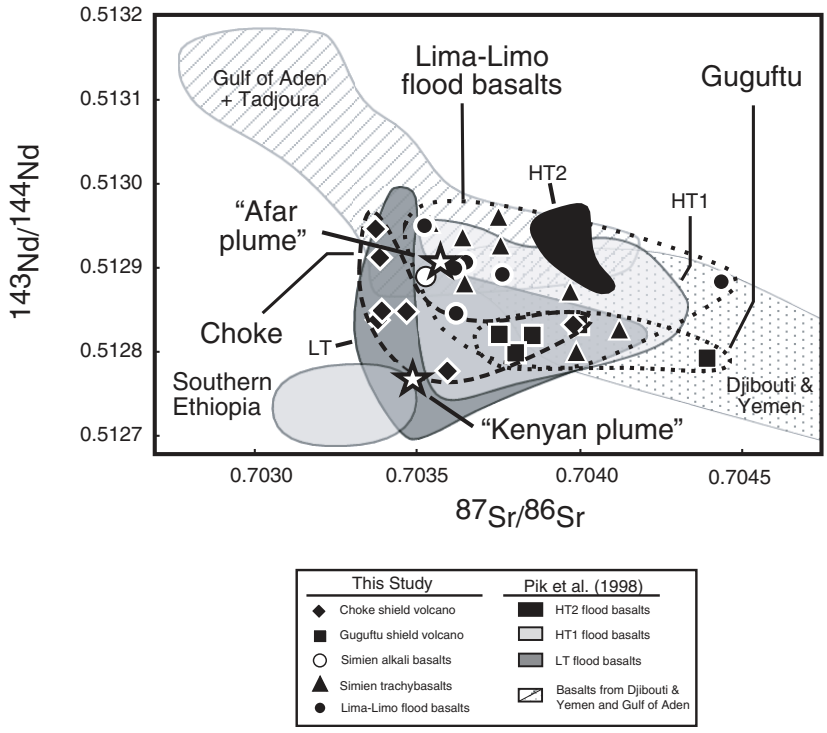

Fig. 14. Nd and Sr isotope compositions of Ethiopian volcanic rocks. The isotopic composition labelled 'Afar plume' was defined by Baker *et al.* (1996*b*, 2002) using the data of Vidal *et al.* (1991) and Schilling *et al.* (1992); the composition of the 'Kenyan plume' is from Rogers *et al.* (2000). Other sources of data: Barrat *et al.* (1990); Deniel *et al.* (1994); Baker *et al.* (1996*b*, 2000); Pik *et al.* (1999).

(<100 m) units of HT1 alkali basalt. It appears that eruption started 30 Myr ago in a restricted region in the Lima Limo region, where LT-type lavas formed a volcanic pile that thinned significantly to the south and east.

(3) Between the towns of Lalibela, Desse and Bora, flows of the HT2 magma type are strongly deformed and commonly have dips from 20 to 60° (Merla *et al.*, 1979; Berhe *et al.*, 1987). Our field observations, like those of Pik *et al.* (1998), suggest that this deformation was synchronous with eruption of the HT2 flows.

How do the alkali lavas fit into the picture? The Karoo sequence in South Africa opened with minor nephelinite eruptions, but all other basalts are tholeiitic (Erlank, 1984; Marsh *et al.*, 1997). In the Deccan, Paraná–Etendeka, Madagascar and Coppermine River plateaux (Cox & Hawkesworth, 1985; Peate *et al.*, 1992; Griselin & Arndt, 1996; Storey *et al.*, 1997), alkaline rocks are absent or restricted to minor syenitic intrusions. In the Siberian flood basalt province, alkaline rocks form volumetrically important units both below and above the main tholeiitic sequence (Wooden *et al.*, 1993; Sharma, 1997). The compositions of Siberian alkali basalts resemble Pik *et al.*'s HT1 type; Siberian alkali picrites have trace element characteristics very similar to the HT2 type. Olivine-phyric rocks with compositions broadly similar to the HT1 and HT2 magma types are also reported in East Greenland (Tegner *et al.*, 1998; Larsen *et al.*, 2003). Rocks of the alkali series therefore are not unique to the Ethiopian province, but in the other provinces such rocks form a relatively minor component of sequences dominated by monotonous low-Ti tholeiitic basalt. In the Ethiopian volcanic plateau, low-Ti tholeiites erupted in a short pulse around 30 Ma and are restricted to a small region in the NW of the province. Alkaline rocks have a wider distribution, in both space and time. Alkali picrites of the HT2 type started to erupt around 31 Ma (Figs 1 and 5), slightly before the main peak of tholeiitic flood volcanism, and alkaline flood and shield volcanism persisted well after the main tholeiitic peak.

The relative volumes of flood and shield volcanoes in the northern part of the plateau can be estimated as follows. In Fig. 1, the total area covered by flood basalts is roughly 400 km × 600 km. The thickness of the pile decreases from about 1·5 km at Lima Limo in the north to near zero near Alem Ketema in the south. If the average thickness is 0·75 km the total volume of flood basalts is $400 \times 600 \times 0{\cdot}75 = 1{\cdot}8 \times 10^5\ \mathrm{km}^3$. Currently about 20% of the surface of the plateau is covered by shields; before erosion they may have covered one-third. The summits of the shields are about 1·5 km above the flood basalt surface. Because the volume of a cone-shaped shield is one-third of that of a cylinder with the same

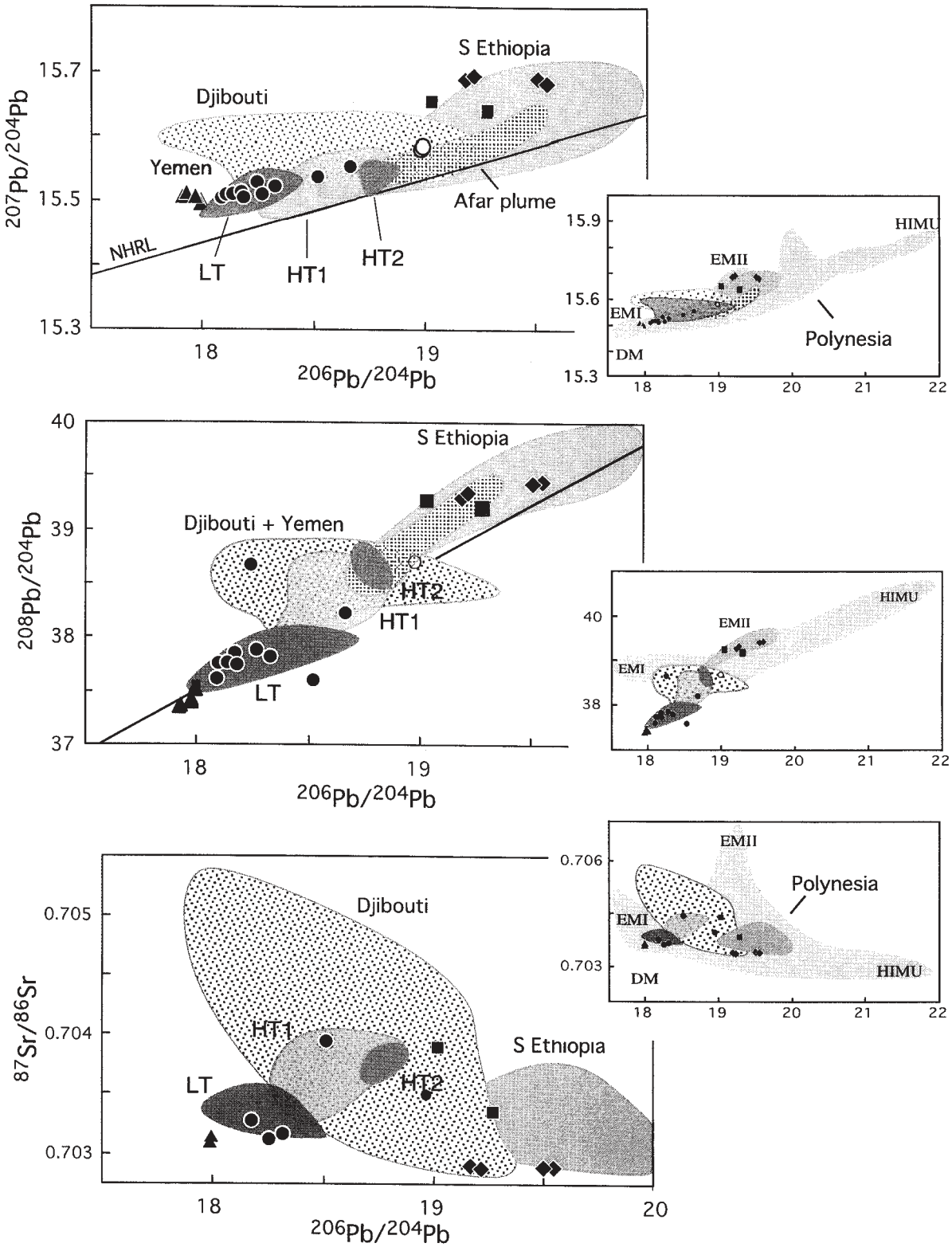

Fig. 15. Pb and Sr isotope compositions of Ethiopian volcanic rocks compared with compositions from other parts of the Horn of Africa. The composition labelled 'Afar plume' was defined by Baker *et al.* (1996*b*, 2002) using the data of Vidal *et al.* (1991) and Schilling *et al.* (1992). The compositions of the rocks from French Polynesia, shown in the insets, are from the GEOROC data base (http://georoc.mpch-mainz.gwdg.de/). Other sources of data: Barrat *et al.* (1990); Deniel *et al.* (1994); Baker *et al.* (1996*b*, 2000); Pik *et al.* (1999).

radius, the total volume of the shields is about 1/3 × 1/3 × 1·5 × 400 × 600 or ~4 × 10^4 km^3. On this basis, we calculate that the volume of the shields was about 20% of that of the flood basalts. The magmatic flux during the 1 Myr period of flood volcanism was about 0·18 km^3/year, far greater than that during the periods of shield volcanism (~0·008 km^3/year if the Choke and Guguftu shields, each with a volume of about 4000 km^3, formed within a 1 Myr period around 23 Ma).

To summarize, the northern Ethiopian volcanic plateau is not a thick, monotonous, rapidly erupted pile of undeformed, flat-lying tholeiitic basalts. Instead, it consists of a number of volcanic centres of variable magmatic character and age. The earliest flood volcanics are tholeiitic in some regions and alkaline in others. The tholeiitic Simien shield surmounts tholeiitic flood basalts and the two probably form parts of the same magmatic system. The flood volcanism was protracted, starting with a major peak of activity between 31 and 30 Ma in the northern part of the plateau, then migrating to the south. The 23 Ma Choke and Guguftu shields in the central northern part of the plateau are alkaline and they overlie a thin sequence of 23 Ma alkaline flood basalts. Finally, still younger silica-undersaturated lavas erupted from 11 Ma (Guna) to recent times, in shields or small cones, in various parts of province.

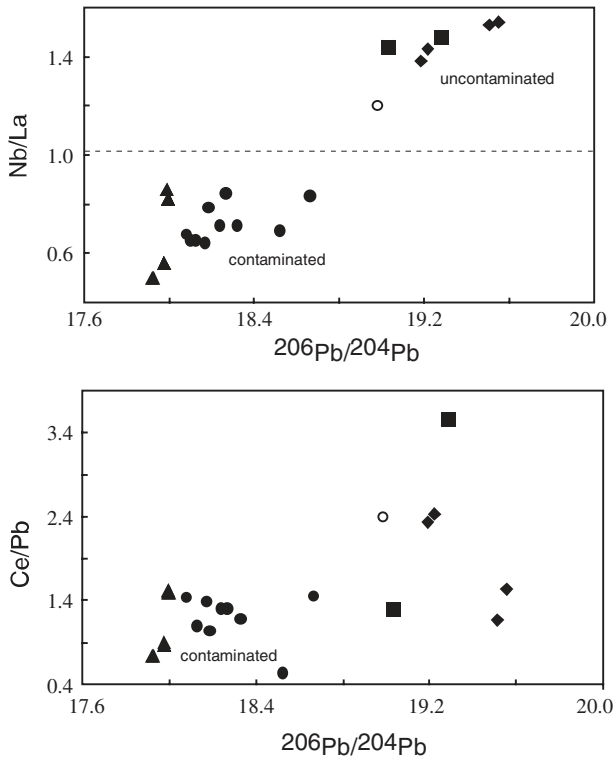

Fig. 16. Correlation of Nb/La and Ce/Pb with $^{206}Pb/^{204}Pb$ illustrating the unradiogenic Pb isotopic ratios of crustally contaminated LT flood basalts.

Petrogenesis

An important petrological challenge posed by the Ethiopian volcanic series, and to a lesser extent other provinces, is to explain the relationship between the tholeiites and the different types of alkaline rocks. More specifically, we must account for simultaneous eruption, at 30 Ma, of LT tholeiites in one part of the province and HT1 or HT2 magmas in another; and the broad transition, during the period 30–20 Ma, from mixed tholeiitic–alkaline magmatism to exclusively alkaline magmatism. We need to establish what part(s) of the mantle melted to form these magmas, and how the composition of the source and the conditions of melting influenced the magma composition.

Tholeiitic and alkaline magmatism ~30 Myr ago

The tholeiitic basalts have relatively low concentrations of incompatible trace elements, sloping HREE patterns, and negative Nb anomalies (Table 5 and Figs 10 and 11). Their Nd and Sr isotopic compositions plot in the middle of the field for all Ethiopian lavas (Fig. 14), but their Pb isotopic compositions (Fig. 15) are unusually non-radiogenic. Baker *et al.* (2000) have argued that Oligocene tholeiitic flood basalts in Yemen, part of the Ethiopian plateau before the opening of the Red Sea, were contaminated with continental crust. Using a combination of trace elements and Nd–Sr–Pb–O isotopes, they showed that the compositions of these basalts were strongly influenced by the assimilation of late Proterozoic lower crust. Pik *et al.* (1999) invoked a similar process to explain the compositions of LT tholeiites from the Lima Limo region.

Our data support this interpretation. The tholeiitic basalts of the Simien shield and underlying flood volcanics have persistently low Nb/La, a reliable trace element index of crustal contamination, and low $^{206}Pb/^{204}Pb$ (Fig. 16), whereas alkali basalts from the late veneer on the Simien shield, samples from all other shields, and the HT1 and HT2 lavas of Pik *et al.* (1999), have high Nb/La and $^{206}Pb/^{204}Pb$. Although there is more scatter in the Ce/Pb vs $^{206}Pb/^{204}Pb$ diagram, probably because of Pb mobility, the correlation persists. It appears that the tholeiitic magmas were susceptible to crustal contamination whereas the alkali magmas were unaffected. The same behaviour is seen in the Siberian flood volcanics (Wooden *et al.*, 1993; Sharma, 1997) where a persistent crustal signature is present in the tholeiites but absent in alkaline volcanic rocks. Arndt *et al.* (1998) attributed this contrasting behaviour to differences in volatile contents. Higher volatile contents in the alkaline magmas drive these magmas to the surface without interaction with crustal rocks

Table 5: Average compositions of principal volcanic series normalized to 7% MgO

	LT tholeiites	HT1 series	HT2 series
n:	83	14	14
SiO_2	50·73 (1·2)*	48·35 (1·9)	46·42 (1·3)
TiO_2	1·94 (0·4)	2·06 (0·4)	5·48 (0·7)
Al_2O_3	15·46 (1·0)	16·53 (1·5)	9·81 (0·6)
Fe_2O_3	12·59 (1·1)	12·87 (1·5)	14·43 (0·7)
MgO	7 (0)	7 (0)	7 (0)
CaO	9·28 (1·1)	9·31 (1·5)	12·71 (0·8)
Na_2O	2·58 (0·4)	2·94 (0·9)	1·98 (0·4)
K_2O	0·47 (0·3)	1·01 (0·3)	1·46 (0·3)
Nb	7·77 (3·3)	31·2 (15·8)	67·9 (12·0)
Zr	137·6 (40·6)	157·7 (50·3)	492·6 (82·8)
Y	29·5 (6·6)	28·0 (7·9)	40·1 (4·9)
Pb	2·27 (0·9)	2·94 (1·2)	3·58 (0·9)
Th	0·92 (0·4)	2·70 (1·3)	5·19 (1·2)
U	0·29 (0·1)	0·60 (0·3)	1·35 (0·3)
La	10·4 (3·4)	23·2 (10·1)	50·1 (10·1)
Ce	25·6 (8·1)	48·9 (20·4)	117·8 (22·7)
Nd	17·1 (5·0)	25·3 (9·1)	68·5 (12·3)
Sm	4·59 (1·2)	5·56 (1·7)	14·8 (2·5)
Eu	1·57 (0·4)	1·87 (0·5)	4·34 (0·7)
Gd	5·23 (1·2)	5·70 (1·6)	12·7 (2·1)
Dy	5·10 (1·1)	4·83 (1·3)	8·39 (1·2)
Er	2·72 (0·6)	2·67 (0·8)	3·47 (0·4)
Yb	2·33 (0·5)	2·39 (0·7)	2·45 (0·2)
Lu	0·34 (0·1)	0·36 (0·1)	0·33 (0·0)

*Standard deviation.
n, number of analyses used to calculate averages. Before calculating the averages, the samples were normalized to 7% MgO by adding or subtracting olivine with the composition Fo_{85}. Although this procedure is only approximate because it fails to take into account the changing olivine composition and the crystallization of pyroxene and plagioclase in the more evolved basalts, it is sufficient to provide a basis for comparison of the trace element contents of the three rock types.

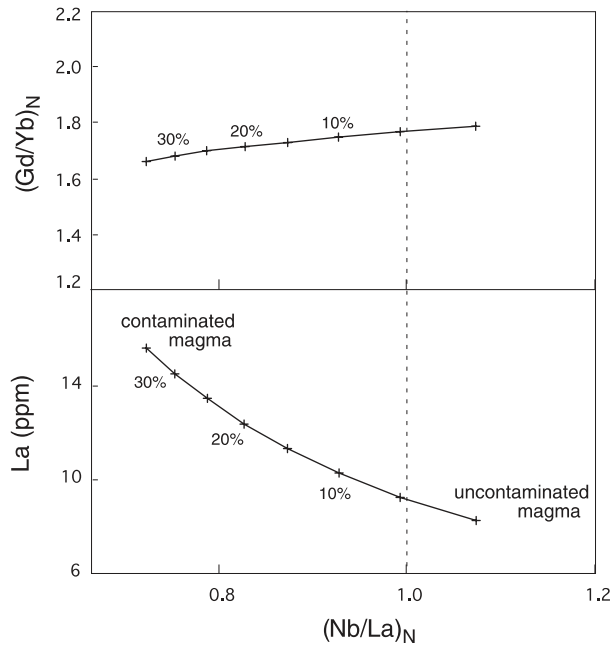

Fig. 17. Results of a calculation in which the effects of crustal contamination on the LT flood basalts are removed. It should be noted that the Gd/Yb ratio, a measure of the slope of the normalized HREE pattern, changes minimally during contamination.

whereas the volatile-poor, higher density tholeiites stall, and became contaminated, in large crustal magma chambers.

The composition of the parental magma of the tholeiites can be calculated by stripping off the chemical effects of contamination and fractional crystallization. This was done using a numerical procedure, starting with the average composition of the tholeiitic basalts (Table 5), subtracting average continental crust and adding olivine in the ratio 4:10 until the Nb anomaly was eliminated (Fig. 17). The result, after removing the effects of 30% crystallization and 12% contamination, is a picritic magma containing about 18% MgO, with levels of incompatible elements such as La about half those of the contaminated magma. Because the Gd/Yb ratio of the contaminated basalt is similar to that of the crustal contaminant, the slope of the HREE does not change. Were the isotopic composition of the crustal contaminant known, a similar procedure would give us the isotopic composition of the parental magma. However, although we can assume that the contaminant corresponds to Baker *et al.*'s (1996*b*) Proterozoic mafic granulites, which have low Pb isotope ratios and plot to the left of the LT tholeiites, their wide range of compositions ($^{206}Pb/^{204}Pb = 15{\cdot}6–18{\cdot}0$) renders meaningless any quantitative modelling. All that can be said is that the isotopic compositions of the uncontaminated LT tholeiites lie somewhere to the right of the LT fields shown in Fig. 15.

The low concentrations of incompatible elements, combined with moderately sloping HREE patterns and the picritic composition of the parental magma, suggest that this magma formed by high degrees of partial melting under conditions in which garnet was retained in the residue. The magmas may have been pooled melts from a melting column that extended from the garnet stability field at >90 km to shallower depths, but the garnet signature in the deep-seated melts would have dominated the signature of melts from the entire melt column.

HT2 lavas contain 10–20 times the contents of incompatible trace elements of the tholeiites (Table 5). More magnesian Ethiopian HT2 lavas have picritic compositions

and contain olivine phenocrysts with up to 86% forsterite (Pik *et al.*, 1998, and our unpublished data). From these compositions we estimate, using Mg–Fe partitioning, that the liquids from which the olivine crystallized contained around 14% MgO. The trace element content of such a liquid, calculated from the average composition of these lavas, has a high concentration of incompatible elements, strongly sloping HREE, low Al/Ti and high Fe. The REE patterns and the low Al/Ti of this magma indicate partial melting under conditions that left a large amount of garnet in the residue; the high MgO and FeO contents suggest melting at considerable depth.

The Nd and Sr isotopic compositions of the two types of magma (LT and HT2), with the exception of one sample with high $^{87}Sr/^{86}Sr$, plot together in a field far from the composition of depleted upper mantle (Fig. 14) and straddling the composition of the Afar mantle plume, as estimated from the data of Vidal *et al.* (1991) and Schilling *et al.* (1992).

We therefore have two types of magma, the trace element poor LT type and the trace element rich HT2, both of which apparently formed around 30 Ma by deep melting of a source with an isotopic composition similar to that of the mantle plume currently beneath the Afar depression. The major difference between the two types is in the level of incompatible trace elements, which differ by a factor of more than 10. There are two obvious ways of explaining such large differences in the levels of incompatible elements; either the degree of partial melting varied widely, or the magmas were derived from sources with different trace element compositions. Either the source region was heterogeneous in terms of composition and/or temperature, or different parts of the mantle source partially melted to form the magmas. The magmas may have come from a heterogeneous sub-lithospheric source, or from heterogeneous lithospheric mantle, or from both.

Was any magma derived from the lithospheric mantle?

The notion that continental flood basalts form by partial melting of the sub-continental lithosphere is firmly entrenched in the geological literature. In numerous papers (e.g. Hawkesworth *et al.*, 1984; Hergt *et al.*, 1989; Lightfoot *et al.*, 1993) typical low-Ti continental flood basalt is said to form in metasomatized sub-continental lithospheric mantle with a distinctive trace element and isotopic composition (enrichment of incompatible elements, negative Nb–Ta–Ti anomalies, high $^{87}Sr/^{86}Sr$ and low $^{143}Nd/^{144}Nd$). In other papers, the sub-continental lithospheric mantle is thought to give rise to magma of very different composition. Larsen *et al.* (2003) suggested that a suite of alkaline picrites in East Greenland—magmas with compositions very similar to those of the Ethiopian HT2 rocks—owe their high trace element concentrations to melting of metasomatized lithospheric mantle. George & Rogers (2002) proposed a lithospheric source for the Getra-Kele alkali basalts in southern Ethiopia, magmas whose trace element and isotope compositions (low $^{87}Sr/^{86}Sr$ and high $^{206}Pb/^{204}Pb$) resemble those of the Choke and Guguftu shield basalts (Fig. 15). Silica-undersaturated alkali basalts, basanites and nephelinites in the East African rift (e.g. Class *et al.*, 1994; Macdonald *et al.*, 2001; Späth *et al.*, 2001) have isotopic compositions and trace element ratios that are thought to preclude an asthenospheric or plume source, and they too are explained as lithosphere melts. What indeed is the compositional range of the lithospheric mantle, and can it give rise to magmas with such diverse chemical characteristics? Is there any concrete evidence that such a wide range of magma types comes from the lithospheric mantle, or is the label 'lithosphere' just given to the source of any magma whose composition is thought to be inconsistent with that of an asthenosphere or plume source? Consider the following arguments.

(1) The major and trace element characteristics of the HT2 magmas suggest that they came from a deep source under conditions that left considerable garnet in the residue. We can use the experimental results of Hirose & Kushiro (1993) and Herzberg & Zhang (1996) to provide more quantitative constraints. The high MgO and FeO contents, the low Al_2O_3/TiO_2 and the strongly sloping HREE of these magmas point to melting under at least 3 GPa pressure, which corresponds to depths greater than 90 km. The contemporaneous LT tholeiites, on the other hand, have lower FeO, higher Al_2O_3/TiO_2 and less fractionated HREE, and they appear to have come from shallower depths.

(2) During plume–lithosphere interaction, the lithosphere, which is the coldest part of the mantle, melts only if its solidus is depressed by the presence of volatiles. Gallagher & Hawkesworth (1992) suggested that an upwelling, essentially anhydrous plume may cause melting in overlying volatile-rich metasomatized lithosphere. There is no evidence, however, neither from the style of eruption, nor from the abundance of vesicles and the mineralogy of the lavas, that those magmas said to come from a lithospheric source were richer in volatiles than contemporaneous plume-derived magmas. The abundance of phlogopite and amphibole in the HT2 magmas (Pik *et al.*, 1998, and our own observations) indicates that these magmas may have had significant water contents, yet the major and trace element contents of these magmas indicate that they came from a deeper source than the apparently anhydrous LT tholeiites. In other words, the volatile-rich source was deeper than the anhydrous source, just the opposite to what is required in Gallagher & Hawkesworth's (1992) model.

(3) Negative K anomalies, such as those observed in the trace element patterns of alkali basalts from the East African rift and many other ultrapotassic magmas, are thought to indicate melting in the presence of amphibole (Class *et al.*, 1994; Späth *et al.*, 2001). Because this mineral is stable only under relatively low temperatures and pressures, such as those in the lithosphere, the presence of such anomalies is cited as evidence of a lithospheric source of the rift basalts. In lavas from northern Ethiopia, negative K anomalies are absent.

(4) Analyses of peridotite xenoliths in volcanic rocks from Ethiopia, Yemen, Saudi Arabia and the Red Sea give some indication of the composition of the lithosphere beneath the Horn of Africa. Their isotopic compositions are highly variable (Henjes-Kunst *et al.*, 1990; Blusztajn *et al.*, 1995; Baker *et al.*, 1998; Baker *et al.*, 2002) and encompass the entire range of compositions measured in Ethiopian volcanic rocks. Although the xenoliths from northern Ethiopia (Roger *et al.*, 1999; F. Bastien, unpublished data, 2001) have depleted Sr and Nd isotopic compositions (low $^{87}Sr/^{86}Sr$ ~0·7025, and high $^{143}Nd/^{144}Nd$ ~0·5132–0·5133) that are very different from those of the lavas in this region, xenoliths of metasomatized peridotite from Yemen (Baker *et al.*, 1998; Baker *et al.*, 2002) have compositions like the Oligocene to Recent volcanic rocks of that region. Their trace element compositions are very different, however. Like many samples of metasomatized lithospheric peridotite, particularly those that interacted with carbonate-rich fluids, these rocks have extremely high ratios of REE to high field strength elements [HFSE; see fig. 2 of Baker *et al.* (1998) and Baker *et al.* (2002)]. Particularly characteristic of these rocks are very large negative Zr and Ti anomalies in their mantle-normalized trace element patterns. As mentioned above, the LT tholeiites have small negative Nb–Ta anomalies, but like other continental tholeiites, their ratios of Zr to REE are close to, or higher than, chondritic values (Griselin & Arndt, 1996). In the Ethiopian alkali lavas (HT2 and HT1) HFSE anomalies are positive or absent and this indicates that these magmas could not have formed by melting of the metasomatized lithosphere identified by Baker *et al.* (1998, 2002).

On balance, the chemical compositions of the lithosphere sampled by the xenolith suites do not correspond to those of the sources of the Ethiopian volcanic rocks and, on the basis of all the arguments presented above, we conclude that melts from the lithospheric mantle did not contribute significantly to the formation of any of the Oligocene lavas from northern Ethiopia. These magmas came from a sub-lithospheric source that was heterogeneous in terms of temperature, or composition, or both.

Conditions in the mantle source of the 30 Ma lavas

The problem is to establish which factor—temperature or composition—had the greatest influence on magma compositions. The most enriched HT2 magmas contain more than 60 ppm of La, a level 100 times greater than that of primitive mantle. If primitive mantle were the source, the degree of melting must have been less than 1%; if the source was depleted, the percentage would have been still lower. In the LT tholeiites, La concentrations are far lower and REE patterns are less fractionated (lower La/Yb). When the effects of crustal contamination are eliminated, the calculated La content is around 6 ppm. If these magmas came from the same source as the HT2 lavas, the degree of partial melting must have been 10 times greater. The similarity of isotopic compositions for contamination-corrected tholeiites and HT2 lavas suggests that the sources were indeed similar.

Our view of the melting process that produced the 30 Ma tholeiites and HT2 lavas is as follows. For reasons developed in a later section, we envisage melting not in a discrete mantle plume but in a broad, heterogeneous region of mantle upwelling. During ascent, the hotter, more enriched portions were the first to intersect the peridotite solidus and the first to melt. Magmas from these regions erupted as the HT2 basalts and picrites. As mentioned above, these rocks are located in a region characterized by significant deformation of the lava series. On the basis of our preliminary observations, this deformation appears to have been synchronous with the eruption of the lavas. The character of the deformation is consistent with extension in the underlying basement, which suggests that the emplacement of these unusual rocks may have been facilitated by fractures in the underlying lithosphere.

Synchronous melting in cooler parts of the upwelling mantle source produced larger volumes of higher-degree melts and these erupted as LT flood basalts.

Shield volcanism during the period 23–10 Ma

The period from 30 to 10 Ma saw the transition from flood to shield volcanism. The two ~23 Ma volcanoes that we investigated consist entirely of HT1 type alkali lavas and they directly overlie flood basalts of similar overall composition, but with distinctly different Pb isotopic ratios. At present we do not have sufficient age data to establish the chronology of the underlying flows, but a possible interpretation is that flood volcanism in the north–central part of the plateau started with the emplacement, 30 Myr ago, of LT flows from the Simien volcanic centre, then continued around 23 Myr ago with the emplacement of the HT1 series shields in the middle of the northern part of the plateau (Figs 1 and 18). Then, from 20 to 10 Ma, alkali volcanics erupted from dispersed sites such as the late veneer on the Simien shield and the entire Guna shield.

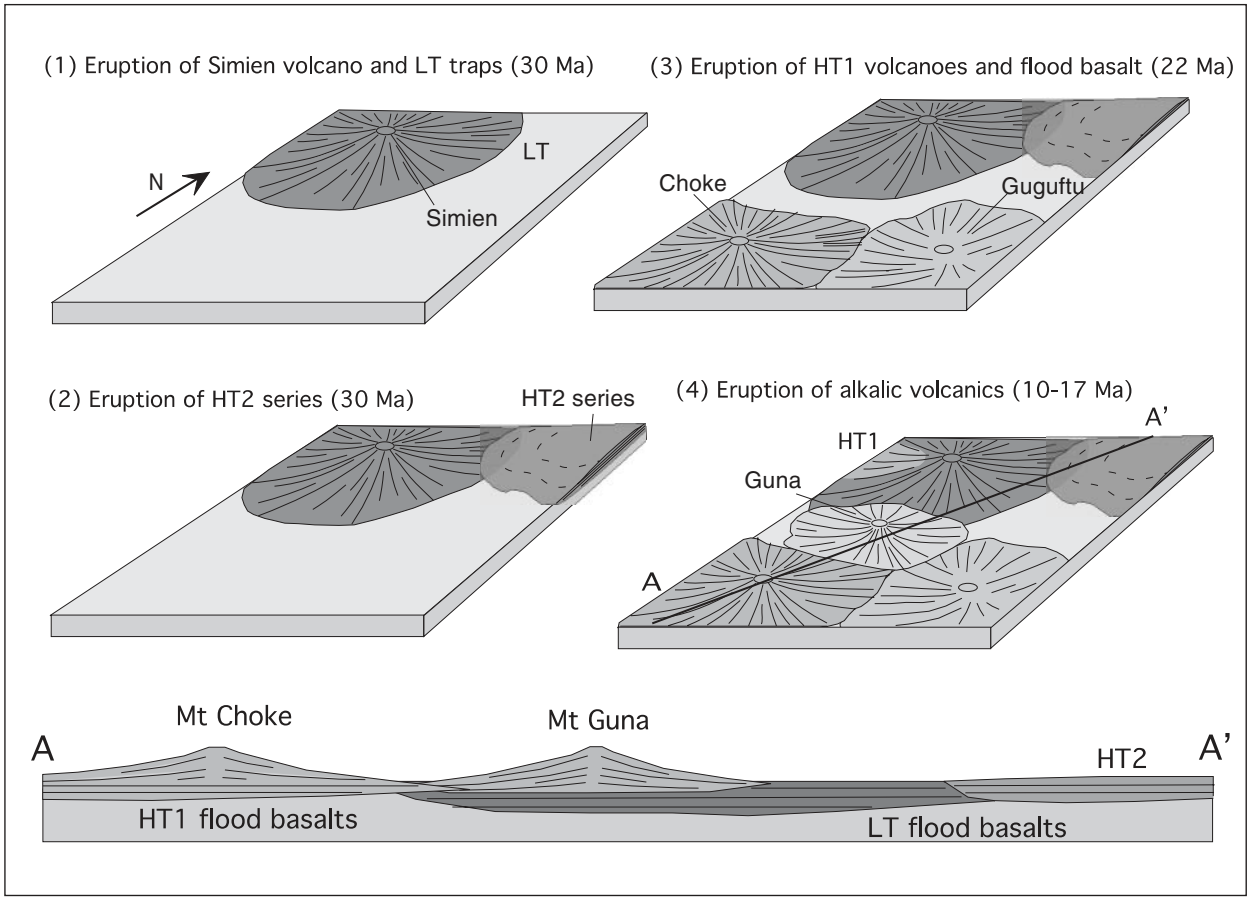

Fig. 18. Four stages in the formation of the northern Ethiopian plateau.

The compositions of the 23 Ma lavas are very different from those of the Oligocene flood volcanics. The absence of Nb anomalies and radiogenic Pb isotopic compositions indicate that these lavas were not contaminated with crustal material. Although their Nd and Sr isotopic compositions plot within the same broad field as the older lavas, their Pb isotopic compositions are distinct, being characterized by higher $^{206}Pb/^{204}Pb$, $^{207}Pb/^{204}Pb$ and $^{208}Pb/^{204}Pb$ ratios than any other lava from northern Ethiopia. Each volcano has a unique combination of Nd, Sr and Pb isotopic compositions. The Choke basalts have the most extreme composition, being characterized by high Pb isotope ratios and low $^{87}Sr/^{86}Sr$. This combination corresponds quantitatively to that of the HIMU mantle component, which is reported to be present both in lavas from the Afar depression (Deniel *et al.*, 1994) and in the mantle lithosphere adjacent to the Red Sea (Chazot & Bertrand, 1993). The 45–30 Ma Getra-Kele basalts in southern Ethiopia (Figs 14 and 15) have a similar composition, which was attributed by Stewart & Rogers (1996) and George & Rogers (2002) to be a characteristic of their source in the mantle lithosphere.

Nature of the mantle source of Ethiopian volcanic rocks: comparison with the Pacific superswell

In the insets in Fig. 15, we show the range of Pb–Sr isotopic compositions recorded in volcanic rocks from French Polynesia in the South Pacific. We refer to this region because it gives some indication of the extremely wide range of compositions that can be present in sub-lithospheric mantle. Although the compositions of lavas on some of the French Polynesian islands indicate some interaction with the oceanic lithosphere (Chauvel *et al.* 1997), the contaminants are attributed to recent metasomatism by earlier erupted magmas and are not thought to be a characteristic of ancient lithosphere. The comparison between the isotopic compositions of lavas from the Ethiopian and Polynesian provinces reveals two important points. First, the compositions of all Ethiopian lavas are far removed from that of the HIMU end-member, as represented by samples from the Austral Islands in French Polynesia (Chauvel *et al.*, 1992). Second, all non-contaminated Ethiopian lavas plot around the centre of the Polynesian field, far from all the more extreme compositions of mantle components such as EMI, EMII,

DMM and HIMU. The compositions recorded in Ethiopia are well within the range tapped by melting in various parts of the Polynesian superswell. This is true of the compositions of all Ethiopian lavas, except those contaminated with continental crust: it includes not only the estimated compositions of the 'Afar plume' [as defined by Baker *et al.* (1996, 2002) using data of Vidal *et al.* (1991) and Schilling *et al.* (1992)] and the 'Kenyan plume' (Rogers *et al.*, 2000), but also the compositions of all magmas that have been said to come from a lithospheric source. On the basis of this comparison, rather than assigning specific compositions to various plumes or to different parts of the sub-continental lithospheric mantle, we propose instead that the composition of the mantle beneath northern Africa was heterogeneous in much the same way as the mantle that is currently welling up beneath the southern Pacific.

Except along its margins and in major river valleys, the entire Ethiopian volcanic plateau currently stands above 2000 m in altitude. According to Jestin & Huchon (1992) and Menzies *et al.* (1992), the uplift took place concurrently with, or very soon after, eruption of the flood basalts, 30 Myr ago, and since that time the high altitudes have been maintained. It is most unlikely that this uplift is due to the thermal or compositional influence of the Oligocene plume, which should have dissipated by now. Instead, the present elevation of the plateau is normally attributed to dynamic support from a thermally anomalous upwelling portion of the present upper mantle. In fact, the Horn of Africa has been shown on the basis of mantle tomography studies (Nyblade & Robinson, 1994; Gurnis *et al.*, 2000; Ritsema & van Heijst, 2000; Nyblade, 2002) to be underlain by a broad zone of low-velocity, probably low-density, mantle that extends in a broad swath from northern to southern Africa. The anomalous mantle beneath Africa is one of two such regions, the other being the Pacific superswell. In other words, the mantle beneath northern Africa has an anomalous thermal character similar in many ways to that beneath the southern Pacific.

In view of these observations, and as for the 30 Ma lavas, we attribute the compositions of the post-Oligocene Ethiopian lavas to those of different parts of a complex, heterogeneous region of mantle upwelling. We do not exclude the possibility that elements of these compositions could have been transferred by migration of fluids to the base of the lithosphere, and it is possible that such short-lived metasomatized sources could have contributed to the formation of magmas, as envisaged by Späth *et al.* (2001). However, these parts of the lithosphere only temporarily acquired the distinctive compositions of components that were inherent to the superswell itself.

The formation of the large shields is thus attributed to melting of the hotter and more fusible parts of the superswell. These parts may have risen separately as secondary plumes from the main body of the swell, as envisaged by Davaille *et al.* (2003). In the South Pacific, the products of such melting erupt onto a fast-moving oceanic plate to form chains of oceanic islands. Woodhead & McCulloch (1989), Chauvel *et al.* (1992), Woodhead & Devey (1993) and White & Duncan (1996) have shown that the compositions of the various chains in the Polynesian archipelagoes reflect their derivation from a wide range of sources. The melt products become mixed through the superposition of one chain on another. The north African plate moves much more slowly and the products of melting of hot, more fusible parts of the source erupt more or less at one place, over a protracted period, to form the large volcanic shields. The distinctive compositions of the Choke and Guguftu shields, and more generally the nature of all the volcanic rocks throughout the Horn of Africa, can be explained, in our opinion, by melting in regions of anomalously hot material dispersed within the slowly upwelling mantle source.

The final question is how to explain the transition from mixed tholeiitic–alkaline magmatism to exclusively alkaline magmatism. The problem is accentuated because interpretation of structural data suggests that rifting and thinning of the lithosphere did not start in northern Ethiopia before 30 Ma, but was well advanced by 23 Ma. Mantle upwelling beneath the thinned lithosphere normally would lead to an increase in the extent of partial melting, and thus to a change in magma type in the opposite sense to what we observe: instead of a transition from tholeiite to alkaline magma, we should see the opposite. Three processes might explain a global decrease in the degree of melting: (1) the 7 Myr that elapsed were sufficient to allow significant cooling of the mantle source; (2) hot material from the central core of the source migrated laterally, to be replaced at the site of melting by cooler material; (3) the residue left after extraction of the LT magmas was light and refractory and it accumulated beneath the lithosphere to create a barrier that limited the amount of partial melting in the underlying mantle. To distinguish between these models requires quantitative modelling of melting and melt extraction in a complex zone of mantle upwelling. This work is currently under way and the results will be reported in a later paper.

CONCLUSIONS

(1) The Ethiopian volcanic plateau is not a thick, monotonous, rapidly erupted pile of undeformed, flat-lying tholeiitic basalts. Instead, it consists of a number of volcanic centres with different magmatic character and with a large range of ages.

(2) The shield volcanoes are magmatically similar to the underlying flood basalts—the tholeiitic Simien shield overlies tholeiitic flood basalts, and the alkaline Choke

and Guguftu shields overlie alkaline flood basalts. The change in volcanic style is driven not by a change in the compositions of the magmas but probably by the tectonic setting and a decrease in magma flux.

(3) Three main types of magma, distinguished by their major and trace element compositions, are recognized in the northern part of the plateau. Tholeiitic and alkaline types erupted synchronously, around 30 Ma, at the start of plateau volcanism but later magmatism was exclusively alkaline. Large differences in the contents of incompatible elements are explained in terms of differences in source composition and in the degree of partial mantling. The lavas that built the plateau did not come from metasomatized lithospheric mantle, but from a broad region of mantle upwelling that was heterogeneous in terms of both temperature and composition.

ACKNOWLEDGEMENTS

Funding for this research was provided by the French CNRS (programmes IDYL, Corne de l'Afrique and Interieur de la Terre) and by BHP Billiton. One of us (B.K.) benefited from a Eurodoc fellowship. Claude Maerschalk, Catherine Chauvel and Eric Lewin are thanked for help in the chemistry laboratory, mass spectrometric analyses and fruitful discussions. The comments of M. Menzies, B.-M. Jahn and J. Scoates on the manuscript and the journal reviews by Joel Baker, Lotte Larsen and Marjorie Wilson are greatly appreciated.

SUPPLEMENTARY DATA

Supplementary data for this paper are available on *Journal of Petrology* online.

REFERENCES

Arndt, N. T., Chauvel, C., Czamanske, G. & Fedorenko, V. (1998). Two mantle sources, two plumbing systems: tholeiitic and alkaline magmatism of the Maymecha River basin, Siberian flood volcanic province. *Contributions to Mineralogy and Petrology* **133**, 297–313.

Ayalew, D., Marty, B., Yirgu, G. & Pik, R. (1999). Geochemical and isotopic (Sr, Nd and Pb) characteristics of volcanic rocks from southwestern Ethiopia. *Journal of African Earth Sciences* **29**, 381–391.

Baker, J., Snee, L. & Menzies, M. A. (1996*a*). A brief Oligocene period of flood volcanism in Yemen: implications for the duration and rate of continental flood basalt volcanism at the Afro-Arabian triple junction. *Earth and Planetary Science Letters* **138**, 39–55.

Baker, J., Thirlwall, M. & Menzies, M. A. (1996*b*). Sr–Nd–Pb isotopic and trace element evidence for crustal contamination of plume-derived flood basalts: Oligocene flood volcanism in western Yemen. *Geochimica et Cosmochimica Acta* **60**, 2559–2581.

Baker, J., Chazot, G., Menzies, M. A. & Thirlwall, M. F. (1998). Metasomatism of the shallow mantle beneath Yemen by the Afar plume—implications for mantle plumes, flood volcanism and intraplate volcanism. *Geology* **26**, 431–434.

Baker, J., MacPherson, C. G., Menzies, M. A., Thirlwall, M. F., Al-Kadasi, M. & Mattey, D. P. (2000). Resolving crustal and mantle contributions to continental flood volcanism, Yemen; constraints from mineral oxygen isotope data. *Journal of Petrology* **41**, 1805–1820.

Baker, J., Chazot, G., Menzies, M. A. & Thirlwall, M. (2002). Lithospheric mantle beneath Arabia: a Pan-African protolith modified by the Afar and older plumes, rather than a source for continental flood volcanism. In: Menzies, M. A., Klemperer, S. L., Ebinger, C. J. & Baker, J. (eds) *Volcanic Rifted Margins. Geological Society of America, Special Papers* **362**, 65–80.

Barberio, M. R., Donati, C., Donato, P., Yirgu, G., Peccerillo, A. & Wu, T. W. (1999). Petrology and geochemistry of Quaternary magmatism in the northern sector of the Ethiopian Rift between Debre Zeit and Awash Park. *Acta Vulcanologica* **11**, 69–81.

Barrat, J. A., Jahn, B. M., Joron, J. L., Auvray, B. & Hamdi, H. (1990). Mantle heterogeneity in NE Africa: evidence from Nd isotopic composition and hygromagmaphile element geochemistry of basaltic rocks from the Gulf of Tadjoura and southern Red Sea regions. *Earth and Planetary Science Letters* **101**, 233–247.

Barrat, J. A., Keller, F., Amossé, J., Taylor, R. N., Nesbitt, R. W. & Hirata, T. (1996). Determination of rare earth elements in sixteen silicate reference samples by ICP-MS after Tm addition and ion exchange separation. *Geostandards Newsletter* **20**, 133–139.

Barrat, J. A., Blichert-Toft, J., Gillet, P. & Keller, F. (2000). The differentiation of eucrites: the role of *in situ* crystallization. *Meteoritics and Planetary Science* **35**, 1087–1100.

Berhe, S. M., Desta, B., Nicoletti, M. & Teferra, M. (1987). Geology, geochronology and geodynamic implications of the Cenozoic magmatic province in W and SE Ethiopia. *Journal of the Geological Society, London* **144**, 213–226.

Blusztajn, J., Hart, S. R., Shimizu, N. & McGuire, A. V. (1995). Trace-element and isotopic characteristics of spinel peridotite xenoliths from Saudi Arabia. *Chemical Geology* **123**, 53–65.

Chauvel, C. and Blichert-Toft, J. (2001). A hafnium isotope and trace element perspective on melting of the depleted mantle. *Earth and Planetary Science Letters* **190**, 137–151.

Chauvel, C., Hofmann, A. W. & Vidal, P. (1992). HIMU–EM: the French Polynesian connection. *Earth and Planetary Science Letters* **110**, 99–119.

Chauvel, C., McDonough, W., Guille, G., Maury, R. & Duncan, R. (1997). Contrasting old and young volcanism in Rurutu Island, Austral chain. *Chemical Geology* **139**, 125–143.

Chazot, G. & Bertrand, H. (1993). Mantle sources and magma–continental crust interactions during early Red Sea–Aden rifting in Southern Yemen: elemental and Sr, Nd, Pb isotope evidence. *Journal of Geophysical Research* **98**, 1818–1835.

Class, C., Altherr, R., Volker, F., Eberz, G. & McCulloch, M. T. (1994). Geochemistry of Pliocene to Quaternary alkali basalts from the Huri Hills, northern Kenya. *Chemical Geology* **113**, 1–22.

Coulié, E. (2001). Chronologie $^{40}Ar/^{39}Ar$ et K/Ar de la dislocation du plateau éthiopien et de la déchirure continentale dans la Corne de l'Afrique depuis 30 Ma. Ph.D. thesis, Université de Paris Sud, Orsay.

Coulié, E., Quideleur, X., Gillot, P.-Y., Courtillot, V., Lefèvre, J.-C. & Chiesa, S. (2003). Comparative K–Ar and Ar/Ar dating of Ethiopian and Yemenite Oligocene volcanism: implications for timing and duration of the Ethiopian traps. *Earth and Planetary Science Letters* **206**, 477–492.

Courtillot, V. E. & Renne, P. R. (2003). On the ages of flood basalt events. *Comptes Rendus de l'Académie des Sciences, Geosciences* **335**, 113–140.

Cox, K. G. & Hawkesworth, C. J. (1985). Geochemical stratigraphy of the Deccan Traps at Mahabaleshwar, Western Ghats, India, with implications for open-system magmatic processes. *Journal of Petrology* **26**, 355–377.

Davaille, A., Le Bars, M. & Carbonne, C. (2003). Thermal convection in a heterogeneous mantle. *Comptes Rendus de l'Académie des Sciences, Geoscience* **335**, 141–156.

Deniel, C., Vidal, P., Coulon, C., Vellutini, P. J. & Piguet, P. (1994). Temporal evolution of mantle sources through continental rifting: the volcanism of Djibouti (Afar). *Journal of Geophysical Research* **99**, 2853–2869.

Duncan, R. A., Hooper, P. R., Rehacek, J., Marsh, J. S. & Duncan, A. R. (1997). The timing and duration of the Karoo igneous event, southern Gondwana. *Journal of Geophysical Research* **102**, 18127–18138.

Eggins, S. M., Woodhead, J. D., Kinsley, L. P. J., Sylvester, P., McCulloch, M. T., Hergt, J. M. & Handler, M. R. (1997). A simple method for the precise determination of 40 or more trace elements in geological samples by ICPMS using enriched isotope internal standardisation. *Chemical Geology* **134**, 311–326.

Erlank, A. J. (1984). *Petrogenesis of the Volcanic Rocks of the Karoo Province. Special Publication of the Geological Society of South Africa* **13**, 395 pp.

Gallagher, K. & Hawkesworth, C. (1992). Dehydration melting and the generation of continental flood basalts. *Nature* **258**, 57–59.

George, R. M. & Rogers, N. W. (2002). Plume dynamics beneath the African plate inferred from the geochemistry of the Tertiary basalts from southern Ethiopia. *Contributions to Mineralogy and Petrology* **144**, 286–304.

Griselin, M. & Arndt, N. T. (1996). Plume–lithosphere interaction and crustal contamination during formation of Coppermine River basalts, Northwest Territories, Canada. *Canadian Journal of Earth Sciences* **34**, 958–975.

Gurnis, M., Mitrovica, J. X., Ritsema, J. & van Heijst, H. J. (2000). Constraining mantle density structure using geological evidence of surface uplift rates: the case of the African Superplume. *Geochemistry, Geophysics, Geosystems* **1**, 1999GC000035.

Hawkesworth, C. J., Marsh, J. S., Duncan, A. R., Erlank, A. J. & Norry, M. J. (1984). The role of continental lithosphere in the generation of the Karoo volcanic rocks: evidence from combined Nd- and Sr- isotope studies. *Special Publication of the Geological Society of South Africa* **13**, 341–354.

Henjes-Kunst, F., Altherr, R. & Baumann, A. (1990). Evolution and composition of the lithospheric mantle underneath the western Arabian peninsula: constraints from Sr–Nd isotope systematics of mantle xenoliths. *Contributions to Mineralogy and Petrology* **105**, 460–472.

Hergt, J. M., Chappell, B. W., McCulloch, M. T., McDougall, I. & Chivas, A. R. (1989). Geochemical and isotopic constraints on the origin of the Jurassic dolerites of Tasmania. *Journal of Petrology* **30**, 841–883.

Herzberg, C. & Zhang, J. (1996). Melting experiments on anhydrous peridotite KLB-1: compositions of magmas in the upper mantle and transition zone. *Journal of Geophysical Research* **101**, 8271–8295.

Hirose, K. & Kushiro, I. (1993). Partial melting of dry peridotites at high pressures: determination of compositions of melts segregated from peridotite using aggregates of diamond. *Earth and Planetary Science Letters* **114**, 477–489.

Hofmann, A. W. (1988). Chemical differentiation of the Earth: the relationship between mantle, continental crust, and oceanic crust. *Earth and Planetary Science Letters* **90**, 297–314.

Hofmann, C., Courtillot, V., Feraud, G., Rochette, P., Yirgu, G., Ketefo, E. & Pik, R. (1997). Timing of the Ethiopian flood basalt event and implications for plume birth and global change. *Nature* **389**, 338–341.

Jerram, D. A. (2002). The volcanology and facies architecture of flood basalts. In: Menzies, M. A., Klemperer, S. L., Ebinger, C. J. & Baker, J. (eds) *Magmatic Rifted Margins. Geological Society of America, Special Publications* **362**.

Jerram, D. A. & Robbe, O. (2001). Building a 3-D geologic model of a flood basalt: an example from the Etendeka, NW Namibia. *Electronic Geoscience* **6**(1), 1–15.

Jestin, F. & Huchon, P. (1992). Cinématique et déformation de la jonction triple mer Rouge–golfe d'Aden–Rift éthiopien depuis l'Oligocène. *Bulletin de la Société Géologique de France* **163**, 125–133.

Justin Visentin, E., Nicoletti, M., Tolomeo, L. & Zanettin, B. (1974). Miocene and Pliocene volcanic rocks of the Addis Ababa–Debra Berhan area (Ethiopia). *Bulletin of Volcanology* **38**, 237–253.

Lanphere, M. A., Dalrymple, G. B., Fleck, R. S. & Pringle, M. S. (1990). Intercalibration of mineral standards for K–Ar and 40 Ar–39 Ar age measurements. *EOS Transactions, American Geophysical Union* **71**, 1658.

Larsen, L. M., Pedersen, A. K., Sundvoll, B. & Frei, R. (2003). Alkali picrites formed by melting of old metasomatized lithospheric mantle: Manîtdlat Member, Vaigat Formation, Paleocene of West Greenland. *Journal of Petrology* **44**, 3–38.

Lightfoot, P. C., Hawkesworth, C. J., Hergt, J., Naldrett, A. J., Gorbachev, N. S., Fedorenko, V. A. & Doherty, W. (1993). Remobilization of the continental lithosphere by mantle plumes: major-, trace-element and Sr-, Nd-, and Pb-isotope evidence from picritic and tholeiitic lavas of the Noril'sk district Siberian Trap, Russia. *Contributions to Mineralogy and Petrology* **114**, 171–188.

MacDonald, G. A. & Katsura, T. (1964). Chemical composition of Hawaiian lavas. *Journal of Petrology* **5**, 82–133.

Macdonald, R., Rogers, N. W., Fitton, J. G., Black, S. & Smith, M. (2001). Plume–lithosphere interactions in the generation of the basalts of the Kenya Rift, East Africa. *Journal of Petrology* **42**, 877–900.

Manhès, G., Minster, J.-F. & Allègre, C. J. (1978). Comparative uranium–thorium–lead and rubidium–strontium study of the Saint Severin amphoterite: consequences for early solar system chronology. *Earth and Planetary Science Letters* **39**, 14–24.

Marsh, J. S., Hooper, P. R., Rehacek, J., Duncan, R. A. & Duncan, A. R. (1997). Stratigraphy and age of Karoo Basalts of Lesotho and implications for correlations within the Karoo igneous province. In: Mahoney, J. J. & Coffin, M. E. (eds) *Large Igneous Provinces: Continental, Oceanic and Planetary Flood Volcanism. Geophysical Monograph, American Geophysical Union* **100**, 247–272.

Menzies, M., Baker, J., Bosence, D., Dart, C., Davison, I., Hurford, A., Al-Kadasi, M., McKlay, K., Nichols, G., Al-Subbary, A. & Yelland, A. (1992). The timing of magmatism, uplift and crustal extension: preliminary observations from Yemen. In: Storey, B. C., Alabaster, T. & Pankhurst, R. J. (eds) *Magmatism and the Causes of Continental Break-up. Geological Society, London, Special Publications* **68**, 293–304.

Menzies, M., Baker, J. & Chazot, G. (2001). Cenozoic plume evolution and flood basalts in Yemen: a key to understanding older examples. In: Ernst, R. E. & Buchan, K. L. (eds) *Mantle Plumes: their Identification through Time. Geological Society of America, Special Papers* **353**, 23–36.

Merla, G., Abbate, E., Canuti, P., Sagri, M. & Tacconi, P. (1979). Geological map of Ethiopia and Somalia and comment with a map of major landforms (scale 1:2,000,000). Rome: Consiglio Nazionale delle Ricerche, **95**.

Mohr, P. (1967). Review of the geology of the Semien Mountains. *Bulletin of the Geophysical Observatory of Addis Ababa* **10**, 79–93.

Mohr, P. (1983*a*). Ethiopian flood basalt province. *Nature* **303**, 577–584.

Mohr, P. (1983*b*). Volcanotectonic aspect of Ethiopian evolution. *Bulletins des Centres de Recherches Exploration–Production Elf-Aquitaine* **7**(1), 157–189.

Mohr, P. & Zanettin, B. (1988). The Ethiopian flood basalt province. In: Macdougall, J. D. (ed.) *Continental Flood Basalts*. Dordrecht: Kluwer Academic, pp. 63–110.

Nyblade, A. A. (2002). Crust and upper mantle structure in East Africa: implications for the origin of Cenozoic rifting and volcanism and the formation of magmatic rifted margins. In: Menzies, M. A., Klemperer, S. L., Ebinger, C. J. & Baker, J. (eds) *Volcanic Rifted Margins. Geological Society of America, Special Papers* **362**, 15–26.

Nyblade, A. A. & Robinson, S. W. (1994). The African Superswell. *Geophysical Research Letters* **21**, 765–768.

Peate, D. W., Hawkesworth, C. J. & Mantovani, M. S. M. (1992). Chemical stratigraphy of the Paraná lavas (South America): classification of magma types and their spatial distribution. *Bulletin of Volcanology* **55**, 119–139.

Pedersen, A. K., Larsen, L. M., Pedersen, G. K. & Dueholm, K. S. (1996). Filling and plugging of a marine basin by volcanic rocks: the Tunoqqu Member of the Lower Tertiary Vaigat Formation on Nuussuag, central West Greenland. *Bulletin Grønlands Geologiske Undersogelse* **171**, 5–28.

Piccirillo, E., Justin Visentin, E., Zanettin, B., Joron, J. L. & Treuil, M. (1979). Geodynamic evolution from plateau to rift: major and trace element geochemistry of the central eastern Ethiopian Plateau volcanics. *Neues Jahrbuch für Geologie und Paläontologie, Abhandlungen* **158**, 139–179.

Pik, R., Deniel, C., Coulon, C., Yirgu, G., Hoffmann, C. & Ayalew, D. (1998). The northwestern Ethiopian Plateau flood basalts: classification and spatial distribution of magma types. *Journal of Volcanology and Geothermal Research* **81**, 91–111.

Pik, R., Deniel, C., Coulon, C., Yirgu, G. & Marty, B. (1999). Isotopic and trace element signatures of Ethiopian basalts: evidence for plume–lithospheric interactions. *Geochimica et Cosmochimica Acta* **63**, 2263–2279.

Planke, S. & Eldholm, O. (1994). Seismic response and construction of seaward dipping wedges of flood basalts. *Journal of Geophysical Research* **99**, 9263–9278.

Ritsema, J. & van Heijst, H. (2000). New seismic model of the upper mantle beneath Africa. *Geology* **28**, 63–66.

Rochette, P., Tamrat, E., Feraud, G., Pik, R., Courtillot, V., Ketefo, E., Coulon, C., Hoffmann, C., Vandamme, D. & Yirgu, G. (1998). Magnetostratigraphy of the Ethiopian traps. *Earth and Planetary Science Letters* **164**, 497–510.

Roger, S., Dautria, J.-M., Coulon, C., Pik, R., Yirgu, G., Michard, A., Legros, P. & Ayalew, D. (1999). An insight on the nature, composition and evolution of the lithospheric mantle beneath the north-western Ethiopian plateau: the ultrabasic xenoliths from the Tana Lake Province. *Acta Vulcanologica* **11**, 161–168.

Rogers, N., Macdonald, R., Fitton, J. D., George, R., Smith, M. & Barreiro, B. (2000). Two mantle plumes beneath the East African rift system: Sr, Nd and Pb isotope evidence from Kenya Rift basalts. *Earth and Planetary Science Letters* **176**, 387–400.

Schilling, J.-G., Kingsley, R. H., Hanan, B. B. & McCully, B. L. (1992). Nd–Sr–Pb isotopic variations along the Gulf of Aden: evidence for Afar mantle plume–continental lithosphere interaction. *Journal of Geophysical Research* **97**, 10927–10966.

Sharma, M. (1997). Siberian traps. Large igneous provinces: continental, oceanic and planetary flood volcanism. In: Mahoney, J. J. & Coffin, M. E. (eds) *Large Igneous Provinces: Continental, Oceanic and Planetary Flood Volcanism. Geophysical Monograph, American Geophysical Union* **100**, 273–296.

Späth, A., Le Roex, A. P. & Opiyo-Akech, N. (2001). Plume–lithosphere interaction and the origin of continental rift-related alkaline volcanism—the Chyulu Hills volcanic province, southern Kenya. *Journal of Petrology* **42**, 765–787.

Stewart, K. & Rogers, N. (1996). Mantle plume and lithosphere contributions to basalts from southern Ethiopia. *Earth and Planetary Science Letters* **139**, 195–211.

Storey, M., Mahoney, J. J. & Saunders, A. D. (1997). Cretaceous basalts in Madagascar and the transition between plume and continental lithosphere mantle sources. In: Mahoney, J. J. & Coffin, M. E. (eds) *Large Igneous Provinces: Continental, Oceanic and Planetary Flood Volcanism. Geophysical Monograph, American Geophysical Union* **100**, 95–122.

Tegner, C., Lesher, C. E., Larsen, L. M. & Watt, W. S. (1998). Evidence from the rare-earth-element record of mantle melting for cooling of the Tertiary Iceland plume. *Nature* **395**, 591–594.

Ukstins, I. A., Renne, P. R., Wolfenden, E., Baker, J., Ayalew, D. & Menzies, M. (2002). Matching conjugate volcanic rifted margins: $^{40}Ar/^{39}Ar$ chrono-stratigraphy of pre- and syn-rift bimodal flood volcanism in Ethiopia and Yemen. *Earth and Planetary Science Letters* **198**, 289–306.

Vidal, P., Deniel, C., Vellutini, P. J., Piguet, P., Coulon, C., Vincent, J. & Audin, J. (1991). Changes of mantle source in the course of a rift evolution. *Geophysical Research Letters* **18**, 1913–1916.

Violle, P. Y. (1999). Relations entre la géomorphologie et la lithologie des trapps d'Ethiopie. Diplôme d'Études Approfondies de l'Université Joseph Fourier, Grenoble II, 31 pp.

Weis, D., Demaiffe, D., Cauët, S. & Javoy, M. (1987). Sr, Nd, O and H isotopic ratios in Ascension Island lavas and plutonic inclusions: cogenetic origin. *Earth and Planetary Science Letters* **82**, 255–268.

White, W. M. & Duncan, R. A. (1996). Geochemistry and geochronology of the Society Islands: new evidence for deep mantle recycling. In: Basu, A. R. & Hart, S. R. (eds) *Earth Processes: Reading the Isotopic Code.* Washington, DC: American Geophysical Union, **95**, 183–206.

White, W. M., Albarède, F. & Telouk, P. (2000). High-precision analysis of Pb isotope ratios by multi-collector ICP-MS. *Chemical Geology* **167**, 257–270.

Widdowson, M. (1997). Tertiary paleosurfaces of the SW Deccan, Western India: implications for passive margin uplift. In: Widdowson, M. (ed.) *Palaeosurfaces: Recognition, Reconstruction and Palaeoenvironmental Interpretation. Geological Society, London, Special Publications* **120**, 221–248.

Widdowson, M. & Cox, K. G. (1996). Uplift and erosional history of the Deccan Traps, India: evidence from laterites and drainage patterns of the Western Ghats and Konkan Coast. *Earth and Planetary Science Letters* **137**, 57–69.

Wolde, B. & Widenfalk, L. (1994). Petrochemical and geochemical constraints on Cenozoic volcanism in Ethiopia. *African Geosciences Reviews* **1**, 475–494.

Wooden, J. L., Czamanske, G. K., Fedorenko, V. A., Arndt, N. T., Chauvel, C., Bouse, R. M., King, B. W., Knight, R. J. & Siems, D. F. (1993). Isotopic and trace-element constraints on mantle and crustal contributions to Siberian continental flood basalts, Noril'sk area, Siberia. *Geochimica et Cosmochimica Acta* **57**, 3677–3704.

Woodhead, J. D. & Devey, C. W. (1993). Geochemistry of the Pitcairn seamounts, I: source character and temporal trends. *Earth and Planetary Science Letters* **116**, 81–99.

Woodhead, J. D. & McCulloch, M. T. (1989). Ancient seafloor signals in Pitcairn Island lavas and evidence for large amplitude, small length-scale mantle heterogeneities. *Earth and Planetary Science Letters* **94**, 257–273.

Zanettin, B. (1992). Evolution of the Ethiopian Volcanic Province. *Memorie Lincee Scienze Fisiche e Naturali* **1**, 155–181.

Zanettin, B. (1993). On the evolution of the Ethiopian volcanic province. In: Abbate, E., Sagri, M. & Sassi, F. P. (eds) *Geology and Mineral Resources of Somalia and Surrounding Regions.* Firenze: Istituto Agronomico per l'Oltremare, pp. 279–310.

Zanettin, B. & Justin Visentin, E. (1974). The volcanic succession in central Ethiopia, 2: The volcanics of the western Afar and Ethiopia

rift margins. *Memorie degli Istituti di Geologia e Mineralogia dell'Universita di Padova* **31**, 1–19.

Zanettin, B. & Justin Visentin, E. (1975). *Tectonical and Volcanological Evolution of the Western Afar Margin (Ethiopia). Afar Depression of Ethiopia.* Stuttgart: Schweizerbart, pp. 300–309.

Zanettin, B., Gregnanin, A., Justin Visentin, E., Mezzacasa, G. & Piccirillo, E. M. (1976). *New Chemical Analyses of the Tertiary Volcanics from the Central Ethiopian Plateau.* Consiglio Nazionale delle Ricerche, Istituto di Mineralogia e Petrografia. Padova: Universita di Padova, pp. 1–43.

Zanettin, B., Justin Visentin, E. & Piccirillo, E. M. (1978). Volcanic succession, tectonics and magmatology in central Ethiopia. *Atti e Memorie dell'Accademia Patavina di Scienze, Lettere ed Arti* **90**, 5–19.